

2700.

OPTIMUM PARAMETERS OF
ASYMMETRICALLY SLOTTED STRUCTURES

A MASTER OF SCIENCE THESIS

in

Electrical and Electronics Engineering

Middle East Technical University

By

Ahmet DİRİKER

December, 1987


T. C.
Yükseköğretim Kurulu
Dokümantasyon Merkezi

Approval of the Graduate School of Natural and Applied
Sciences,



Prof. Dr. Halim DOGRUSÖZ

Director

I certify that this thesis satisfies all the requirements
as a thesis for the Master of Science degree in Electrical
and Electronics Engineering,


Prof. Dr. Canan TOKER
Chairman of the Department

We certify that we have read this thesis and that in our
opinion it is fully adequate, in scope and quality as a
thesis for the Master of Science degree in Electrical and
Electronics Engineering,


Assoc. Prof. Dr. Bülent ERTAN
Supervisor

Examining Committee in Charge:

Assoc. Prof. Dr. Aydın ERSKAK
Assoc. Prof. Dr. Muammer ERMIŞ
Assoc. Prof. Dr. Bülent ERTAN
Asst. Prof. Dr. Yıldırım ÜÇTUĞ
Dr. Müjdat TOHUMCU








ABSTRACT

OPTIMUM PARAMETERS OF ASYMMETRICALLY SLOTTED STRUCTURES

DIRIKER AHMET

Msc. Degree in Electrical and Electronics Engineering

Supervisor: Assoc. Prof. Dr. Bülent ERTAN

December 1987, 132 pages

Due to advantages that originate from its simple magnetic structure and driver configuration, switching reluctance motor (SRM) drives are regarded as a new alternative for other drive types. However in order to be competitive with known motor types, optimum design of SRM is of utmost importance.

Contrary to classical machines, the complex nature of the geometry and high saturation of this motor makes impossible to analytically compute the performance functions. Due to this factor for achieving optimum design parameter values is more difficult in this case. Current design techniques generally depend on experi-

mentally obtained information or numerically computed data. For obtaining accurate values of parameters, field solutions should be used. However, this is not practical since it is very time consuming process.

In this thesis, optimum values of air-gap parameters of asymmetrically slotted structures are found by using computer programmes. To do this, a straight forward method recently developed for computation of steady-state average torque of symmetrically slotted SRM's is applied to asymmetrically slotted SRM's. Input data for this work is normalized Permeance vs flux density curves of symmetrically slotted structures. At the end of this work accurate values of optimum design of SRM's are found under different mmf and magnetic loading limits. The thesis also describes the optimization technique developed for the purpose above.

Ö Z E T

EŞİT OLMAYAN KUTUPLU YAPILARIN OPTİMUM PARAMETRELERİ

DİRİKER Ahmet

Yüksek Lisans Tezi, Elektrik ve Elektronik Müh. Bölümü

Tez Yönetmeni: Doç. Dr. Bülent ERTAN

Aralık 1987, 132 Sayfa

Manyetik yapısının ve sürücü devresinin basitliğinden kaynaklanan üstünlüklerinden dolayı, Anahtarlı Relüktans Motorlu (ARM) tahrik sistemleri diğer tahrik sistemleri için yeni bir seçenek olarak görülmektedir. Bununla beraber, diğer sistemlerle tam bir rekabet için ARM'lerin optimum tasarımı önem kazanmaktadır.

Klasik motorların aksine karmaşık doğası ve ağır saturasyon, bu motorların performans fonksiyonlarının analitik olarak ifade edilmesini imkansız kılmaktadır. Bu durumda, optimum tasarım parametrelerinin elde edilmesi daha da güçleşmektedir. Halihazırdaki tasarım yöntemleri genellikle deneysel bilgilere veya

nümerik hesaplara dayanmaktadır. Tasarım parametrelerinin hasas olarak elde edilmesi için alan çözümlerinin kullanılması gerekir. Ancak bu ise çok zaman alıcı hesaplamaları gerektirdiğinden, pratik bir yaklaşım değildir.

Bu tezde stator ve rotor kutup genişlikleri birbirine eşit olmayan ARM'lerin optimum hava-aralığı parametreleri bilgisayar yardımıyla hesaplanmıştır. Bunun için daha önce eşit kutuplu ARM'lerin ortalama karalı çalışma momentinin hesaplanması için geliştirilen bir metod, bu defa eşit olmayan kutuplu ARM'lere uyarlanmıştır. Bu çalışmada, daha önce eşit kutuplu yapılar için hesaplanmış alan permeans verileri kullanılmıştır. Tez çalışmasının sonunda değişik manyetik yükleme ve mmf limitleri için optimum ARM tasarımının genel bir çerçevesi çizilmiştir. Bu tezde söz konusu amaç için geliştirilmiş bir optimizasyon metodu da tanımlanmıştır.

ACKNOWLEDGEMENTS

I would like to express my gratitude to my supervisor, Assoc. Prof. Dr. Bülent Ertan not only, for his great help during my master thesis but also encouragements at every stage.

I would also like to thank Dr. Müjdat Tohumcu for his helps.

I would also like to thank my sister Pınar Ergen who typed the text very carefully within a very short time, and Coşkun Korkut and Filiz Başlar for their help in producing the drawings which are very important for my thesis.

TABLE OF CONTENTS

	<u>Page</u>
ABSTRACT	iii
ÖZET	v
ACKNOWLEDGEMENTS	vii
LIST OF TABLES	xii
LIST OF FIGURES	xiii
CHAPTER	
1. INTRODUCTION	1
1.1 Drive Types & Growing Importance of Switching Reluctance Motors (SRM)	1
1.2 Brief Information About Previous Works on SRM..	3
1.3 Aim of This Thesis	5
1.4 Content of This Thesis	5
1.5 Brief Information On Operating Principles of SRM	6
1.6 Conclusion	10
2. ENERGY FACTOR CONCEPT & TORQUE	11
2.1 Introduction	11
2.2 Normalization	11

2.3 Unit Doubly Salient Structure	14
2.4 Torque	15
2.4.1 Flux Waveform	15
2.4.2 Flux Mmf Contour	17
2.4.3 Torque and Energy Factor	20
2.4.4 Importance of Energy Factor	22
2.5 Computation of Energy Factor	22
2.5.1 Permeance Calculation of Asymmetrically Slotted Structure	25
2.5.1.1 Tooth Width & Normalized Displace- ment of Symmetrical Pair	25
2.5.1.2 λ/g of Symmetrical Pair	26
2.5.1.3 Flux Density (B_t) of Symmetrical Pair	27
2.6 Conclusion	29
3. COMPUTATION OF ENERGY FACTOR	31
3.1 Introduction	31
3.2 Preparation of Input Data	31
3.2.1 Obtaining F vs B_t Curves From Available Data	33
3.2.2 Extrapolation of F vs B_t Curves	36
3.2.3 Computation of Permeance Data For Symmetrically Slotted Structures	39
3.3 Steps of the Procedure For Computing Energy Factor Data	40

3.3.1	Computation of Permeance Data For Asymmet- rically Slotted Structures	40
3.3.2	Computation of Permeance Data For Struc- tures Having Unavailable Parameter Values ..	43
3.3.3	Obtaining Mmf vs B_t Curves of Asymmet- rically Slotted Structures	48
3.3.4	Computation of Energy Factor	49
3.4	Observations On The Obtained Energy Factor Data ..	70
3.5	Conclusion	83
4.	OPTIMIZATION	88
4.1	Introduction	88
4.2	General Optimization Approach	88
4.2.1	Independent Motor Parameters	89
4.2.2	Constraints	90
4.3	Theory of Optimization Method Used in this Work ..	91
4.4	Application of the Method	92
4.5	Result of Optimization	96
4.6	Effect of Mmf Limits On Optimum Values of Parameters	101
4.7	Effect of $B_p(\max)$ Limits On Optimum Values Of Parameters	101
4.8	Conclusion	106
5.	CONCLUSION	109

LIST OF REFFERENCES	115
APPENDIX A: CUBIC SPLINE INTERPOLATION	117
APPENDIX B: DESCRIPTIONS OF PROGRAMMES USED IN THE WORK	121



LIST OF TABLES

<u>Table</u>		<u>Page</u>
3.5	Interpolation Procedure of Structures Having Unavailable Parameter Values In The Data	46
3.7	Energy Factor Data	52
4.1	Optimization Results Concerning 3 Different Local Maximas	98
4.2	Optimization Results Concerning 5 Different Local Maximas	98
4.3	Optimum Air-gap Parameters With Respect To Different Mmf Limits	102
4.4	Optimum Air-Gap Parameters With Respect To Different $B_{p(max)}$ Limits	102
4.5	Optimum Designs With Respect To Different Mmf Limits and $B_{p(max)}$ Limits	104

LIST OF FIGURES

<u>Figure</u>	<u>Page</u>
1.1 Basic Structure of 4 Phase SRM	7
1.2 Motion of 3 Phase, 4 Pole SRM	8
1.3 In and Out Positions Of SRM	10
2.1 Air-Gap Region Of SRM	12
2.2 A Doubly Salient Geometry and Unity Doubly Salient Structure	14
2.3 A Typical Triangular Flux Waveform	17
2.4 A Typical ϕ -Mmf Contour	18
2.5 Obtaining of Flux Density (B_t) - Mmf Contour.	19
2.6 An Asymmetrical Pair And Corresponding Symmetrical Pair	24
2.7 Changing in λ_r Value In Obtaining Corresponding Symmetrically Slotted Structure	27
3.1 Original B_t vs Mmf Curves And Curve Found By Cubic Spline Interpolation Technique	35
3.2 Oscillations Of B_t vs Mmf Curves Caused By Cubic Spline Interpolation Technique	37
3.3 Extrapolation Of B_t vs F Curves	38
3.4 Normalized Permeance vs B_t Curves Of Asymmetrically Slotted Structure	42

3.6	Flux Waveform For Different Conduction Periods	50
3.8	Energy Factor vs X_{ni} Curves	71
3.9	Energy Factor vs X_{ni} Curves	72
3.10	Energy Factor vs X_{ni} Curves	74
3.11	Energy Factor vs λ/g Curves	75
3.12	Energy Factor vs X_{ni} Curves	76
3.13	Energy Factor vs t_r/λ Curves	78
3.14	Energy Factor vs t_s/λ , t_r/λ Curves	80
3.15	Energy Factor vs t_s/λ , t_r/λ Curves	81
3.16	Energy Factor vs Mmf Limit Curves	84
4.6	Energy Factor vs $B_{p(max)}$ Curves	105

CHAPTER 1

INTRODUCTION

1.1 DRIVE TYPES & GROWING IMPORTANCE OF SWITCHING RELUCTANCE MOTOR (SRM)

During the last 20-25 years to exploit developments in semiconductor technology improved forms of electrical drives are introduced. However, until late sixties DC motors were unique alternative whenever speed control was concerned. At that time, DC motors were treated as variable speed motors and AC motors were regarded as constant speed motors. In DC motors, speed control is simply achieved by controlling its terminal voltage or field current with additional resistors. This situation has changed in sixties with the introduction of drives which use controlled rectifiers or choppers instead of additional resistors. Later various inverter circuits were developed for induction machine speed control. Although an induction motor is cheaper, the drive is usually more complicated particularly if thyristors are used. In induction motors, speed can be controlled over a wide range by varying the terminal voltage together with frequency. Transistorized inverters are much more simpler than thyristorized inverters however, voltage-current ratings of available transistors are smaller than thyristors. As a result induction motor drives of larger sizes, especially are more

expensive than DC drives still dominate in larger sizes. However, for low power applications, inverter-fed induction machines have already been a serious commercial alternative for DC drives. In addition, DC drives have serious problems originating from the motor due to weight, size and maintenance problems, particularly in explosive or dusty atmospheres.

For some 20-25 years there have been predictions that motor robustness will increase and the cost of power electronics will fall and AC or brushless-motor based systems will dominate conventional DC drives. However, this has not happened, the cost of power electronics has not fallen sufficiently. For that reason, even now DC motor dominates controlled drives technology but it is not a unique alternative.

In recent years designers offer a third alternative to the competition between DC and AC drives. This alternative is the switching reluctance motor drives (SRM). It has some advantages as mentioned below.

. This type of motor has a very simple magnetic structure. Motor contains the windings only on the stator side. This winding is a concentrated winding. There is no winding on stator side.

. It can offer high system efficiency and high controllability. It can be used for both speed and position control.

. Its drive circuit is also simpler. Since the operation of reluctance motor is independent of the direction current flow in the windings yielding particularly economical and

reliable power conditioning circuits having fewer power-semiconductors and the drive provides low cost and maintenance. As compared to the DC motor, a further advantage is that it is a brushless machine.

. Whenever speed control is concerned, SRM drives offer a good result and if a high resolution is not desired, good position control can be obtained as well.

. In addition, if Torque/Volume ratio improves and becomes comparable asynchronous motors, the usage field of SRM is likely to become wider.

1.2 BRIEF INFORMATION ABOUT PREVIOUS WORKS ON SRM

The advantages of SRM mentioned above has made investigation of optimum parameter of SRM an important problem for design engineers. Although a lot has been written about SRM's, further work is needed to solve the design problems. Difficulties arise since the working principle of SRM highly depends on the heavy saturation of magnetic material, the design problem is very complex. Present design practice generally depends on experimentally obtained results common sense and analysis. General design constraints are introduced to define a range of parameters which result in a feasible design. Some performance functions such as steady-state average torque, starting torque, efficiency etc. are not taken into account or treated in a rough manner.

As discussed below a more through analysis method has been introduced in the recent years. However, optimization of parameters for the purpose of maximizing the out-

put of an SRM is still a problem of interest, particularly because such commercial devices have asymmetrical slotting for which little has been done. This problem has been investigated in some detail for symmetrical slotting case which presents a simpler problem. Work on SRM's can be briefly summarized as follows.

Early published work on SRM's belongs to Unnewehr and Koch, Blenkinsop, Byrne and Lacy, Baushand and Rieke. Unnewehr and also Koch who presented a disc type SRM in 1974. In 1976 a phase single stock SRM is analyzed by Blenkinsop. It showed only the basic principles of operation of SRM. In 1977, Koch developed a linear theory of SRM, in order to investigate the performance of SRM's. In 1979 Corda presented his results on the design of a 0.75 Kw SRM. Corda, in his work, formulated linear analysis for the performance calculations of a SRM in a very systematic manner. He set out a number of different design criteria which are necessary for a reversible drive with self starting capability. In his work, Corda also directed his attention towards treating the nonlinear work of Lawrenson, Stephenson, Blenkinsop, Corda and Fulton published in 1980. The work lays basic principles of SRM structure and operation and offers some general principles for a practical design. Davis, Ray, Blake discussed various inverter circuit options as SRM driver configuration.

Lawrenson discussed the recent significant developments in SRM drives his paper in 1983. In his work the importance and advantages of such drives were emphasized.

In 1984, Chappell, Ray, Blake published a paper which discussed applications where microprocessors has been used in the control unit of SRM drives.

In 1982 Ertan shows an analytical method of static torque and inductance curve prediction for symmetrically slotted doubly salient devices in his published work.

In 1985 Tohumcu offers a method for optimizing the symmetrical slotted SRM in his Phd thesis.

1.3 AIM OF THIS THESIS

Correct design of the airgap geometry has an important role in torque production capability of an SRM. SRM's may have asymmetrical slottings and as far as the authors know an answer for correct choice of geometry for non-linear magnetic circuit conditions does not exist.

The purpose of this thesis have been to identify optimum air-gap region parameters from the point of view of torque production of asymmetrically slotted SRM's.

This would normally involve a series of numerical magnetic field solutions, due to highly saturated and position dependent saturation of such devices under practical conditions. But in this thesis an approach based on numerically calculated permeance data has been used as explained in chapter 2.

1.4 CONTENT OF THIS THESIS

In optimum design, to know the average steady-state torque produced of that motor has vital importance.

In SRM, because of heavy saturation analytical expression of steady state average torque are not available as being other performance functions. Then instead of using the analytical expression, torque can be computed by means of various numerical field solutions. But by these method, solution can be obtained after thousands of times iterations which is a very time consuming process. Then, an easier method based on the permeance data prepared by making numerical field solutions has been used.

In chapter 2 this method is explained for asymmetrically slotted Srm's and the concept of energy factor is introduced.

In chapter 3 the process of computation energy factor for several structures of SRM by using the method described in chapter 2 is presented. During this computation process a digital computer programs have been used and practical motor conditions has been assumed. The obtained energy factor data is also discussed in this chapter.

In chapter 4 a general idea about optimization technique is described. A search method used in this thesis called "A Form Of Direction Of Search" is explained and used for finding optimum SRM structure.

In chapter 5 the results obtained during this work are discussed and concluded.

1.5 BRIEF INFORMATION ON WORKING PRINCIPLES OF SRM

Switching reluctance motor (SRM) is a kind of

step motor which is designed to rotate a specific number of degrees for each electrical pulse produced by its control circuit. Depending upon the pulse rate and the load torque including inertia effects, the motor follows the axis of air-gap magnetic field by virtue of reluctance torque. The basic structure of SRM is shown in fig.(1.1)

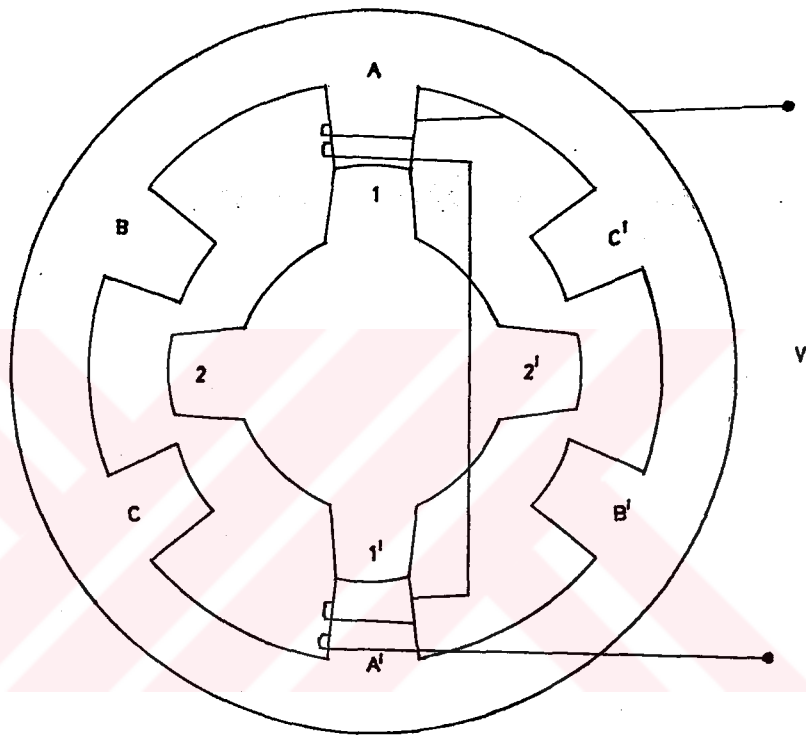


Fig. 1.1. Basic structure of 4 phase SRM

As it is understood from its name, it is a doubly salient structure. Salient poles are placed on both rotor and stator side. In order to provide continuous motion number of stator poles must be unequal to the number of rotor poles. There are no windings on rotor side but on stator poles there are simple concentrated winding. A second bifilar winding is wound on each stator pole which provides energy recovery. This winding has a vital importance in

production of highest torque.

The set of windings called phases are separately excited by means of a proper sequence.

The counter clockwise motion of SRM is shown in fig. 1.2 for giving an idea of its working principle.

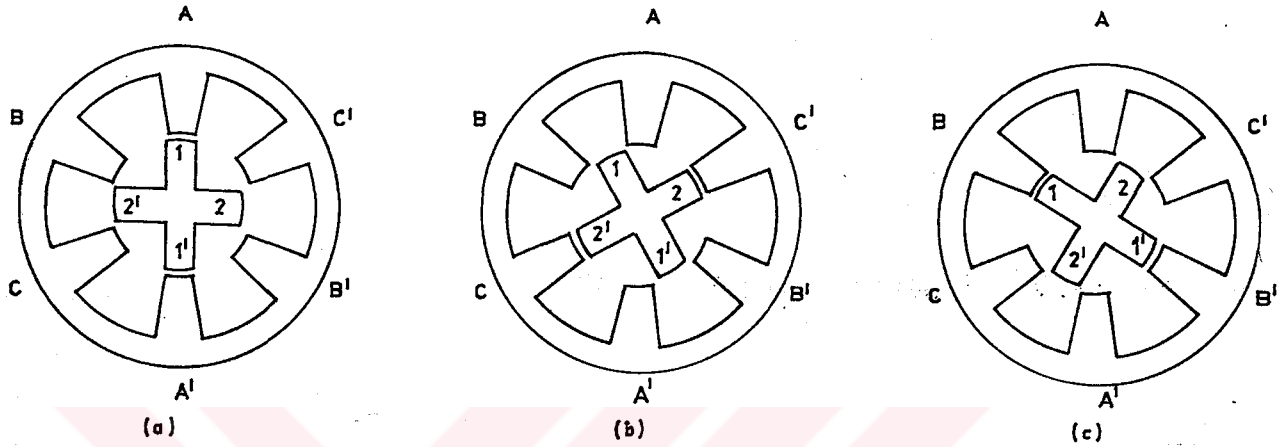


Fig. 1.2 . Motion of 3 phase, 4 pole SRM

The motor shown in fig. 1.2 is 3 phase SRM with 4 rotor poles. At part "a" of fig. 1.2 phase A is energized, in part "b" phase C is energized and part "c" phase B is energized. If this A C B sequence is repeated then and a counter clockwise motion is obtained. For reversing the direction of motion, sequence of excitation should be A, B, C..... .

As may be easily noticed from the explanation, above rotor is displaced by a certain amount everytime a new phase is excited. The distance travelled when excitation pattern is changed is called the stepping angle denoted by α and is given by eq. 1.1

$$\alpha = \frac{2\pi}{qN_r} \quad (1.1)$$

Where q is the number of phases and N_r is the number of rotor teeth.

During the motion, the instant at which each phase is to be energized to maximize torque, is determined according to the information taken from the rotor position transducer.

The following terminology is always used throughout this work.

Switch-on instant: Is the instant phase energized. After switch-on instant energy begins to flow from the supply to the related phase winding. Position of rotor poles will be aligned to stator poles which have excited phase winding.

Switch-off instant: Is the instant when the current of main switching element is turned off. After this instant energy begins to flow from the phase winding to the supply.

Conduction Period: For a given phase it is a period defined as the time interval between switch-on and switch-off instants.

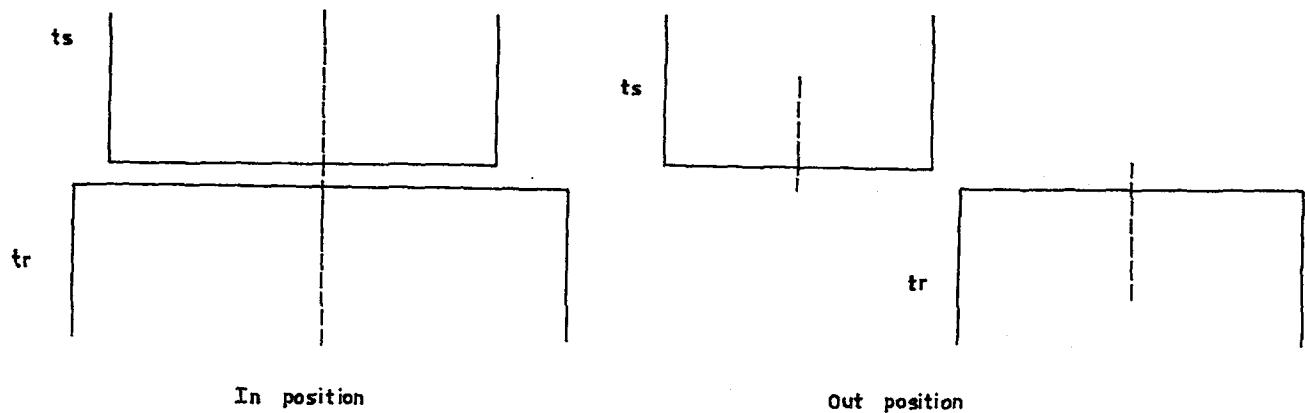


Fig. 1.3. IN and OUT positions of SRM

In and out positions: The position in which rotor and stator teeth are fully aligned when a phase is energized is called the "IN" position. As an example of a pair of teeth in this position may be seen in fig. 1.3 and also in 1.3-a where alignment occurs under phase A.

In this position permeance is maximum. If rotor and stator teeth are fully out of alignment, this position is called the "OUT" position which is shown in fig. 1.3-b and in fig. 1.3-a for phases B and C.

In this chapter a Switching Reluctance Motor has been briefly presented. In the next chapter a simple method for calculation of steady state average torque is explained with the help of energy factor concept.

CHAPTER 2

ENERGY FACTOR CONCEPT & TORQUE

2.1 INTRODUCTION

The performance functions and motor parameters of doubly salient switching reluctance motor can not be simply defined by analytical expressions as conventional DC and AC motors because of high saturation.

Therefore in place of defining analytical expression, it is useful to use data which are computed or measured in experimental means. Computed data may be obtained by numerical field solutions. But it is a very time consuming process. Design engineers need simple and straightforward techniques which give quick results. In literature some design techniques have been developed. But unfortunately none of them for a sufficient background for design. Ertan⁽³⁾ and Tohumcu⁽⁵⁾ have offered a new optimization method for symmetrically slotted SRM's by computing average steady-state torque.

This technique for calculating average torque of asymmetrically slotted SRM's will be summarized in this chapter.

2.2 NORMALIZATION

It is very convenient to define the position of

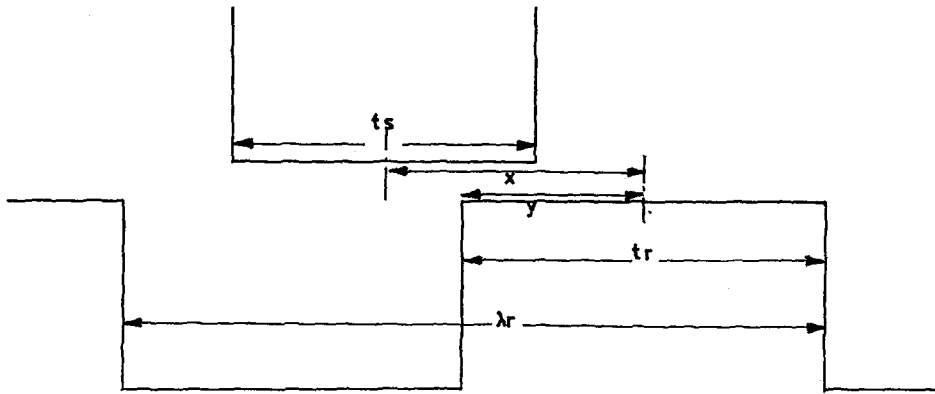


Fig. 2.1. Air-gap region of SRM

In this fig., λ_r denotes rotor pole pitch, t_r and t_s denote, rotor and stator teeth widths y is overlap and x is the displacement between center lines of stator and rotor poles.

Then position knowledge should be expressed as a function of rotor pole pitch λ_r . Any position can be converted to normalized displacement by using following relationship.

$$x_n = \frac{2x}{\lambda_r} \quad (2.1)$$

Where λ_r is the rotor pole pitch, x and x_n displacement and normalized displacement.

If rotor displaces as $\lambda_r/2$ rotor and stator poles are fully un-aligned which is an out position as mentioned in section (1.5). In normalized form

$$X_n = \frac{2}{\lambda_r} \times \frac{\lambda_r}{2} = 1$$

On the other hand, $X=0$ means axis of stator and rotor poles are fully aligned then,

$$X_n = \frac{2}{\lambda_r} \times 0 = 0$$

Then 'in' position in normalized form in zero and 'out' position is 1.

The parameter λ_r is very important motor parameter in obtaining of optimum SRM as explained in the next section. Therefore it is very convenient to express pole widths as a fraction of λ_r . In normalized form λ_r is equal to 2.

Then normalized stator and rotor teeth widths are defined as follows,

$$t_{sn} = \frac{t_s}{\lambda_r} \quad t_{rn} = \frac{t_r}{\lambda_r} \quad (2.2)$$

Switch-on, off and conduction period must be also thought as in normalized form. In this work these parameters are used in normalized form, which are denoted as,

X_{ni} - normalized switch-on position

X_{nx} - normalized switch-off position

X_{nc} - normalized conduction period

where $X_{nc} = X_{ni} - X_{nx}$

2.3 UNIT DOUBLY SALIENT STRUCTURE

Unit doubly salient structure (udss) is the scaled model of the original geometry. Udss is very useful tool in computing steady state average torque. The original geometry and udss are shown in fig. 2.2.

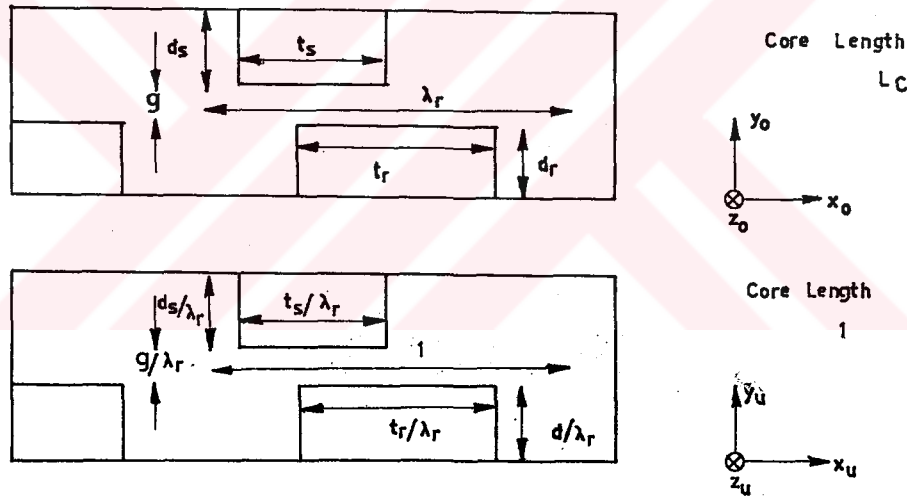


Fig. 2.2. A Doubly Salient Geometry and Unity Doubly Salient Structure

Udss is very convenient tool as far as analysis is concerned, because of the reason that is a general structure with unity rotor pole pitch and core length. All dimensions which are in transverse plane obtained by the factor λ_r and in axial dimensions by $1/L_c$ which are shown below.

$$X_o = \lambda_r X_u$$

$$Y_o = \lambda_r Y_u \quad (2.3)$$

$$Z_o = L_c Z_u$$

where subscripts "o" and "u" refer the original geometry and udss. Udss carries all nature of the actual geometry to the scaled model. One can obtain magnetic quantities and parameters of original geometry in transverse plane by λ_r and in axial dimension, by $1/L_c$ as shown below,

<u>UDSS</u>	<u>ORIGINAL</u>
T_s / λ_r	t_s
g / λ_r	g
1	λ
1	L_c

and for magnetic quantities

$$F_o = \lambda_r F_u$$

$$\phi_o = \lambda_r L_c \phi$$

2.4 TORQUE

2.4.1 FLUX WAVE FORM

Since practical motor conditions are assumed during this work, a constant voltage source is to be considered to be driving the winding instead of constant current source, as in most practical cases. If the supply voltage is V_s to corresponding phase, then the voltage equation is,

$$V_s = R_s I + N_t \frac{d\theta}{dt} \quad (2.5)$$

If the stator resistance is neglected, then

$$V_s = N_t \frac{d\theta}{dt} \quad (2.6)$$

let

$$V_s = V \quad \text{for} \quad X_{ni} \ll X_n \ll X_{nx}$$

and

$$V_s = -V \quad \text{for} \quad X_{ni+1} \ll X_n \ll X_{nx+1}$$

The reason of applying minus voltage is to decay the current in the phase in which is turned off and avoid breaking torques. In other words, voltage can be expressed as,

$$V_s = N_t \frac{d\theta}{dt} = N_t \frac{d\theta}{dx_n} \frac{dx_n}{d\theta} \frac{d\theta}{dt} = \frac{N_t N_r}{\pi} w \frac{d\theta}{dx_n} \quad (2.7)$$

where w is speed of the motor, N_t is the number of turns per phase and X_n normalized displacement.

Let $k = \frac{N_t N_r}{\pi} w$ then, $V_s = k \frac{d\phi}{dx_n}$ (2.7)

$\phi_p = \frac{V_s (X_{nx} - X_{ni})}{k}$ or $\phi_p = \frac{V_s X_{nc}}{k}$

Then for $V_s = V$ and $V_s = -V$ the flux waveform becomes triangular in shape as shown in fig. 2.3.

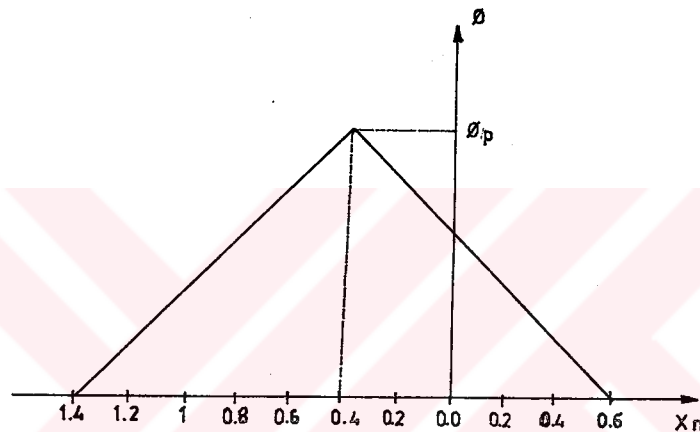


Fig.2.3 A typical triangular flux waveform.

2:4:2 FLUX - MMF CONTOUR

Since constant voltage source is assumed, the locus of flux vs mmf curve depends on the variation of flux with time with motion, the flux contour is generally of the shape shown in fig.2.4. The flux axis may be replaced with flux density B_t if needed.

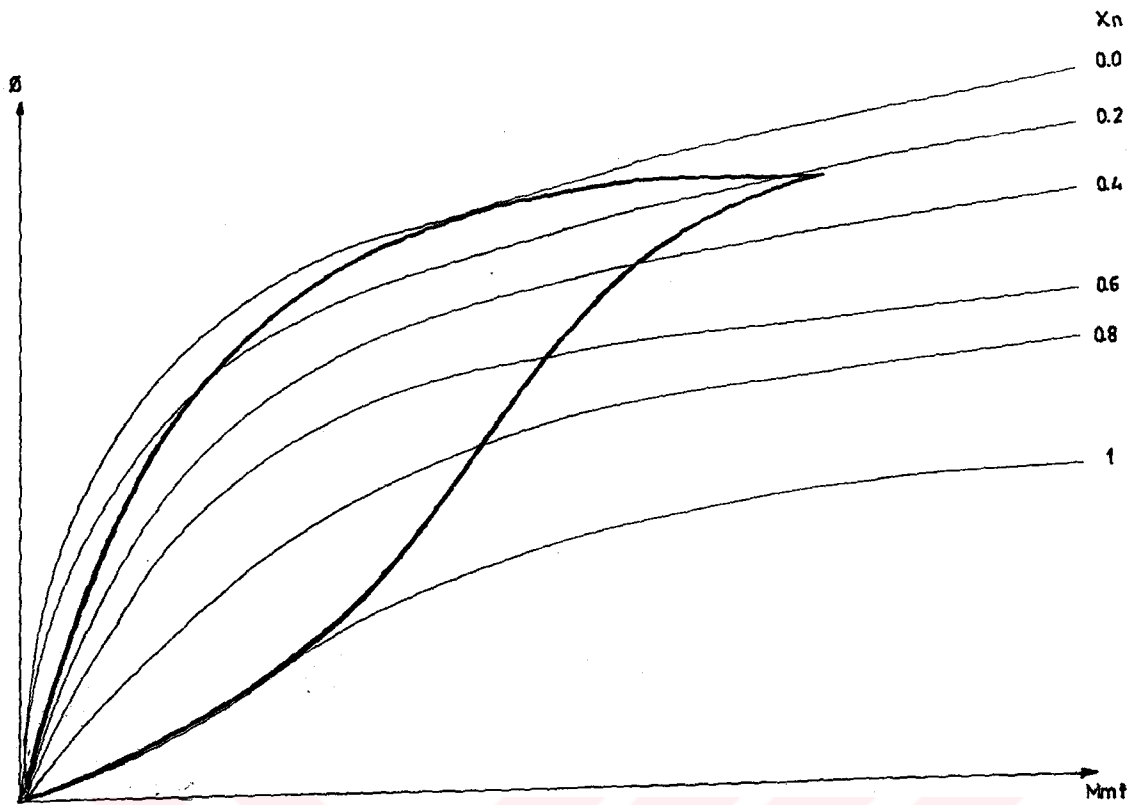


Fig.2.4 A typical ϕ - mmf contour.

The manner in which flux vs mmf contour is obtained here may be illustrated by the help of fig. 2.5. In fig. 2.5-a the flux waveform of an SRM is obtained for $X_{ni} = -1.4$ as shown. To construct flux vs mmf (or B_t vs mmf) contour several positions are chosen, for example -0.8 and -0.2 on the curve. Flux density B_t vs mmf curve of these positions must be available. These may be obtained by using the technique described in section 2.5.1 with the aid of this curve, several points of the flux - mmf contour may be obtained and the complete curve may be constructed. The area of this contour is very important in computing average steady-state torque as will be explained in the next section.

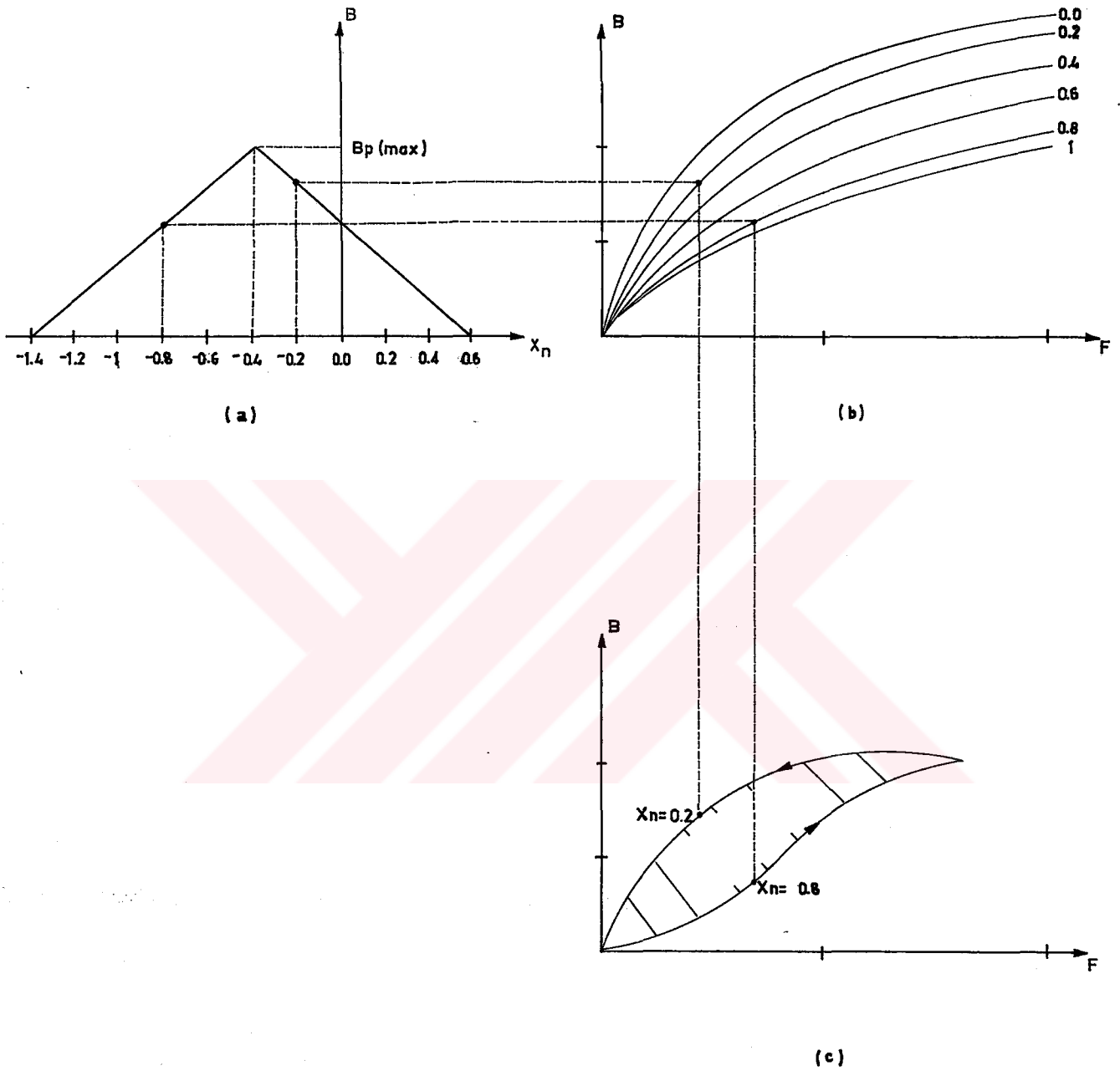


Fig 2.5. Obtaining of flux-density vs mmf contour

2.4.3 TORQUE AND ENERGY FACTOR

In any structure which has N_s as number of stator pole and N_r as number of rotor pole, the torque produced by each stator pole is,

$$T = \frac{\partial w'}{\partial \theta} \quad (2.8)$$

where w' is coenergy and θ is angular position.

In one cycle, the average torque produced by each pole is,

$$T_{av} = \frac{\Delta w'}{\Delta \theta} \quad \text{where} \quad \Delta \theta = \frac{2\pi}{N_r} \quad (2.9)$$

$$T = \frac{\Delta w'}{2\pi} N_r \quad (2.10)$$

If all the stator poles are excited, then the obtained torque is,

$$T_{av} = N_s \frac{N_r}{2\pi} \Delta w' \quad (2.11)$$

As seen from the above equation, average torque can be computed by using coenergy change. Coenergy can be computed by using mmf vs B_t curves for certain switch-on and switch-off positions as explained in previous section.

Since udss is a scaled model of original geometry (SRM), when the size of main structure are taken into account, the coenergy of original SRM can be found, from

equation (2.12) in terms of energy factor.

$$\Delta w' = \lambda_r L_c \Delta w'_u \quad (2.12)$$

Where $\Delta w'_u$ is total change in coenergy of udss and it is called Energy Factor and denoted by E in the rest of this work. Briefly, the average steady-state torque produced by SRM in terms of udss can be expressed as,

$$T_{av} = \frac{N_s N_r}{2\pi} \lambda_r^2 L_c E \quad (2.13)$$

In terms of motor volume, the average torque expression can be rearranged as follows,

$$V_r = \frac{d^2}{4} \pi L_c = \frac{\lambda_r^2 N_r}{4\pi} \quad (2.14)$$

then torque expression becomes,

$$T_{av} = 2 \frac{N_s}{N_r} V_r E \quad (2.15)$$

If only one stator phase is excited then the effective volume is,

$$V_{eff} = 2 \frac{V_r}{N_r} \quad (2.16) \text{ (Since flux passes only}$$

two pole) then,

$$T_{av} = N_s V_{eff} E \quad (2.17)$$

2.4.4 IMPORTANCE OF ENERGY FACTOR

As seen from the previous section, computing average steady-state torque of any SRM, it is necessary that energy factor should be known as well as the other dimensions of the motor as may be seen from equation (2.17). The importance of energy factor may be briefly explained as follows; it is sufficient to know the energy factor of corresponding udss of desired SRM. If energy factor is known, the only thing to do is calculate the average torque of an SRM of any size with the same parameters to it with SRM volume parameter which is described in previous section. Therefore it is possible to calculate the torque for a SRM which have different volume or magnetic geometry by using energy factor of related udss. This method provides simplicity in designing SRM air-gap parameters.

2.5 CALCULATION OF ENERGY FACTOR

For computing energy factor of any udss the followings must be known,

- , Normalized switch-on and switch-off positions
- , Supply voltage or magnetic loading
- , F vs B curves of related udss for different normalized displacement X_n .

Normalized switch-on and switch-off positions and supply voltage depend on the designer choice. In otherwords, they may be parameters for adjusting of

output steady-state torque as in this work. However, F vs B curves depend on the characteristic of the magnetic material. Therefore, they have to be given to the designer.

Available data as an input for this work is permeance data for symmetrically slotted structures. Since this work is interested with asymmetrically slotted structures, it is necessary to know the permeance data for asymmetrically slotted pairs. If this permeance data are obtained, then it is simple to calculate MMF data by using the following equality,

$$F = \frac{\phi}{P} = \frac{B_r t_s}{P} \quad (2.18)$$

A method for obtaining permeance data for asymmetrically slotted structures by using permeance data or symmetrical pairs is presented in the next section.

2.5.1 PERMEANCE CALCULATION OF ASYMMETRICALLY SLOTTED STRUCTURES

Any asymmetrical teeth pair of udss can be represented with two symmetrical pairs by using the method developed by Ertan⁽³⁾. One of these symmetrical pair represents rotor side of the original asymmetrical geometry as shown in fig. 2.6. According to this method a permeance of asymmetric teeth pair can be computed by using the

using the following equalities.

$$P = \frac{2P_a P_b}{P_a + P_b} \quad \text{or in normalized form,}$$

$$P_n = \frac{2P_{na} P_{nb}}{P_{na} + P_{nb}} \quad (2.19)$$

Where P is the permeance of desired asymmetrical pair and P_a, P_b are the permeances of corresponding symmetrical teeth pairs.

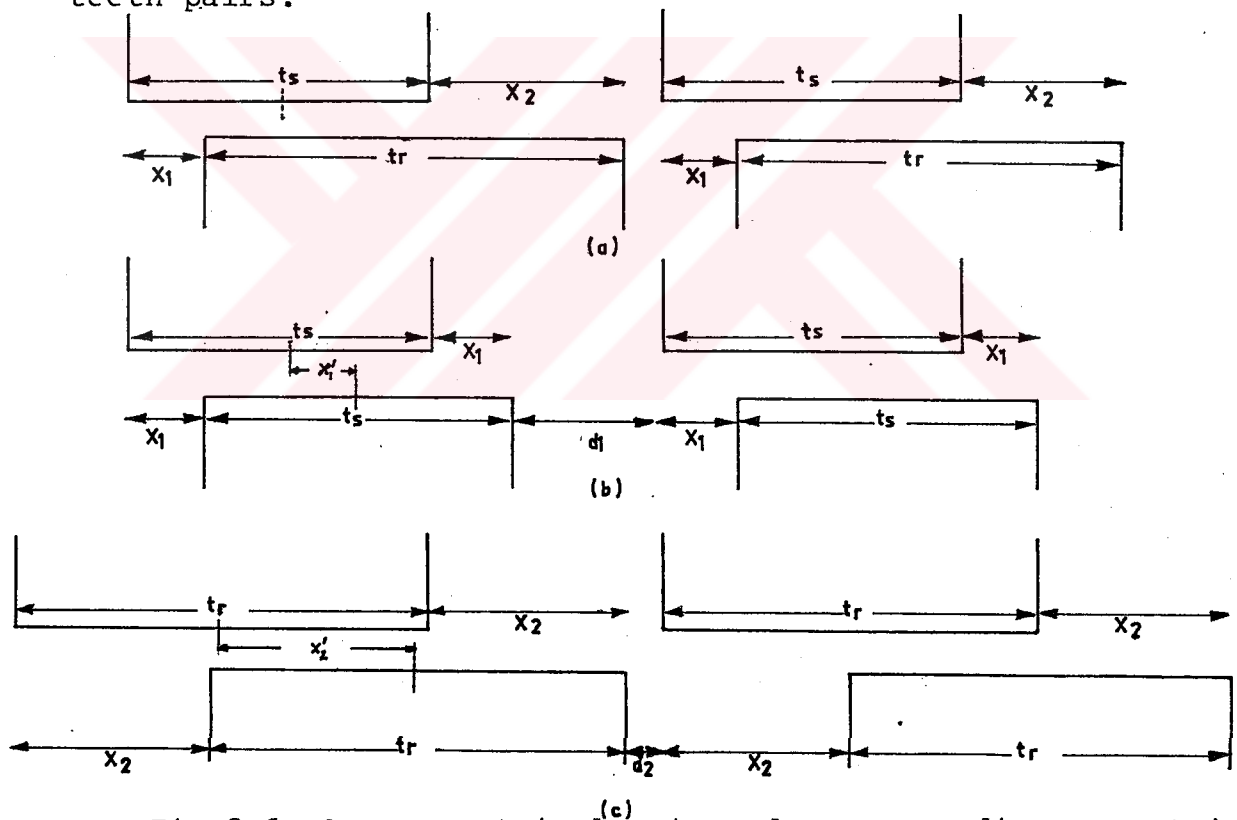


Fig 2.6. An asymmetrical pair and corresponding symmetrical pair,

However, any symmetrical geometry can not represent the original asymmetrical geometry. As mentioned above, corresponding symmetrical pairs should be used.

Therefore, parameters of symmetrical pairs which will represent the original geometry must be identified.

2.5.1.1 TOOTH WIDTH OF SYMMETRICAL PAIR

(Tooth Width): As mentioned above, rotor and stator side of asymmetrical teeth pair can be represented by two separate symmetrical teeth pairs. If rotor and stator tooth width of asymmetrical pair are t_{sn} and t_{rn} , then one of the symmetrical pair has rotor-stator tooth width is t_{sn} and the other has t_{rn} as shown in fig. 2.6.

For X_n (normalized displacement): As mentioned in section 2.2 a normalized displacement X_n can be written as,

$$X_{na} = \frac{2X}{\lambda_r} \quad (2.20)$$

where X is the distance between center lines of stator and rotor teeth. In this cases, X is equal to X'_1 for fig. 2.6-b and X'_2 for fig. 2.6-c. Then,

$$X_{nb} = \frac{X'_1}{\lambda_r/2} \quad \text{and} \quad X_{nc} = \frac{X'_2}{\lambda_r/2}$$

where subscripts b and c define symmetric geometry b and c in fig. 2.6. Then they can also written, as follows;

$$X_{nb} = X_{na} + t_{sn} - t_{rn}$$

$$X_{nc} = X_{na} + t_{rn} - t_{sn} \quad (2.21)$$

where subscript c defines asymmetrical structure.

2.5.1.2 λ/g OF SYMMETRICAL PAIR

The distances d_1 and d_2 which are illustrated in fig. 2.7 must be at least equal to $25g$ for the validity of this method for SRM. This because flux from the excited pole is forced to cross to rotor to the opposite excited poles on the stator. Hence for all practical purposes adjacent stator poles may be regarded as non-existent. As shown by Ertan $25g$ is a sufficient distance to stimulate this position.

What happens when asymmetrical pairs are replaced with symmetrical ones and necessity to adapt the measure described here may be better explained with an example. Consider fig. 2.7. When the stator tooth 2 is replaced with rotor tooth the distance between S_2 and R_1 is reduced to d^1 . If a numerical field solution in which the distance between adjacent pairs is small (i.e. smaller the specified above) because of the flux crossing to the other pair, permeance calculations would result in a value different to the case in which this distance is longer. Hence the calculated value would not be appropriate for SRM torque calculation. Therefore, a constrain which overcome this problem may be written as,

$$\lambda_b = \text{Max} (\lambda_r, t_s + X_1 + 25 g)$$

$$\lambda_c = \text{Max} (\lambda_r, t_r + X_2 + 25 g) \quad (2.22)$$

or it can be written in the following normalized form,

$$\frac{\lambda_b}{g} = \text{Max} \left[\frac{\lambda_r}{g}, \left(t_{sn} + \frac{X_{nb}}{2} \right) \frac{\lambda_r}{g} + 25 \right]$$

(2.23)

$$\frac{\lambda_c}{g} = \text{Max} \left[\frac{\lambda_r}{g}, \left(t_{rn} + \frac{X_{nc}}{2} \right) \frac{\lambda_r}{g} + 25 \right]$$

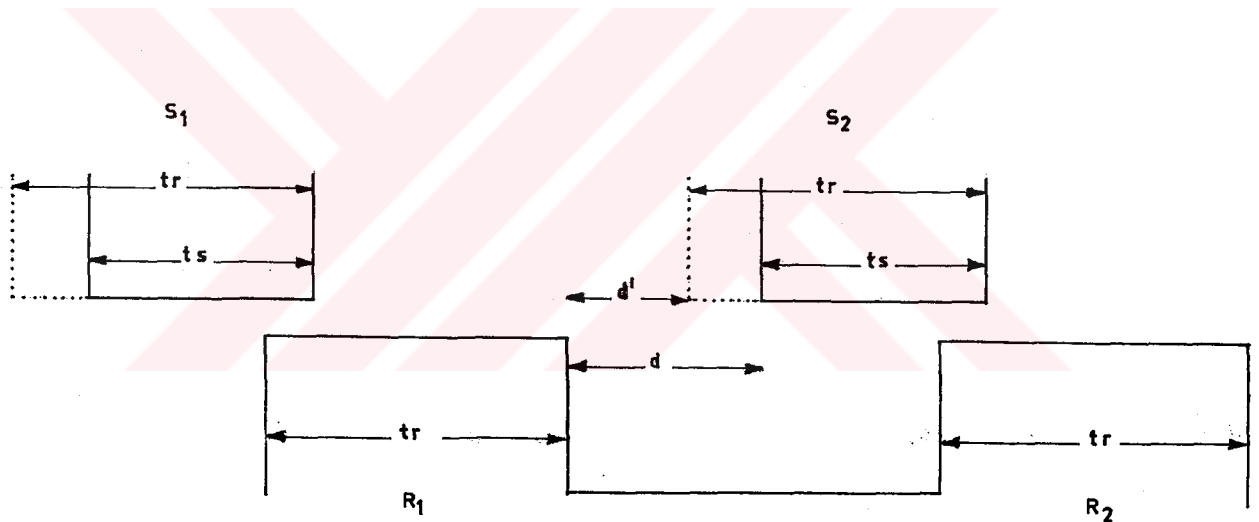


Fig 2.7. Changing in λ_r value in obtaining corresponding symmetrically slotted structure

2.5.1.3 FLUX DENSITY OF SYMMETRICAL PAIRS

If the stator flux density is B_{ts} , then rotor flux density can be written in terms of B_{ts} as,

$$B_{tr} = B_{ts} \frac{t_{sn}}{t_{rn}} \quad \text{since } \phi_s = \phi_r \quad (2.24)$$

where t_{sn} and t_{rn} are teeth width of stator and rotor poles of asymmetrical structure and ϕ_s , ϕ_r are fluxes of asymmetrical structures.

Therefore, if stator flux density is B_t for original asymmetrical pair than symmetrical pair which represents stator side has flux density $B_b = B_t$ and symmetrical pair which represents rotor side has flux density

$$B_c = B_a \frac{t_{sn}}{t_{rn}} .$$

After identifying all the parameters for corresponding symmetric structures, P_a and P_b is searched from the related P vs B_t curves which are input of this work, and obtained permeance values are applied to equation (2.19).

The identification procedure of symmetric structure parameters may be clarified with the aid of an example.

Let the asymmetrical structure has the following air-gap parameters,

$$\frac{\lambda_r}{g} = 40 \quad : \quad t_{sn} = 0.3 \quad : \quad t_{rn} = 0.4 \quad : \quad X_n = 0.2$$

and $B = 0.5$ tesla

For symmetric structure which has stator, tooth width

$$\cdot t_{sn} = t_{rn} = 0.3$$

$$\cdot X_{na} = 0.1 \quad (\text{by using (2.21)})$$

$$\cdot B_s = 0.5 \text{ Tesla}$$

$$\cdot \lambda_a/g = 40 \quad (\text{by using constrain (2.23)})$$

For symmetric structure which represents rotor side of asymmetrical structure,

$$\cdot t_{sn} = t_{rn} = 0.4$$

$$\cdot X_{na} = 0.3 \quad (\text{by using (2.21)})$$

$$\cdot B_s = 0.375$$

$$\cdot \lambda_b/g = 47 \quad (\text{by using (2.23)})$$

2.6 CONCLUSION

In this chapter, a summary of the theory of calculation of steady-state average torque for any SRM by the help of corresponding udss has been presented.

Additionally, the method for obtaining permeance of any asymmetrical structure by using the permeance of corresponding symmetrical structures has been also described.

By the help of the information given here, the computation of energy factor data for asymmetrical udss are given in the next section.



CHAPTER 3

COMPUTATION OF ENERGY FACTOR

3.1 INTRODUCTION

This chapter attempts to calculate energy factor data for a proper range of air-gap parameters of Udss by the help of the method given in the previous chapter.

The procedure for the application of this method is described step by step during this chapter. The obtained energy factor data at the end of this procedure is very useful for observing the effect of air-gap parameters on energy factor variations.

Additionally, since Mmf vs B_t curves obtained here, are used as input data for optimization of air-gap parameters given in next chapter, this part of the work has a vital importance for achieving the purpose of this thesis.

Descriptions for some important programs used in this part of the work are presented in Appendix B.

3.2 PREPARATION OF INPUT DATA

As mentioned in chapter 2, it is possible to obtain permeance data for asymmetrically slotted structures by using the permeance data of symmetrically

slotted structures. By using this approach energy factor of asymmetrically slotted SRM may be computed. The available data for this work is P vs B_t curves of symmetrically slotted structures computed by Ertan. However, these data has a λ/g range between 40 and 70. Practical SRM's assume much higher λ/g ratios. Since this work considers the practical SRM conditions, this data should be expanded to $\lambda/g = 250$ which is practically possible. This may be done by extrapolation the available data with respect to λ/g . The alternative way to expand permeance data is to use numerical field solution techniques however, this is a lengthy task and a research matter in itself and therefore not attempted here.

Fortunately, this data has been already extrapolated by Tohumcu for his Phd work, however it is in B_t vs F form. Therefore it should be converted to F vs B_t form in order to obtain P vs B curves. Furthermore, as discussed in section (3.2.2), it is essential that the data covers the same B_t range. This however was not the case and therefore further manipulation of the data was necessary.

Briefly, the preparation of the P vs B_t data in this work, involves the following sub-steps.

- 1. Obtain F vs B_t curves from available B vs F curves.
- 2. Extrapolate F vs B_t curves with respect to

B so that all curves have same B axis range,

, Obtain P vs B_t curves,

All above sub-steps has been realized by the help of digital computer programs,

3.2.1 OBTAINING F vs B_t CURVES FROM AVAILABLE DATA

Available data is in the form of F vs B_t curves with respect to several values of the parameters λ/g , t_{sn} , X_n . To obtain intermediate values for F vs B_t curves, an interpolation method should be used. First of all Cubic Spline Interpolation method has been tried since it is capable of giving accurate result. The description of this method is given in Appendix A. However, during this application with 8 points on each curve it has been observed that although it gives very accurate results for the curves which have low λ/g values (i.e., less than $\lambda/g = 100$), for high values it gives some errors. As may be seen from the fig. 3.1 while λ/g value increases the curves get sharper. In this fig. the points which represent these curves are also denoted. As seen from this fig., at linear part of the F vs B curves having high λ/g values there are no available point. In other words, shape of such F vs B curves is not defined sufficiently. Therefore, no information is given to the cubic spline method about linear part of such curves. As a result since this part of the curve is not known by the method, it passes a curve which causes errors as shown

by dotted line in fig. 3.1. However curves having low λ/g (i.e. 40-70) value, are smoother and linear part is well defined. Therefore, since the available data which represent the curve are sufficient, cubic spline method gives accurate result for such curves.

Nevertheless the results indicate that whatever the interpolation method is, these curves should be defined properly.

Therefore, in order to overcome this problem number of points in that part of the curves has been increased.

To do this, all B_t vs F curves are drawn by using available data and from these graphs useful points are added to the available data. Therefore number of points to represent each curve is increased from 8 to 13.

However, with this new form of the data, this method is found to cause oscillations in interpolation as shown in the fig. 3.2. %0.5 error is possible which probably comes from reading the values from graphs while inputting them to enter program. Although these reading errors are very small, they destroy linearity of the linear part of the curves. Hence, cubic spline method passes a curve through these additional points which cause oscillations. This oscillation is not considerable in this interval since data density is high because of the additional points. However, after this mmf interval since there are no additional points, the peak value of the

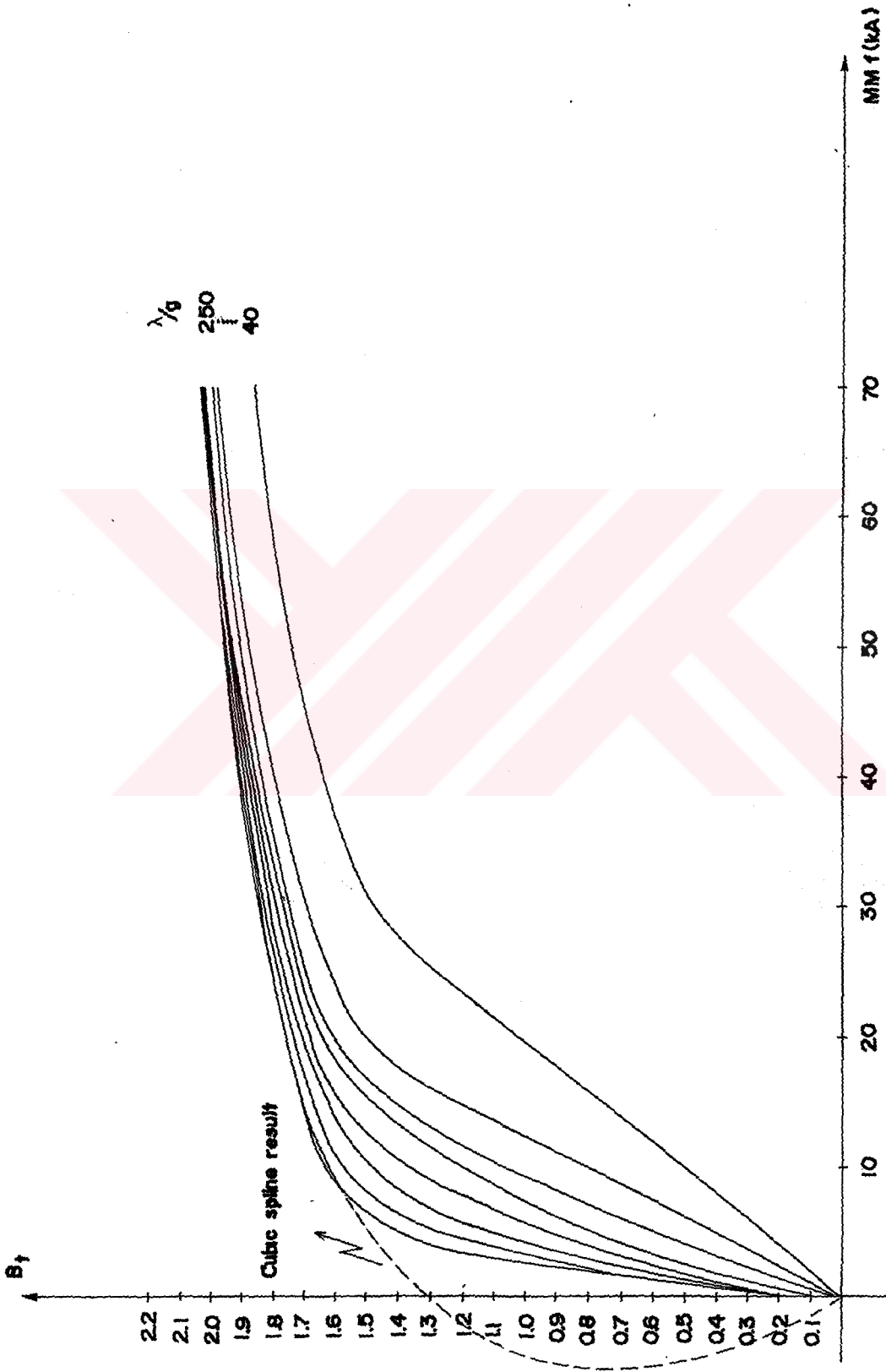


Fig. 3.1.1: Original B_t vs Mef Curves and Curve found by Cubic Spline Interpolation Technique

oscillation increases as shown in fig. 3.2.

Therefore, it is understood that these oscillations may be avoided if the data read from the graphs are very accurate and if more supplementary points are added along the curve for interpolation. However, to read the data from graphs in desired accuracy for the cubic spline is not possible since it is very sensitive even the error percentage is below 0.5% which is very difficult to provide. On the other hand to add supplementary points along the curve is not a practical solution.

Therefore, because of the above reasons it is decided that trying linear interpolation method would be worthwhile.

In order to obtain accurate result, the additional points mentioned in cubic spline work has been used in linear interpolation application. It is observed that in this method, F vs B curves could be interpolated with an error of 1.5% at most when compared with the drawn graphs.

3.2.2 EXTRAPOLATION F vs B_t CURVES

After obtaining F vs B curves as in previous step, it is observed that some of them do not reach up to 2.1 T especially for the curve having high X_n values. However, since it is necessary to obtain all the F vs B

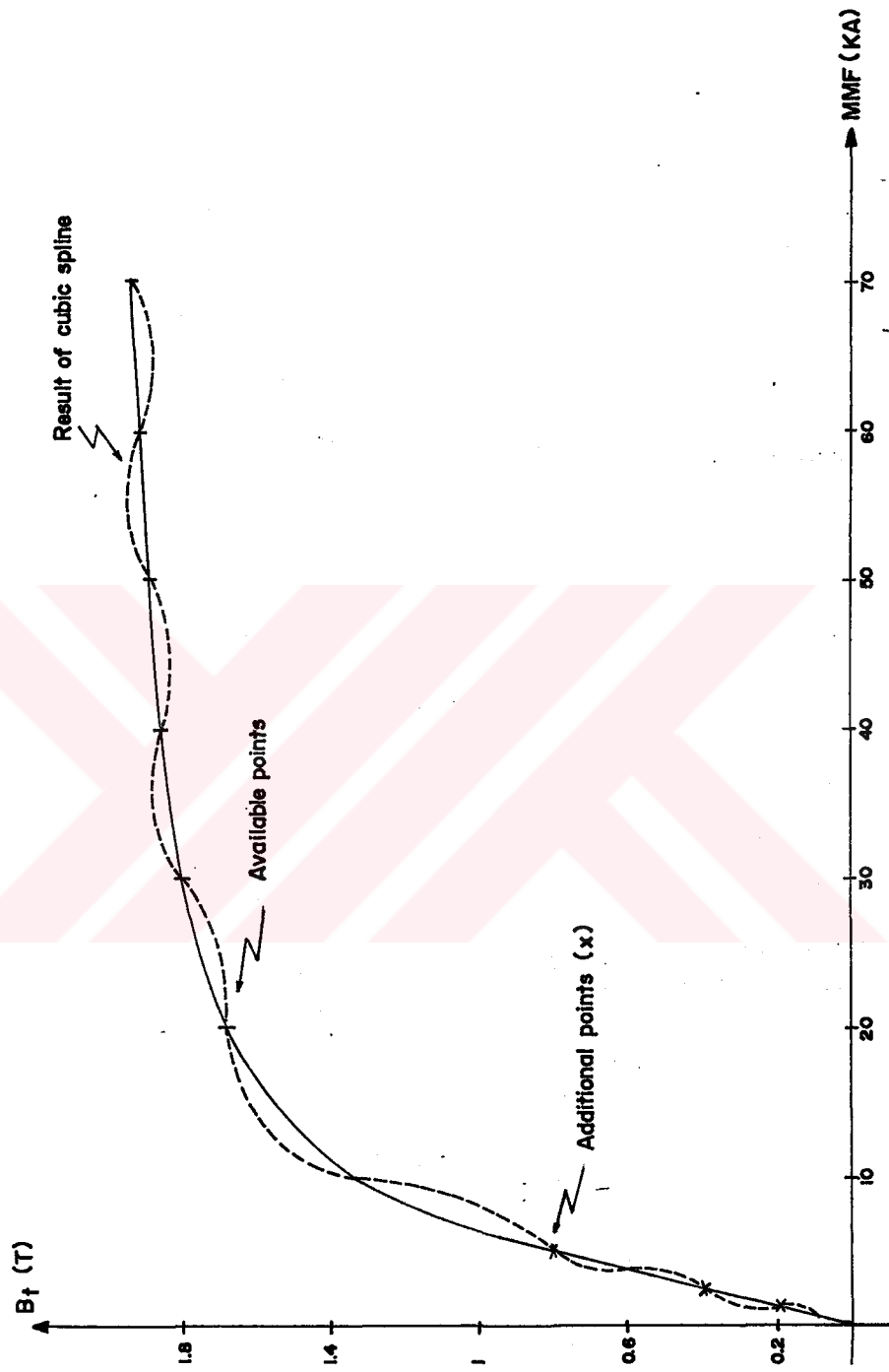


Fig. 3.1.2. Oscillations of B_t vs F Curves Caused by Cubic Spline Interpolation Technique

in the same B range for the further part of this thesis, curves which do not cover sufficient range should be extrapolated with respect to B_t .

To do this, for the curves which do not reach up to $B=2.1T$, a straight line is passed between last two points of such curve, as shown in fig. 3.3.1a. However, this approach is found to cause some F vs B curves which have low λ/g value, cross other curves which have higher λ/g values as shown in fig 3.3.1a by the dotted lines. This however is not possible in practice due to the nature of $B - H$ curve of the material used. In fact these curves are expected to be asymptotical and therefore all curves are made asymptotical with respect to curve having λ/g value 250 as shown in fig. 3.3.1a.

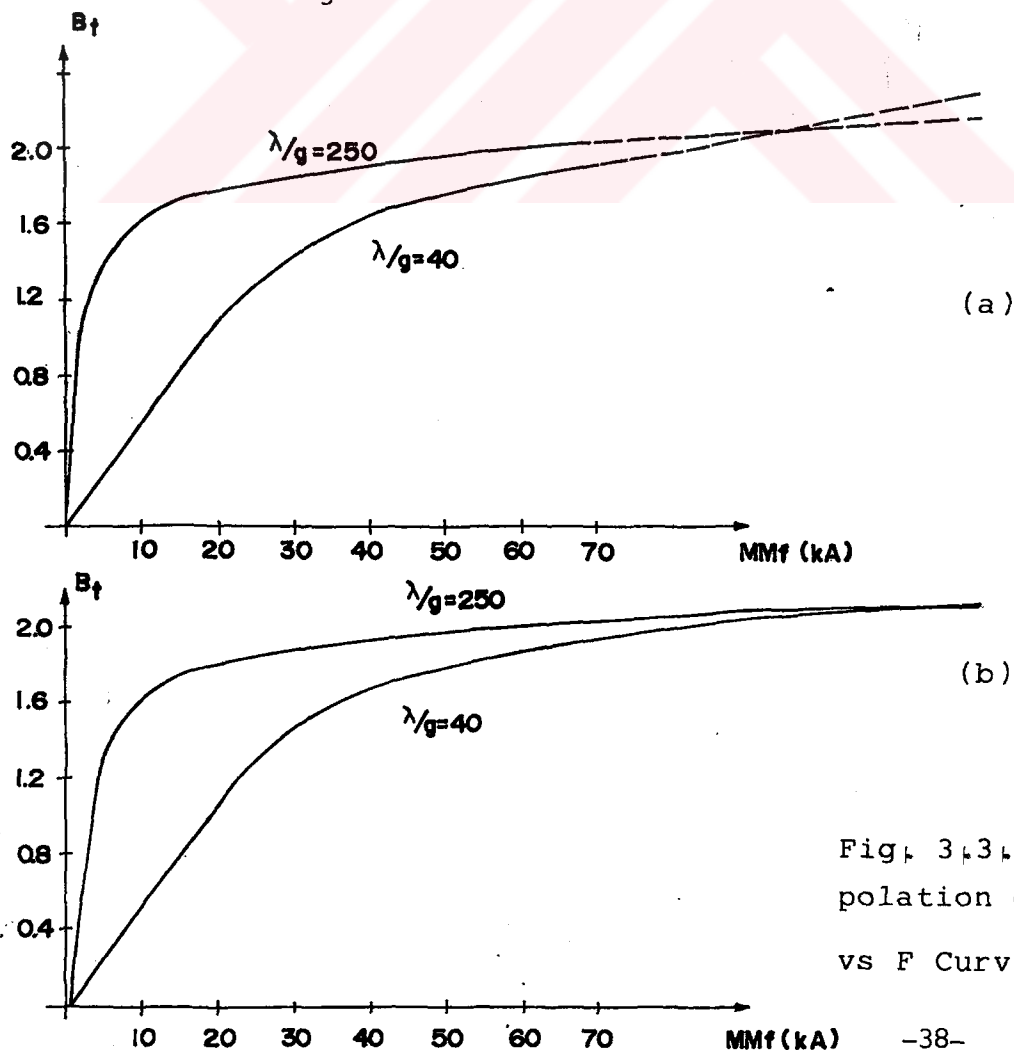


Fig. 3.3. Extrapolation of B_t vs F Curves

3.2.3 COMPUTATION OF PERMEANCE DATA FOR SYMMETRICALLY SLOTTED STRUCTURES

This is the last step for preparation of data for the procedure given in section (3.2).

The permeance of any structure may be obtained by using the following equation

$$P = \frac{B_t * t_{sn}}{F} \quad 3.1$$

Where t_{sn} is normalized tooth width and F is mmf value of entire structure under flux density B_t .

In this step of the work, permeance data of symmetrically slotted structures is obtained by using equation 3.1 and B vs F data. Permeance data covers each combination of the following values of parameters,

λ/g : 40, 70, 100, 130, 160, 190, 220, 250

t/λ : 0.3, 0.4, 0.5

X_n : 0.0, 0.2, 0.4, 0.6, 0.8, 1

B_t : 0.1, 0.2, 0.3, 0.4, 0.5, 0.6, 0.7, 0.8, 0.9, 1.0, 1.1, 1.2, 1.3, 1.4, 1.5, 1.6, 1.7, 1.8, 1.9, 2.0, 2.1

Therefore, at the end of this step the permeance data has been prepared for the main procedure of computation of energy factor given in the next section.

3.3 STEPS OF THE PROCEDURE FOR COMPUTING ENERGY FACTOR DATA

For obtaining energy factor data of asymmetrically slotted Udss, the procedure described below is followed in this work. For this purpose permeance data of symmetrically slotted structure which have been prepared in previous section are used.

- Computation of Permeance data of asymmetrically slotted structure.
- Computation of Mmf vs B data of asymmetrically slotted structure.
- Computation of energy factor of asymmetrically slotted structure.

The detailed description of application of above procedure is given in the next sections.

3.3.1 COMPUTATION OF PERMEANCE DATA OF ASYMMETRICALLY SLOTTED UDSS.

As presented in chapter 2, permeance data of asymmetrically slotted structures may be obtained from the permeance vs B data of symmetrically slotted structures by using the following equation

$$P = \frac{2P_a P_b}{P_a + P_b} \quad 3.2$$

Where P_a and P_b are permeances of corresponding symmetrical pairs. The parameters of these two corresponding symmetrical pairs should be identified as given in chapter 2.

In this section of the work, the method summarized above has been applied with the aid of a computer program and the permeance data has been obtained for asymmetrical pairs by using available P vs B data as discussed above. The description of this program is presented in Appendix B.

Typical normalized Permeance vs Flux density (B_t) curves for structures, having different tooth widths are shown in fig. 3.4. As seen from this figure, after a certain value of B , structure having asymmetrical tooth widths as higher permeance value with respect to symmetrical pairs. The reason for this situation may be as follows. As seen from fig. 3.4 the asymmetrical pair is the combination of these two symmetrical pairs. As remembered in chapter 2, if stator flux density is B_s then rotor flux density B_r is,

$$B_{tr} = B_{ts} \frac{t_{sn}}{t_{rn}} \quad 3.3$$

$\lambda/g = 70$
 $X_n = 0.4$

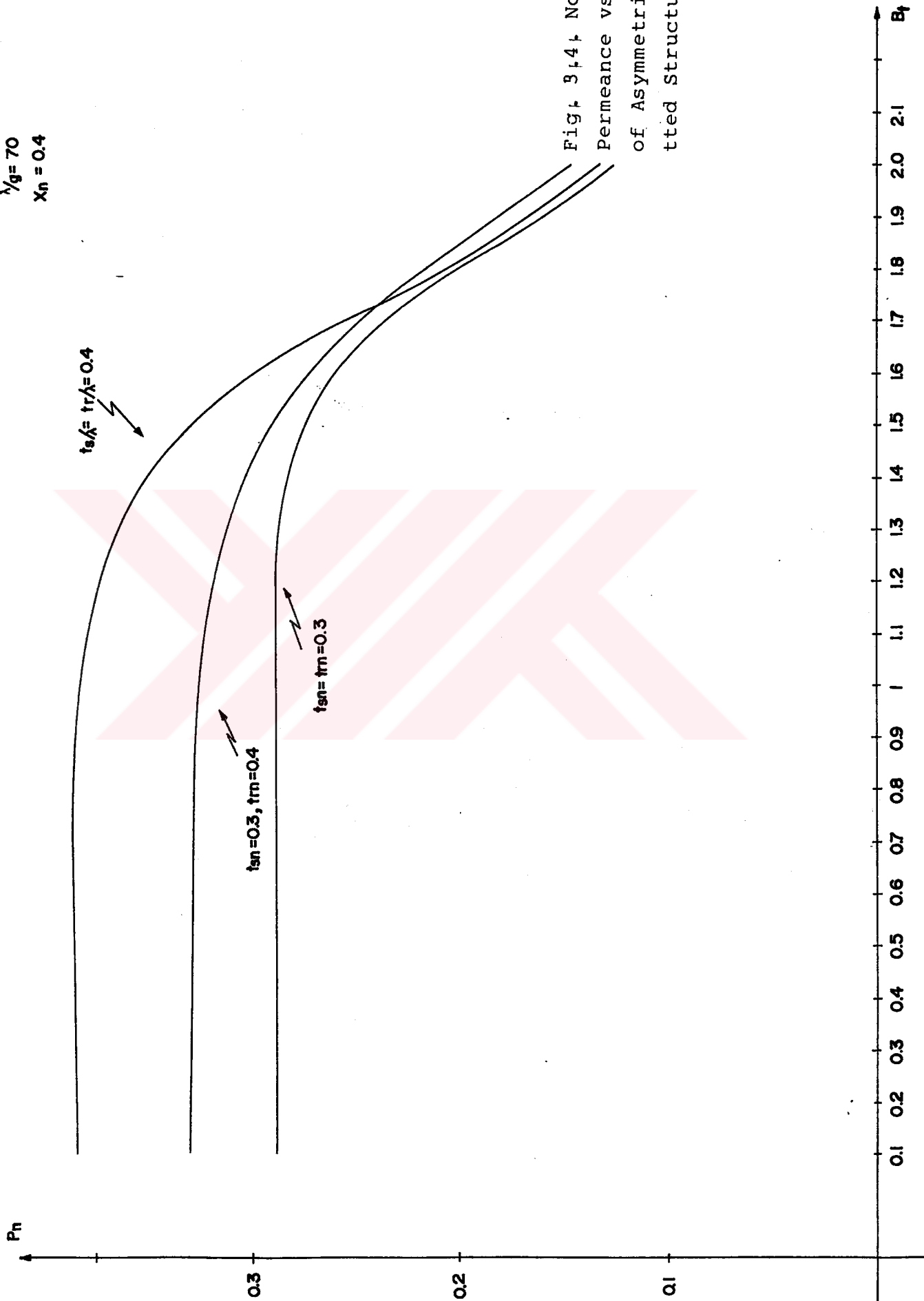


Fig. 3.4. Normalized Permeance vs B_t Curve of Asymmetrically Slopped Structure

Since $t_r/\lambda = t_s/\lambda$ then $B_{tr} < B_{ts}$ for an asymmetrical pair: But for symmetrical pairs $B_{tr} = B_{ts}$. Therefore for a certain value of stator flux density B_{ts} , while stator-rotor parts of symmetrical pairs and stator part of asymmetrical pair saturate, rotor part of asymmetrical pair is not in saturation region at that instant since $B_{tr} < B_{ts}$. Therefore, permeance of asymmetrical pair is higher than symmetrical pair for this particular figure.

The permeance data obtained at the end of this step is for combinations of the following parameter values.

B_t : 0.1, 0.2, 0.3, 0.4, 0.5, 2.1
 λ/g : 40, 70, 100, 130, 250
 t_s/λ : 0.3, 0.4, 0.5
 t_r/λ : 0.3, 0.4, 0.5
 x_n : 0.0, 0.2, 0.4, 0.6, 0.8, 1

3.3.2 COMPUTATION OF PERMEANCE DATA FOR STRUCTURES HAVING UNAVAILABLE PARAMETER VALUES

As summarized in the previous section the parameters of corresponding symmetrical pairs should be identified for computing the permeance of asymmetrical pair. However, if the identified parameter values are unavailable in the data, then an interpolation method should

be used. It is known from the section (3.2) that cubic spline interpolation method is very accurate if the intervals of independent variable of related curve are equal.

The input data for this step of the work provides this property for each parameter. However, in order to be accurate since cubic spline method needs all the points which represent the related curve, it requires enormous computer time consumption when compared with linear interpolation as described below. (In this part of the work cubic spline has been tried but after 18 hour of running of the program no result has been achieved on IBM PC X T).

Because of this, linear interpolation method has been used for computation of permeance data for asymmetrical structures.

If only one parameter is unavailable, the procedure followed for obtaining permeance of that structure is simple, but if more than one parameter are unavailable then this procedure becomes quite complex. In order to illustrate the procedure for such a situation, it may be better to give an example.

Suppose that parameters of symmetrical pair have following values:

$$t_s/\lambda = t_r/\lambda = 0.4: X_n = 0.3: \lambda/g = 47 : B_t = 0.375$$

The parameter values for which permeance data for symmetrical pairs are available have been given in section (3,3,1). Therefore, for the example here parameters B_t , X_n and λ/g have values that are not available in data set. Then the permeance at these values should be interpolated in proper order. This order which depends on the user choice is as follows in this work.

$$B_t, X_n, t/\lambda, \lambda/g$$

Since linear interpolation method is used, the pivotal points of intermediate values should be defined as,

$$0.2 \geq X_{ni} \geq 0.4$$

$$40 \geq (\lambda/g)_i \geq 70$$

$$0.3 \geq B_{ti} \geq 0.4$$

$$i = 1, 2, 3, 4, 5$$

The interpolation procedure for this particular example may be illustrated by the help of table (3,5). In this table, the values in the parenthesis refer the parameter values of entire structures according to the above parameter order. Boxes contain, per-

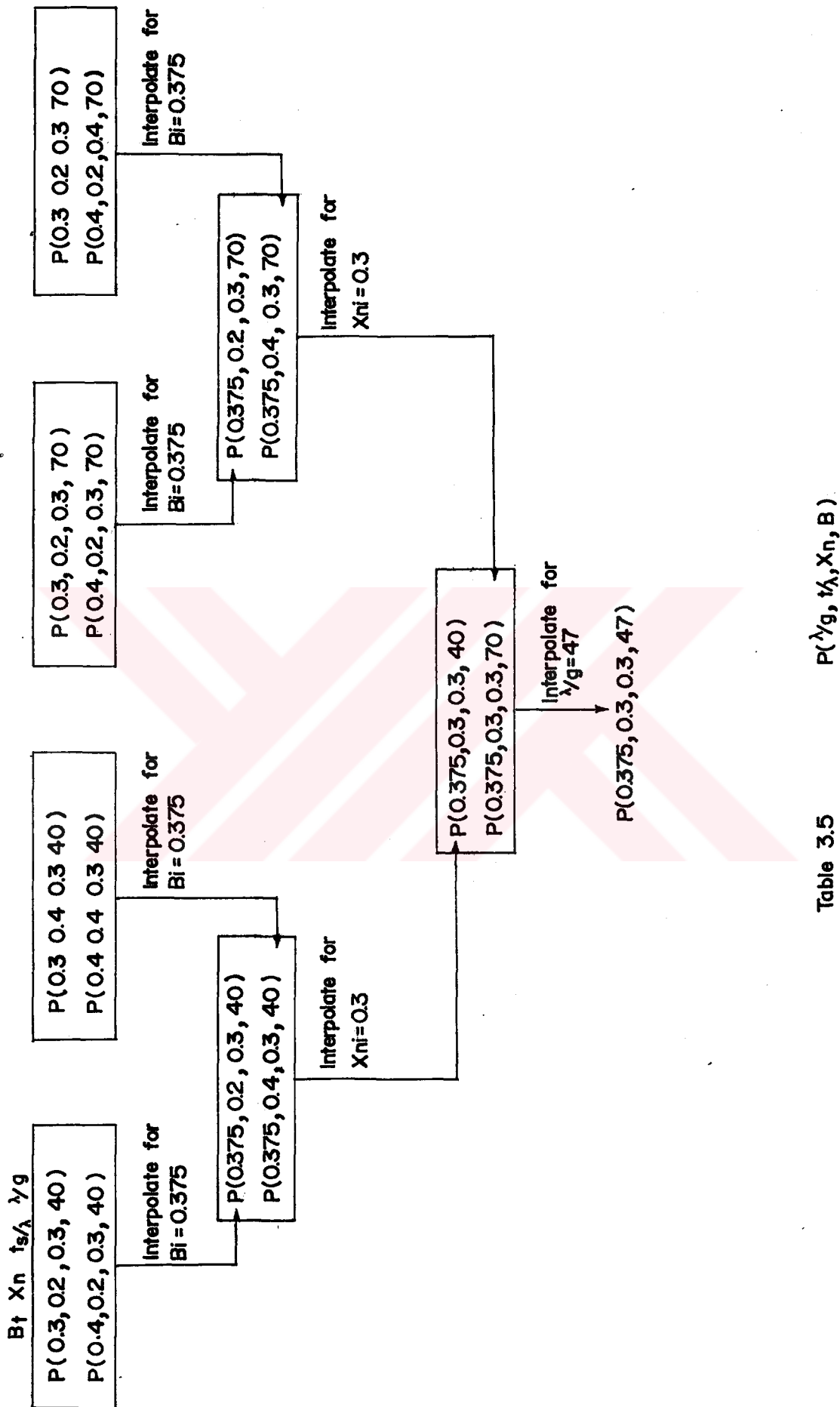


Table 3.5 $P(\lambda/g, t_s/\lambda, X_n, B)$

Fig. 3.5 Interpolation Procedure of Structure Having Unavailable Parameter Values in the Data

means of two separate structures which are denoted by $P(B, X_n, t_s/\lambda, \lambda/g)$. The parameters of these two structures have same values except one parameter which is interpolated.

Arrows show the structure which a permeance value is obtained after the entire interpolation. Levels A, B, C refer interpolations with respect to $B_t, X_n, \lambda/g$.

As seen from this table, number of interpolations required is 7. However if cubic spline is used for the same example, number of interpolation would be 57. This difference occurs since cubic spline method needs all pivotal points of the curve as mentioned above.

The number of interpolation N may be computed by equation given below for the case which contains more than one parameter having unavailable value.

$$N = n_i (n_{i-1} (n_{i-2} \dots (n_3 (n_2 + 1) + 1) \dots + 1) + 1)$$

$$i = 1, 2, 3, \dots, J \quad (J = 4 \text{ for this work})$$

Where (n_i) is the number of points included in interpolation method for curve of i^{th} parameter. J denotes number of parameters.

At the end of interpolation, the permeance value obtained is P_a according to eq. (3.2) notation.

Similar procedure should be followed for P_b . Therefore, the difference in the number of interpolations between two methods increases from the point of view of obtaining permeance of asymmetrically slotted structures. Whenever this comparison is done for computation of whole data of permeance for asymmetrical structures, it is understood that this difference becomes enormous. Therefore, this comparison explains why cubic spline has not been used here, although it is able to give very accurate results for this step of the work.

3.3.3 OBTAINING MMF VS B_T CURVES FOR ASYMMETRICAL STRUCTURES

For computation of energy factor data of Udss, the mmf vs B curves should be known as mentioned in chapter 2.

The mmf of certain Udss may be computed as follows.

$$F = \frac{B_t (t_s / \lambda)}{P} \quad (3.5)$$

Where t_s / λ is tooth width over rotor tooth pitch λ , P is the permeance of that structure corresponding to flux density value B_t . P may be found from P vs B curves of that structure. However if input is normalized permeance P_n then it should be converted

to permeance,

$$P = \mu_o (\lambda/g) P_n \quad (3.6)$$

where λ/g is rotor tooth pitch over air-gap length of that structure,

The above equation has been adopted in to the computer program and it has been used to construct F vs B curves for all the parameters for which permeance curve is calculated. In other words this data is available for the combinations of the following parameter values,

$$B_t : 0.0, 0.1, 0.2, 0.3, \dots, 2.1$$

$$t_s/\lambda : 0.3, 0.4, 0.5$$

$$t_r/\lambda : 0.3, 0.4, 0.5$$

$$x_n : 0.0, 0.2, 0.4, 0.6, 0.8, 1$$

$$\lambda/g : 40, 70, 100, 130, 160, 190, 220, 250$$

3.3.4 COMPUTATION OF ENERGY FACTOR

In chapter 2, the theory and the method is described for obtaining energy factor from mmf vs B curves. In that chapter, it is shown that approximate stator pole flux waveform for a SRM is in triangular

form when it is excited by a constant voltage and with the negligible phase winding resistance,

Since flux of stator having tooth width t_s/λ is,

$$\phi = B_t \times t_s/\lambda \quad (3.7)$$

then flux density waveform has a similar shape. But if flux density waveform is taken into account the obtained B vs mmf contour should be multiplied with t_s/λ for computing energy factor.

The peak value $B_p(\max)$ of this waveform may be called as maximum average flux density. This occurs for unity conduction period(8). Therefore for normalized conduction periods less than unity, waveform does not reach the peak value $B_p(\max)$ as shown in fig. 3.6.

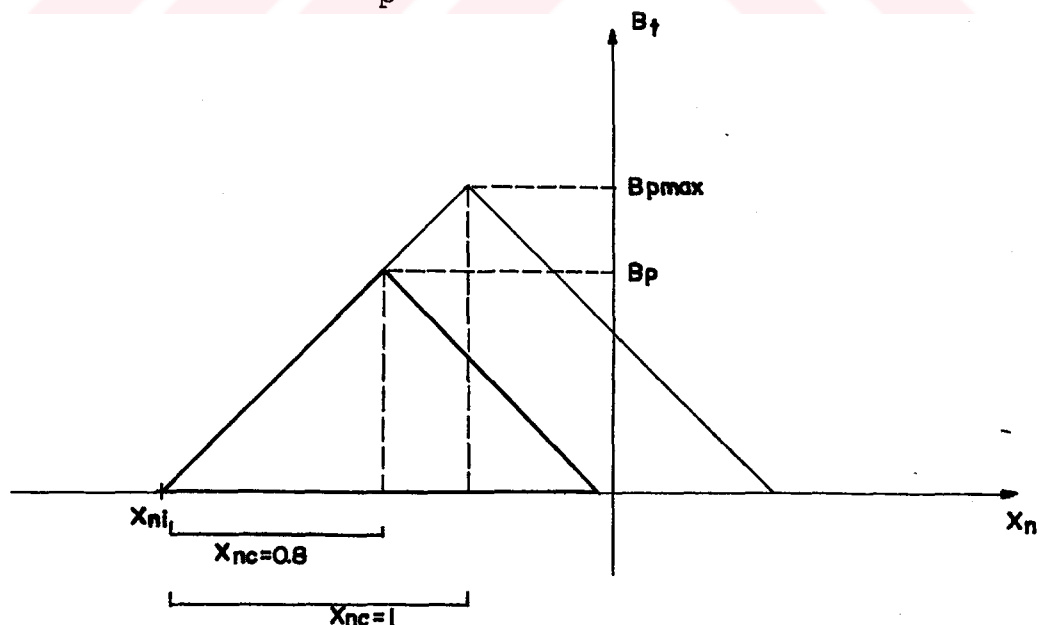


Fig. 3.6 Flux Waveform for Different Conduction Periods

The value of B_p may be limited by the magnetic material used unless bounded by current limit action. Since, practical motor conditions are assumed during this work, current limit action should be taken into consideration. An upper limit of 70 kAT is assumed for mmf value for the current limit action of the drive. Therefore, the peak value of flux density waveform may not reach to $B_{p(max)}$ because of two reasons given below,

- 1) Normalized conduction period may be less than unity
- 2) The mmf value is less than the limit due to current limit action.

The procedure for obtaining energy factor is given in chapter 2. The description and flow-chart of the program used for calculating the energy factor with the restriction mentioned here, is given in Appendix B. The energy factor data has been computed and tabulated in table (3.7) for the combination of the following parameter values,

$$X_{nc} : 0.6, 0.8, 1$$

$$B_{P(max)} : 1.1, 1.3, 1.5, 1.7, 1.9, 2.1$$

$$\lambda/g : 40, 70, 100, 130, 160, 190, 220, 250$$

$$t_s/\lambda : 0.3, 0.4, 0.5$$

ENERGY FACTOR DATA Table(3,7)

Xnc	Bp(max)	L/G	Ts	Tr	XNI: -1.8	-1.6	-1.4	-1.2	-1	-0.8
1.0	1.1	40.0	0.3	0.3	3.41	5.26	4.72	2.64	0.00	-2.64
1.0	1.1	40.0	0.3	0.4	2.53	3.70	3.24	1.84	0.00	-1.84
1.0	1.1	40.0	0.3	0.5	1.82	2.49	2.12	1.21	0.00	-1.21
1.0	1.1	40.0	0.4	0.4	4.33	5.91	4.92	2.81	0.00	-2.81
1.0	1.1	40.0	0.4	0.5	2.34	3.26	2.92	1.73	0.00	-1.73
1.0	1.1	40.0	0.5	0.5	2.86	4.00	3.54	2.06	0.00	-2.06
1.0	1.1	70.0	0.3	0.3	3.71	5.65	5.15	2.89	0.00	-2.89
1.0	1.1	70.0	0.3	0.4	2.86	4.05	3.43	1.90	0.00	-1.90
1.0	1.1	70.0	0.3	0.5	1.94	2.68	2.22	1.22	0.00	-1.22
1.0	1.1	70.0	0.4	0.4	4.59	6.05	5.03	2.83	0.00	-2.83
1.0	1.1	70.0	0.4	0.5	2.52	3.37	2.85	1.61	0.00	-1.61
1.0	1.1	70.0	0.5	0.5	3.17	4.16	3.24	1.82	0.00	-1.82
1.0	1.1	100.0	0.3	0.3	3.98	5.83	5.15	2.83	0.00	-2.83
1.0	1.1	100.0	0.3	0.4	2.90	4.09	3.43	1.88	0.00	-1.88
1.0	1.1	100.0	0.3	0.5	1.92	2.61	2.11	1.14	0.00	-1.14
1.0	1.1	100.0	0.4	0.4	4.75	6.39	5.16	2.81	0.00	-2.81
1.0	1.1	100.0	0.4	0.5	2.66	3.40	2.73	1.49	0.00	-1.49
1.0	1.1	100.0	0.5	0.5	3.32	4.12	2.97	1.49	0.00	-1.49
1.0	1.1	130.0	0.3	0.3	4.13	5.93	5.20	2.80	0.00	-2.80
1.0	1.1	130.0	0.3	0.4	2.93	4.12	3.42	1.86	0.00	-1.86
1.0	1.1	130.0	0.3	0.5	1.92	2.60	2.04	1.10	0.00	-1.10
1.0	1.1	130.0	0.4	0.4	4.68	6.56	5.25	2.77	0.00	-2.77
1.0	1.1	130.0	0.4	0.5	2.68	3.36	2.57	1.37	0.00	-1.37
1.0	1.1	130.0	0.5	0.5	3.34	3.94	2.66	1.28	0.00	-1.28
1.0	1.1	160.0	0.3	0.3	4.24	6.03	5.23	2.75	0.00	-2.75
1.0	1.1	160.0	0.3	0.4	2.96	4.12	3.37	1.82	0.00	-1.82
1.0	1.1	160.0	0.3	0.5	1.94	2.58	1.97	1.07	0.00	-1.07
1.0	1.1	160.0	0.4	0.4	4.59	6.40	5.26	2.74	0.00	-2.74
1.0	1.1	160.0	0.4	0.5	2.63	3.26	2.43	1.26	0.00	-1.26
1.0	1.1	160.0	0.5	0.5	3.31	3.80	2.42	1.11	0.00	-1.11
1.0	1.1	190.0	0.3	0.3	4.29	6.07	5.26	2.73	0.00	-2.73
1.0	1.1	190.0	0.3	0.4	2.96	4.10	3.32	1.78	0.00	-1.78
1.0	1.1	190.0	0.3	0.5	1.93	2.58	1.94	1.06	0.00	-1.06
1.0	1.1	190.0	0.4	0.4	4.45	6.58	5.18	2.70	0.00	-2.70
1.0	1.1	190.0	0.4	0.5	2.61	3.19	2.35	1.18	0.00	-1.18
1.0	1.1	190.0	0.5	0.5	3.37	3.74	2.30	1.04	0.00	-1.04
1.0	1.1	220.0	0.3	0.3	4.32	6.07	5.27	2.72	0.00	-2.72
1.0	1.1	220.0	0.3	0.4	2.94	4.06	3.27	1.75	0.00	-1.75
1.0	1.1	220.0	0.3	0.5	1.92	2.57	1.93	1.05	0.00	-1.05
1.0	1.1	220.0	0.4	0.4	4.32	6.52	5.07	2.63	0.00	-2.63
1.0	1.1	220.0	0.4	0.5	2.58	3.12	2.27	1.12	0.00	-1.12
1.0	1.1	220.0	0.5	0.5	3.37	3.75	2.24	1.00	0.00	-1.00
1.0	1.1	250.0	0.3	0.3	4.34	6.08	5.27	2.71	0.00	-2.71
1.0	1.1	250.0	0.3	0.4	2.94	4.01	3.19	1.70	0.00	-1.70
1.0	1.1	250.0	0.3	0.5	1.90	2.56	1.91	1.03	0.00	-1.03
1.0	1.1	250.0	0.4	0.4	4.23	6.44	4.92	2.54	0.00	-2.54
1.0	1.1	250.0	0.4	0.5	2.52	3.03	2.17	1.07	0.00	-1.07
1.0	1.1	250.0	0.5	0.5	3.39	3.72	2.17	0.98	0.00	-0.98
1.0	1.3	40.0	0.3	0.3	4.67	7.37	6.61	3.68	0.00	-3.68

ENERGY FACTOR DATA (cont.)

Xnc	Bp(max)	L/G	Ts	Tr	XNI:	-1.8	-1.6	-1.4	-1.2	-1	-.8
1.0	1.3	40.0	0.3	0.4		3.54	5.17	4.53	2.58	0.00	-2.58
1.0	1.3	40.0	0.3	0.5		2.56	3.48	2.96	1.70	0.00	-1.70
1.0	1.3	40.0	0.4	0.4		6.04	8.14	7.02	3.96	0.00	-3.96
1.0	1.3	40.0	0.4	0.5		3.27	4.60	4.12	2.43	0.00	-2.43
1.0	1.3	40.0	0.5	0.5		4.05	5.96	4.98	2.94	0.00	-2.94
1.0	1.3	70.0	0.3	0.3		5.12	7.80	7.32	4.13	0.00	-4.13
1.0	1.3	70.0	0.3	0.4		3.96	5.69	4.87	2.70	0.00	-2.70
1.0	1.3	70.0	0.3	0.5		2.69	3.82	3.17	1.71	0.00	-1.71
1.0	1.3	70.0	0.4	0.4		6.01	8.61	7.44	3.97	0.00	-3.97
1.0	1.3	70.0	0.4	0.5		3.58	5.00	4.13	2.30	0.00	-2.30
1.0	1.3	70.0	0.5	0.5		4.67	6.49	4.87	2.60	0.00	-2.60
1.0	1.3	100.0	0.3	0.3		5.43	8.01	7.31	4.06	0.00	-4.06
1.0	1.3	100.0	0.3	0.4		4.01	5.75	4.87	2.67	0.00	-2.67
1.0	1.3	100.0	0.3	0.5		2.63	3.74	3.03	1.62	0.00	-1.62
1.0	1.3	100.0	0.4	0.4		6.32	9.00	7.68	4.05	0.00	-4.05
1.0	1.3	100.0	0.4	0.5		3.77	5.11	4.02	2.15	0.00	-2.15
1.0	1.3	100.0	0.5	0.5		4.92	6.54	4.50	2.31	0.00	-2.31
1.0	1.3	130.0	0.3	0.3		5.65	8.12	7.32	4.04	0.00	-4.04
1.0	1.3	130.0	0.3	0.4		4.03	5.77	4.87	2.64	0.00	-2.64
1.0	1.3	130.0	0.3	0.5		2.61	3.69	2.94	1.55	0.00	-1.55
1.0	1.3	130.0	0.4	0.4		6.33	9.20	7.79	3.97	0.00	-3.97
1.0	1.3	130.0	0.4	0.5		3.86	5.06	3.77	1.98	0.00	-1.98
1.0	1.3	130.0	0.5	0.5		5.02	6.43	4.17	1.97	0.00	-1.97
1.0	1.3	160.0	0.3	0.3		5.85	8.26	7.31	3.94	0.00	-3.94
1.0	1.3	160.0	0.3	0.4		4.07	5.76	4.79	2.59	0.00	-2.59
1.0	1.3	160.0	0.3	0.5		2.63	3.64	2.83	1.51	0.00	-1.51
1.0	1.3	160.0	0.4	0.4		6.33	9.28	7.84	3.86	0.00	-3.86
1.0	1.3	160.0	0.4	0.5		3.88	4.95	3.53	1.81	0.00	-1.81
1.0	1.3	160.0	0.5	0.5		5.05	6.42	3.95	1.64	0.00	-1.64
1.0	1.3	190.0	0.3	0.3		5.93	8.31	7.34	3.87	0.00	-3.87
1.0	1.3	190.0	0.3	0.4		4.07	5.73	4.71	2.54	0.00	-2.54
1.0	1.3	190.0	0.3	0.5		2.63	3.63	2.77	1.50	0.00	-1.50
1.0	1.3	190.0	0.4	0.4		6.29	9.23	7.76	3.82	0.00	-3.82
1.0	1.3	190.0	0.4	0.5		3.89	4.87	3.41	1.70	0.00	-1.70
1.0	1.3	190.0	0.5	0.5		5.15	6.51	3.85	1.55	0.00	-1.55
1.0	1.3	220.0	0.3	0.3		5.99	8.35	7.34	3.80	0.00	-3.80
1.0	1.3	220.0	0.3	0.4		4.06	5.68	4.61	2.49	0.00	-2.49
1.0	1.3	220.0	0.3	0.5		2.63	3.62	2.71	1.49	0.00	-1.49
1.0	1.3	220.0	0.4	0.4		6.16	9.16	7.71	3.71	0.00	-3.71
1.0	1.3	220.0	0.4	0.5		3.89	4.84	3.29	1.61	0.00	-1.61
1.0	1.3	220.0	0.5	0.5		5.24	6.62	3.76	1.48	0.00	-1.48
1.0	1.3	250.0	0.3	0.3		6.03	8.32	7.35	3.78	0.00	-3.78
1.0	1.3	250.0	0.3	0.4		4.02	5.62	4.52	2.40	0.00	-2.40
1.0	1.3	250.0	0.3	0.5		2.60	3.61	2.68	1.49	0.00	-1.49
1.0	1.3	250.0	0.4	0.4		5.95	9.03	7.60	3.64	0.00	-3.64
1.0	1.3	250.0	0.4	0.5		3.83	4.76	3.20	1.52	0.00	-1.52
1.0	1.3	250.0	0.5	0.5		5.32	6.68	3.67	1.46	0.00	-1.46
1.0	1.5	40.0	0.3	0.3		5.61	9.88	8.83	4.93	0.00	-4.93

ENERGY FACTOR DATA (cont.)

Xnc	Bp(max)	L/G	Ts	Tr	XNI:	-1.8	-1.6	-1.4	-1.2	-1	-0.8
1.0	1.5	40.0	0.3	0.4		4.71	6.91	6.03	3.46	0.00	-3.46
1.0	1.5	40.0	0.3	0.5		3.43	4.65	3.96	2.29	0.00	-2.29
1.0	1.5	40.0	0.4	0.4		7.11	10.86	9.63	5.32	0.00	-5.32
1.0	1.5	40.0	0.4	0.5		4.33	6.30	5.59	3.28	0.00	-3.28
1.0	1.5	40.0	0.5	0.5		5.42	8.63	7.02	3.94	0.00	-3.94
1.0	1.5	70.0	0.3	0.3		6.22	10.24	9.85	5.71	0.00	-5.71
1.0	1.5	70.0	0.3	0.4		5.17	7.58	6.63	3.67	0.00	-3.67
1.0	1.5	70.0	0.3	0.5		3.53	5.20	4.37	2.32	0.00	-2.32
1.0	1.5	70.0	0.4	0.4		7.39	11.75	10.42	5.40	0.00	-5.40
1.0	1.5	70.0	0.4	0.5		4.94	7.06	5.72	3.11	0.00	-3.11
1.0	1.5	70.0	0.5	0.5		6.48	9.57	7.35	3.63	0.00	-3.63
1.0	1.5	100.0	0.3	0.3		6.57	10.42	9.90	5.63	0.00	-5.63
1.0	1.5	100.0	0.3	0.4		5.23	7.69	6.63	3.65	0.00	-3.65
1.0	1.5	100.0	0.3	0.5		3.41	5.13	4.21	2.22	0.00	-2.22
1.0	1.5	100.0	0.4	0.4		8.02	12.12	10.80	5.61	0.00	-5.61
1.0	1.5	100.0	0.4	0.5		5.16	7.26	5.66	3.00	0.00	-3.00
1.0	1.5	100.0	0.5	0.5		7.01	9.77	7.06	3.40	0.00	-3.40
1.0	1.5	130.0	0.3	0.3		6.77	10.63	10.03	5.56	0.00	-5.56
1.0	1.5	130.0	0.3	0.4		5.25	7.77	6.64	3.57	0.00	-3.57
1.0	1.5	130.0	0.3	0.5		3.39	5.11	4.07	2.10	0.00	-2.10
1.0	1.5	130.0	0.4	0.4		8.26	12.33	11.10	5.64	0.00	-5.64
1.0	1.5	130.0	0.4	0.5		5.35	7.27	5.43	2.80	0.00	-2.80
1.0	1.5	130.0	0.5	0.5		7.54	9.70	6.44	3.05	0.00	-3.05
1.0	1.5	160.0	0.3	0.3		7.02	10.75	10.06	5.54	0.00	-5.54
1.0	1.5	160.0	0.3	0.4		5.25	7.77	6.61	3.51	0.00	-3.51
1.0	1.5	160.0	0.3	0.5		3.38	5.04	3.97	2.01	0.00	-2.01
1.0	1.5	160.0	0.4	0.4		8.31	12.52	11.34	5.54	0.00	-5.54
1.0	1.5	160.0	0.4	0.5		5.49	7.30	5.15	2.58	0.00	-2.58
1.0	1.5	160.0	0.5	0.5		7.62	9.92	6.44	2.60	0.00	-2.60
1.0	1.5	190.0	0.3	0.3		7.10	10.81	10.11	5.49	0.00	-5.49
1.0	1.5	190.0	0.3	0.4		5.24	7.73	6.53	3.44	0.00	-3.44
1.0	1.5	190.0	0.3	0.5		3.39	5.02	3.91	1.98	0.00	-1.98
1.0	1.5	190.0	0.4	0.4		8.19	12.46	11.44	5.36	0.00	-5.36
1.0	1.5	190.0	0.4	0.5		5.58	7.31	4.93	2.43	0.00	-2.43
1.0	1.5	190.0	0.5	0.5		7.69	10.34	6.33	2.23	0.00	-2.23
1.0	1.5	220.0	0.3	0.3		7.17	10.81	10.12	5.43	0.00	-5.43
1.0	1.5	220.0	0.3	0.4		5.21	7.66	6.42	3.38	0.00	-3.38
1.0	1.5	220.0	0.3	0.5		3.37	5.01	3.85	1.97	0.00	-1.97
1.0	1.5	220.0	0.4	0.4		7.78	12.28	11.43	5.15	0.00	-5.15
1.0	1.5	220.0	0.4	0.5		5.54	7.30	4.74	2.30	0.00	-2.30
1.0	1.5	220.0	0.5	0.5		7.79	10.47	6.33	2.20	0.00	-2.20
1.0	1.5	250.0	0.3	0.3		7.22	10.78	10.11	5.36	0.00	-5.36
1.0	1.5	250.0	0.3	0.4		5.19	7.57	6.29	3.29	0.00	-3.29
1.0	1.5	250.0	0.3	0.5		3.34	4.97	3.79	1.96	0.00	-1.96
1.0	1.5	250.0	0.4	0.4		7.46	12.04	11.34	4.96	0.00	-4.96
1.0	1.5	250.0	0.4	0.5		5.48	7.16	4.57	2.13	0.00	-2.13
1.0	1.5	250.0	0.5	0.5		7.90	10.62	6.23	2.05	0.00	-2.05
1.0	1.7	40.0	0.3	0.3		6.35	11.49	11.56	6.44	0.00	-6.44

ENERGY FACTOR DATA (cont.)

Xnc	Bp(max)	L/G	Ts	Tr	XNI:	-1.8	-1.6	-1.4	-1.2	-1	-0.8
1.0	1.7	40.0	0.3	0.4		5.77	8.91	7.85	4.48	0.00	-4.48
1.0	1.7	40.0	0.3	0.5		4.35	6.10	5.16	2.92	0.00	-2.92
1.0	1.7	40.0	0.4	0.4		6.91	13.58	13.21	7.04	0.00	-7.04
1.0	1.7	40.0	0.4	0.5		5.39	8.50	7.52	4.29	0.00	-4.29
1.0	1.7	40.0	0.5	0.5		6.53	11.46	10.07	5.31	0.00	-5.31
1.0	1.7	70.0	0.3	0.3		6.90	12.57	12.82	7.69	0.00	-7.69
1.0	1.7	70.0	0.3	0.4		6.37	9.76	8.83	4.87	0.00	-4.87
1.0	1.7	70.0	0.3	0.5		4.48	6.84	5.89	3.07	0.00	-3.07
1.0	1.7	70.0	0.4	0.4		7.49	14.79	14.55	7.76	0.00	-7.76
1.0	1.7	70.0	0.4	0.5		6.42	9.68	8.12	4.26	0.00	-4.26
1.0	1.7	70.0	0.5	0.5		8.04	12.95	11.28	5.35	0.00	-5.35
1.0	1.7	100.0	0.3	0.3		7.14	12.89	12.95	7.63	0.00	-7.63
1.0	1.7	100.0	0.3	0.4		6.45	9.91	8.88	4.84	0.00	-4.84
1.0	1.7	100.0	0.3	0.5		4.31	6.78	5.72	2.92	0.00	-2.92
1.0	1.7	100.0	0.4	0.4		8.19	15.38	15.08	8.07	0.00	-8.07
1.0	1.7	100.0	0.4	0.5		6.82	10.02	8.05	4.15	0.00	-4.15
1.0	1.7	100.0	0.5	0.5		8.40	13.32	11.26	5.14	0.00	-5.14
1.0	1.7	130.0	0.3	0.3		7.34	13.10	12.99	7.62	0.00	-7.62
1.0	1.7	130.0	0.3	0.4		6.45	9.97	8.90	4.81	0.00	-4.81
1.0	1.7	130.0	0.3	0.5		4.22	6.71	5.60	2.83	0.00	-2.83
1.0	1.7	130.0	0.4	0.4		8.60	15.59	15.39	8.19	0.00	-8.19
1.0	1.7	130.0	0.4	0.5		7.08	10.09	7.83	3.94	0.00	-3.94
1.0	1.7	130.0	0.5	0.5		8.83	13.51	10.65	4.62	0.00	-4.62
1.0	1.7	160.0	0.3	0.3		7.55	13.23	13.18	7.64	0.00	-7.64
1.0	1.7	160.0	0.3	0.4		6.42	10.08	8.93	4.65	0.00	-4.65
1.0	1.7	160.0	0.3	0.5		4.15	6.71	5.51	2.65	0.00	-2.65
1.0	1.7	160.0	0.4	0.4		8.82	15.95	15.68	8.15	0.00	-8.15
1.0	1.7	160.0	0.4	0.5		7.28	10.23	7.60	3.65	0.00	-3.65
1.0	1.7	160.0	0.5	0.5		9.32	13.79	10.39	4.36	0.00	-4.36
1.0	1.7	190.0	0.3	0.3		7.58	13.31	13.28	7.71	0.00	-7.71
1.0	1.7	190.0	0.3	0.4		6.41	10.08	8.89	4.56	0.00	-4.56
1.0	1.7	190.0	0.3	0.5		4.15	6.71	5.50	2.59	0.00	-2.59
1.0	1.7	190.0	0.4	0.4		8.86	16.15	16.00	7.95	0.00	-7.95
1.0	1.7	190.0	0.4	0.5		7.46	10.43	7.42	3.44	0.00	-3.44
1.0	1.7	190.0	0.5	0.5		9.58	14.40	10.95	3.93	0.00	-3.93
1.0	1.7	220.0	0.3	0.3		7.60	13.29	13.38	7.76	0.00	-7.76
1.0	1.7	220.0	0.3	0.4		6.32	10.05	8.87	4.44	0.00	-4.44
1.0	1.7	220.0	0.3	0.5		4.11	6.73	5.50	2.53	0.00	-2.53
1.0	1.7	220.0	0.4	0.4		8.89	16.18	16.09	7.75	0.00	-7.75
1.0	1.7	220.0	0.4	0.5		7.68	10.53	7.23	3.25	0.00	-3.25
1.0	1.7	220.0	0.5	0.5		9.70	14.88	11.08	3.53	0.00	-3.53
1.0	1.7	250.0	0.3	0.3		7.57	13.27	13.40	7.79	0.00	-7.79
1.0	1.7	250.0	0.3	0.4		6.23	9.95	8.79	4.37	0.00	-4.37
1.0	1.7	250.0	0.3	0.5		4.09	6.71	5.48	2.52	0.00	-2.52
1.0	1.7	250.0	0.4	0.4		8.79	15.89	16.13	7.65	0.00	-7.65
1.0	1.7	250.0	0.4	0.5		7.74	10.51	7.10	3.11	0.00	-3.11
1.0	1.7	250.0	0.5	0.5		9.79	15.12	11.20	3.37	0.00	-3.37
1.0	1.9	40.0	0.3	0.3		6.98	12.38	13.88	8.30	0.00	-8.30

ENERGY FACTOR DATA (cont.)

Xnc	Bp(max)	L/G	Ts	Tr	XNI:	-1.8	-1.6	-1.4	-1.2	-1	-0.8
1.0	1.9	40.0	0.3	0.4		6.35	10.71	9.99	5.71	0.00	-5.71
1.0	1.9	40.0	0.3	0.5		5.33	7.69	6.64	3.68	0.00	-3.68
1.0	1.9	40.0	0.4	0.4		7.13	14.78	15.96	9.26	0.00	-9.26
1.0	1.9	40.0	0.4	0.5		6.09	10.58	9.85	5.63	0.00	-5.63
1.0	1.9	40.0	0.5	0.5		7.22	12.97	13.50	7.38	0.00	-7.38
1.0	1.9	70.0	0.3	0.3		7.23	13.66	15.70	10.25	0.00	-10.25
1.0	1.9	70.0	0.3	0.4		6.94	12.05	11.49	6.32	0.00	-6.32
1.0	1.9	70.0	0.3	0.5		5.37	8.81	7.82	3.99	0.00	-3.99
1.0	1.9	70.0	0.4	0.4		7.49	16.50	18.76	10.83	0.00	-10.83
1.0	1.9	70.0	0.4	0.5		7.41	12.59	11.20	5.70	0.00	-5.70
1.0	1.9	70.0	0.5	0.5		8.35	15.58	16.41	8.05	0.00	-8.05
1.0	1.9	100.0	0.3	0.3		7.25	14.02	16.06	10.38	0.00	-10.38
1.0	1.9	100.0	0.3	0.4		7.04	12.26	11.71	6.39	0.00	-6.39
1.0	1.9	100.0	0.3	0.5		5.16	8.83	7.82	3.87	0.00	-3.87
1.0	1.9	100.0	0.4	0.4		8.00	17.24	19.49	11.59	0.00	-11.59
1.0	1.9	100.0	0.4	0.5		7.80	13.12	11.41	5.78	0.00	-5.78
1.0	1.9	100.0	0.5	0.5		8.57	16.06	16.86	8.05	0.00	-8.05
1.0	1.9	130.0	0.3	0.3		7.42	14.34	16.29	10.51	0.00	-10.51
1.0	1.9	130.0	0.3	0.4		7.10	12.45	11.85	6.34	0.00	-6.34
1.0	1.9	130.0	0.3	0.5		5.09	8.82	7.74	3.70	0.00	-3.70
1.0	1.9	130.0	0.4	0.4		8.43	17.54	19.90	12.03	0.00	-12.03
1.0	1.9	130.0	0.4	0.5		8.19	13.37	11.24	5.54	0.00	-5.54
1.0	1.9	130.0	0.5	0.5		8.60	16.50	16.67	7.33	0.00	-7.33
1.0	1.9	160.0	0.3	0.3		7.48	14.54	16.58	10.68	0.00	-10.68
1.0	1.9	160.0	0.3	0.4		7.05	12.64	11.99	6.25	0.00	-6.25
1.0	1.9	160.0	0.3	0.5		4.96	8.88	7.72	3.59	0.00	-3.59
1.0	1.9	160.0	0.4	0.4		8.79	17.91	20.19	12.53	0.00	-12.53
1.0	1.9	160.0	0.4	0.5		8.46	13.59	11.32	5.32	0.00	-5.32
1.0	1.9	160.0	0.5	0.5		8.89	16.80	16.78	7.45	0.00	-7.45
1.0	1.9	190.0	0.3	0.3		7.51	14.66	16.76	10.86	0.00	-10.86
1.0	1.9	190.0	0.3	0.4		6.99	12.72	12.04	6.12	0.00	-6.12
1.0	1.9	190.0	0.3	0.5		4.93	8.96	7.75	3.50	0.00	-3.50
1.0	1.9	190.0	0.4	0.4		8.93	18.20	20.45	12.54	0.00	-12.54
1.0	1.9	190.0	0.4	0.5		8.72	13.92	11.28	5.00	0.00	-5.00
1.0	1.9	190.0	0.5	0.5		9.18	17.26	17.89	7.42	0.00	-7.42
1.0	1.9	220.0	0.3	0.3		7.56	14.69	16.92	10.98	0.00	-10.98
1.0	1.9	220.0	0.3	0.4		6.90	12.73	12.04	5.93	0.00	-5.93
1.0	1.9	220.0	0.3	0.5		4.89	8.99	7.79	3.41	0.00	-3.41
1.0	1.9	220.0	0.4	0.4		8.98	17.98	20.71	12.70	0.00	-12.70
1.0	1.9	220.0	0.4	0.5		8.80	14.10	11.32	4.75	0.00	-4.75
1.0	1.9	220.0	0.5	0.5		9.28	17.81	18.29	7.09	0.00	-7.09
1.0	1.9	250.0	0.3	0.3		7.52	14.69	16.99	11.04	0.00	-11.04
1.0	1.9	250.0	0.3	0.4		6.78	12.68	11.97	5.78	0.00	-5.78
1.0	1.9	250.0	0.3	0.5		4.87	9.00	7.77	3.33	0.00	-3.33
1.0	1.9	250.0	0.4	0.4		8.94	17.83	20.82	12.70	0.00	-12.70
1.0	1.9	250.0	0.4	0.5		8.84	14.25	11.27	4.48	0.00	-4.48
1.0	1.9	250.0	0.5	0.5		9.42	18.00	18.79	7.03	0.00	-7.03
1.0	2.1	40.0	0.3	0.3		7.46	12.68	14.48	9.24	0.00	-9.24

ENERGY FACTOR DATA (cont.)

Xnc	Bp(max)	L/G	Ts	Tr	XNI:	-1.8	-1.6	-1.4	-1.2	-1	-0.8
1.0	2.1	40.0	0.3	0.4		6.61	11.33	11.75	6.83	0.00	-6.83
1.0	2.1	40.0	0.3	0.5		5.43	8.42	7.86	4.35	0.00	-4.35
1.0	2.1	40.0	0.4	0.4		7.56	14.84	17.43	10.58	0.00	-10.58
1.0	2.1	40.0	0.4	0.5		6.60	11.64	11.78	6.67	0.00	-6.67
1.0	2.1	40.0	0.5	0.5		7.78	13.43	15.70	8.06	0.00	-8.06
1.0	2.1	70.0	0.3	0.3		7.72	14.28	17.61	13.53	0.00	-13.53
1.0	2.1	70.0	0.3	0.4		7.24	13.42	14.53	8.39	0.00	-8.39
1.0	2.1	70.0	0.3	0.5		5.88	10.26	10.28	5.33	0.00	-5.33
1.0	2.1	70.0	0.4	0.4		8.40	16.44	20.97	15.14	0.00	-15.14
1.0	2.1	70.0	0.4	0.5		7.73	13.91	14.81	8.06	0.00	-8.06
1.0	2.1	70.0	0.5	0.5		8.75	15.85	19.96	12.94	0.00	-12.94
1.0	2.1	100.0	0.3	0.3		7.56	14.53	18.21	13.84	0.00	-13.84
1.0	2.1	100.0	0.3	0.4		7.34	13.79	14.92	8.43	0.00	-8.43
1.0	2.1	100.0	0.3	0.5		5.68	10.37	10.36	5.17	0.00	-5.17
1.0	2.1	100.0	0.4	0.4		8.96	17.47	21.98	16.38	0.00	-16.38
1.0	2.1	100.0	0.4	0.5		8.03	14.61	15.45	8.11	0.00	-8.11
1.0	2.1	100.0	0.5	0.5		8.77	16.55	21.20	13.60	0.00	-13.60
1.0	2.1	130.0	0.3	0.3		7.64	14.78	18.65	14.11	0.00	-14.11
1.0	2.1	130.0	0.3	0.4		7.40	14.07	15.20	8.46	0.00	-8.46
1.0	2.1	130.0	0.3	0.5		5.63	10.51	10.40	4.99	0.00	-4.99
1.0	2.1	130.0	0.4	0.4		9.40	17.97	22.53	17.10	0.00	-17.10
1.0	2.1	130.0	0.4	0.5		8.31	15.05	15.54	7.89	0.00	-7.89
1.0	2.1	130.0	0.5	0.5		8.72	16.60	21.54	13.16	0.00	-13.16
1.0	2.1	160.0	0.3	0.3		7.71	15.00	19.17	14.54	0.00	-14.54
1.0	2.1	160.0	0.3	0.4		7.42	14.44	15.52	8.35	0.00	-8.35
1.0	2.1	160.0	0.3	0.5		5.51	10.71	10.51	4.84	0.00	-4.84
1.0	2.1	160.0	0.4	0.4		9.83	18.52	22.95	17.94	0.00	-17.94
1.0	2.1	160.0	0.4	0.5		8.70	15.43	15.73	7.73	0.00	-7.73
1.0	2.1	160.0	0.5	0.5		9.04	16.90	22.14	13.52	0.00	-13.52
1.0	2.1	190.0	0.3	0.3		7.76	15.08	19.48	14.93	0.00	-14.93
1.0	2.1	190.0	0.3	0.4		7.37	14.64	15.75	8.24	0.00	-8.24
1.0	2.1	190.0	0.3	0.5		5.50	10.86	10.70	4.81	0.00	-4.81
1.0	2.1	190.0	0.4	0.4		10.09	18.83	23.29	18.78	0.00	-18.78
1.0	2.1	190.0	0.4	0.5		8.95	15.94	16.21	7.42	0.00	-7.42
1.0	2.1	190.0	0.5	0.5		9.61	17.15	22.70	14.11	0.00	-14.11
1.0	2.1	220.0	0.3	0.3		7.74	15.14	19.72	15.28	0.00	-15.28
1.0	2.1	220.0	0.3	0.4		7.32	14.78	15.86	8.10	0.00	-8.10
1.0	2.1	220.0	0.3	0.5		5.53	10.97	10.87	4.79	0.00	-4.79
1.0	2.1	220.0	0.4	0.4		10.27	18.83	23.39	19.05	0.00	-19.05
1.0	2.1	220.0	0.4	0.5		9.07	16.22	16.35	6.98	0.00	-6.98
1.0	2.1	220.0	0.5	0.5		9.82	17.23	22.94	14.75	0.00	-14.75
1.0	2.1	250.0	0.3	0.3		7.70	15.13	19.83	15.46	0.00	-15.46
1.0	2.1	250.0	0.3	0.4		7.15	14.75	15.84	7.97	0.00	-7.97
1.0	2.1	250.0	0.3	0.5		5.51	11.01	10.94	4.73	0.00	-4.73
1.0	2.1	250.0	0.4	0.4		10.19	18.89	23.60	19.22	0.00	-19.22
1.0	2.1	250.0	0.4	0.5		9.14	16.50	16.43	6.61	0.00	-6.61
1.0	2.1	250.0	0.5	0.5		9.97	17.34	23.40	15.05	0.00	-15.05
0.8	1.1	40.0	0.3	0.3		0.00	2.17	3.24	2.71	1.44	-0.00

ENERGY FACTOR DATA (cont.)

Xnc	Bp(max)	L/G	Ts	Tr	XNI:	-1.8	-1.6	-1.4	-1.2	-1	-0.8
0.8	1.1	40.0	0.3	0.4	0.00	1.65	2.30	1.84	0.97	-0.00	
0.8	1.1	40.0	0.3	0.5	0.00	1.23	1.56	1.21	0.62	-0.00	
0.8	1.1	40.0	0.4	0.4	0.00	2.94	3.74	2.73	1.38	-0.00	
0.8	1.1	40.0	0.4	0.5	0.00	1.53	2.02	1.68	0.93	-0.00	
0.8	1.1	40.0	0.5	0.5	0.00	1.83	2.42	2.01	1.15	-0.00	
0.8	1.1	70.0	0.3	0.3	0.00	2.47	3.51	2.90	1.49	-0.00	
0.8	1.1	70.0	0.3	0.4	0.00	1.90	2.54	1.90	0.92	-0.00	
0.8	1.1	70.0	0.3	0.5	0.00	1.29	1.67	1.20	0.57	-0.00	
0.8	1.1	70.0	0.4	0.4	0.00	3.19	3.88	2.70	1.26	-0.00	
0.8	1.1	70.0	0.4	0.5	0.00	1.69	2.05	1.56	0.77	-0.00	
0.8	1.1	70.0	0.5	0.5	0.00	1.95	2.32	1.76	0.89	-0.00	
0.8	1.1	100.0	0.3	0.3	0.00	2.68	3.69	2.91	1.43	-0.00	
0.8	1.1	100.0	0.3	0.4	0.00	1.98	2.59	1.89	0.87	-0.00	
0.8	1.1	100.0	0.3	0.5	0.00	1.34	1.67	1.13	0.49	-0.00	
0.8	1.1	100.0	0.4	0.4	0.00	3.18	4.09	2.82	1.23	-0.00	
0.8	1.1	100.0	0.4	0.5	0.00	1.76	2.09	1.46	0.66	-0.00	
0.8	1.1	100.0	0.5	0.5	0.00	2.04	2.26	1.50	0.64	-0.00	
0.8	1.1	130.0	0.3	0.3	0.00	2.79	3.79	2.94	1.44	-0.00	
0.8	1.1	130.0	0.3	0.4	0.00	2.04	2.62	1.88	0.84	-0.00	
0.8	1.1	130.0	0.3	0.5	0.00	1.37	1.68	1.09	0.44	-0.00	
0.8	1.1	130.0	0.4	0.4	0.00	3.15	4.15	2.85	1.20	-0.00	
0.8	1.1	130.0	0.4	0.5	0.00	1.76	2.05	1.36	0.57	-0.00	
0.8	1.1	130.0	0.5	0.5	0.00	2.06	2.13	1.28	0.48	-0.00	
0.8	1.1	160.0	0.3	0.3	0.00	2.86	3.86	2.97	1.44	-0.00	
0.8	1.1	160.0	0.3	0.4	0.00	2.08	2.64	1.85	0.80	-0.00	
0.8	1.1	160.0	0.3	0.5	0.00	1.40	1.70	1.06	0.41	-0.00	
0.8	1.1	160.0	0.4	0.4	0.00	3.11	4.13	2.85	1.14	-0.00	
0.8	1.1	160.0	0.4	0.5	0.00	1.72	1.99	1.27	0.50	-0.00	
0.8	1.1	160.0	0.5	0.5	0.00	2.03	2.01	1.14	0.38	-0.00	
0.8	1.1	190.0	0.3	0.3	0.00	2.90	3.90	2.98	1.45	-0.00	
0.8	1.1	190.0	0.3	0.4	0.00	2.10	2.64	1.81	0.77	-0.00	
0.8	1.1	190.0	0.3	0.5	0.00	1.40	1.71	1.05	0.39	-0.00	
0.8	1.1	190.0	0.4	0.4	0.00	3.06	4.07	2.80	1.07	-0.00	
0.8	1.1	190.0	0.4	0.5	0.00	1.70	1.95	1.20	0.46	-0.00	
0.8	1.1	190.0	0.5	0.5	0.00	2.04	1.98	1.08	0.31	0.00	
0.8	1.1	220.0	0.3	0.3	0.00	2.93	3.92	2.99	1.45	-0.00	
0.8	1.1	220.0	0.3	0.4	0.00	2.10	2.63	1.78	0.74	-0.00	
0.8	1.1	220.0	0.3	0.5	0.00	1.40	1.71	1.04	0.38	0.00	
0.8	1.1	220.0	0.4	0.4	0.00	3.01	3.99	2.74	1.03	-0.00	
0.8	1.1	220.0	0.4	0.5	0.00	1.67	1.91	1.15	0.42	-0.00	
0.8	1.1	220.0	0.5	0.5	0.00	2.07	1.95	1.05	0.26	0.00	
0.8	1.1	250.0	0.3	0.3	0.00	2.95	3.93	3.00	1.45	-0.00	
0.8	1.1	250.0	0.3	0.4	0.00	2.10	2.61	1.74	0.71	-0.00	
0.8	1.1	250.0	0.3	0.5	0.00	1.39	1.71	1.03	0.36	-0.00	
0.8	1.1	250.0	0.4	0.4	0.00	3.01	3.90	2.64	1.00	-0.00	
0.8	1.1	250.0	0.4	0.5	0.00	1.64	1.84	1.09	0.39	-0.00	
0.8	1.1	250.0	0.5	0.5	0.00	2.06	1.93	1.03	0.23	-0.00	
0.8	1.3	40.0	0.3	0.3	0.00	3.02	4.54	3.79	2.02	-0.00	

ENERGY FACTOR DATA (cont.)

Xnc	Bp(max)	L/G	Ts	Tr	XNI:	-1.8	-1.6	-1.4	-1.2	-1	-.8
0.8	1.3	40.0	0.3	0.4	0.00	2.30	3.22	2.57	1.36	-0.00	
0.8	1.3	40.0	0.3	0.5	0.00	1.71	2.16	1.68	0.87	-0.00	
0.8	1.3	40.0	0.4	0.4	0.00	4.03	5.26	3.81	1.94	-0.00	
0.8	1.3	40.0	0.4	0.5	0.00	2.13	2.83	2.34	1.29	-0.00	
0.8	1.3	40.0	0.5	0.5	0.00	2.59	3.39	2.82	1.58	-0.00	
0.8	1.3	70.0	0.3	0.3	0.00	3.40	4.91	4.09	2.10	-0.00	
0.8	1.3	70.0	0.3	0.4	0.00	2.66	3.57	2.67	1.30	-0.00	
0.8	1.3	70.0	0.3	0.5	0.00	1.81	2.35	1.70	0.80	-0.00	
0.8	1.3	70.0	0.4	0.4	0.00	4.45	5.38	3.82	1.81	-0.00	
0.8	1.3	70.0	0.4	0.5	0.00	2.36	2.91	2.22	1.09	-0.00	
0.8	1.3	70.0	0.5	0.5	0.00	2.86	3.42	2.49	1.25	-0.00	
0.8	1.3	100.0	0.3	0.3	0.00	3.71	5.13	4.07	2.02	-0.00	
0.8	1.3	100.0	0.3	0.4	0.00	2.75	3.62	2.66	1.24	-0.00	
0.8	1.3	100.0	0.3	0.5	0.00	1.86	2.33	1.61	0.68	-0.00	
0.8	1.3	100.0	0.4	0.4	0.00	4.48	5.72	3.97	1.76	-0.00	
0.8	1.3	100.0	0.4	0.5	0.00	2.52	2.97	2.08	0.94	-0.00	
0.8	1.3	100.0	0.5	0.5	0.00	3.05	3.34	2.20	0.88	-0.00	
0.8	1.3	130.0	0.3	0.3	0.00	3.87	5.25	4.09	2.02	-0.00	
0.8	1.3	130.0	0.3	0.4	0.00	2.82	3.66	2.65	1.18	-0.00	
0.8	1.3	130.0	0.3	0.5	0.00	1.90	2.34	1.55	0.62	-0.00	
0.8	1.3	130.0	0.4	0.4	0.00	4.38	5.87	4.01	1.73	-0.00	
0.8	1.3	130.0	0.4	0.5	0.00	2.53	2.92	1.94	0.81	0.00	
0.8	1.3	130.0	0.5	0.5	0.00	3.12	3.23	1.87	0.68	-0.00	
0.8	1.3	160.0	0.3	0.3	0.00	3.97	5.35	4.10	2.02	-0.00	
0.8	1.3	160.0	0.3	0.4	0.00	2.87	3.68	2.61	1.13	-0.00	
0.8	1.3	160.0	0.3	0.5	0.00	1.94	2.35	1.50	0.58	-0.00	
0.8	1.3	160.0	0.4	0.4	0.00	4.30	5.89	3.99	1.64	-0.00	
0.8	1.3	160.0	0.4	0.5	0.00	2.47	2.83	1.81	0.71	-0.00	
0.8	1.3	160.0	0.5	0.5	0.00	3.07	3.10	1.64	0.54	0.00	
0.8	1.3	190.0	0.3	0.3	0.00	4.03	5.40	4.11	2.04	-0.00	
0.8	1.3	190.0	0.3	0.4	0.00	2.89	3.66	2.57	1.08	-0.00	
0.8	1.3	190.0	0.3	0.5	0.00	1.95	2.35	1.49	0.55	-0.00	
0.8	1.3	190.0	0.4	0.4	0.00	4.21	5.84	3.94	1.55	-0.00	
0.8	1.3	190.0	0.4	0.5	0.00	2.44	2.78	1.71	0.64	0.00	
0.8	1.3	190.0	0.5	0.5	0.00	3.09	3.08	1.58	0.44	-0.00	
0.8	1.3	220.0	0.3	0.3	0.00	4.07	5.43	4.10	2.05	-0.00	
0.8	1.3	220.0	0.3	0.4	0.00	2.89	3.64	2.53	1.04	-0.00	
0.8	1.3	220.0	0.3	0.5	0.00	1.95	2.35	1.49	0.53	-0.00	
0.8	1.3	220.0	0.4	0.4	0.00	4.12	5.77	3.85	1.49	-0.00	
0.8	1.3	220.0	0.4	0.5	0.00	2.42	2.73	1.64	0.59	-0.00	
0.8	1.3	220.0	0.5	0.5	0.00	3.16	3.05	1.53	0.37	-0.00	
0.8	1.3	250.0	0.3	0.3	0.00	4.09	5.44	4.09	2.06	-0.00	
0.8	1.3	250.0	0.3	0.4	0.00	2.92	3.60	2.44	1.00	-0.00	
0.8	1.3	250.0	0.3	0.5	0.00	1.94	2.34	1.48	0.51	-0.00	
0.8	1.3	250.0	0.4	0.4	0.00	4.03	5.67	3.76	1.40	-0.00	
0.8	1.3	250.0	0.4	0.5	0.00	2.37	2.66	1.55	0.55	-0.00	
0.8	1.3	250.0	0.5	0.5	0.00	3.16	3.02	1.52	0.33	-0.00	
0.8	1.5	40.0	0.3	0.3	0.00	4.04	6.05	5.06	2.69	-0.00	

ENERGY FACTOR DATA (cont.)

Xnc	Bp(max)	L/G	Ts	Tr	XNI:	-1.8	-1.6	-1.4	-1.2	-1	-0.8
0.8	1.5	40.0	0.3	0.4	0.00	3.07	4.29	3.44	1.82	-0.00	
0.8	1.5	40.0	0.3	0.5	0.00	2.26	2.88	2.23	1.16	0.00	
0.8	1.5	40.0	0.4	0.4	0.00	5.40	6.99	5.07	2.60	-0.00	
0.8	1.5	40.0	0.4	0.5	0.00	2.84	3.77	3.12	1.71	-0.00	
0.8	1.5	40.0	0.5	0.5	0.00	3.48	4.66	3.77	2.10	0.00	
0.8	1.5	70.0	0.3	0.3	0.00	4.48	6.51	5.52	2.85	-0.00	
0.8	1.5	70.0	0.3	0.4	0.00	3.53	4.76	3.60	1.76	-0.00	
0.8	1.5	70.0	0.3	0.5	0.00	2.40	3.17	2.31	1.08	0.00	
0.8	1.5	70.0	0.4	0.4	0.00	5.83	7.15	5.23	2.44	-0.00	
0.8	1.5	70.0	0.4	0.5	0.00	3.16	3.97	3.01	1.46	-0.00	
0.8	1.5	70.0	0.5	0.5	0.00	3.98	4.88	3.37	1.69	-0.00	
0.8	1.5	100.0	0.3	0.3	0.00	4.92	6.77	5.42	2.74	-0.00	
0.8	1.5	100.0	0.3	0.4	0.00	3.64	4.83	3.58	1.67	-0.00	
0.8	1.5	100.0	0.3	0.5	0.00	2.44	3.12	2.18	0.93	-0.00	
0.8	1.5	100.0	0.4	0.4	0.00	6.00	7.59	5.35	2.39	-0.00	
0.8	1.5	100.0	0.4	0.5	0.00	3.40	4.04	2.84	1.27	0.00	
0.8	1.5	100.0	0.5	0.5	0.00	4.27	4.95	3.07	1.15	-0.00	
0.8	1.5	130.0	0.3	0.3	0.00	5.14	6.92	5.44	2.71	-0.00	
0.8	1.5	130.0	0.3	0.4	0.00	3.71	4.88	3.55	1.60	-0.00	
0.8	1.5	130.0	0.3	0.5	0.00	2.48	3.12	2.09	0.83	-0.00	
0.8	1.5	130.0	0.4	0.4	0.00	5.87	7.86	5.47	2.32	-0.00	
0.8	1.5	130.0	0.4	0.5	0.00	3.45	4.02	2.64	1.10	-0.00	
0.8	1.5	130.0	0.5	0.5	0.00	4.34	4.84	2.69	0.91	-0.00	
0.8	1.5	160.0	0.3	0.3	0.00	5.28	7.07	5.43	2.67	-0.00	
0.8	1.5	160.0	0.3	0.4	0.00	3.78	4.89	3.48	1.52	-0.00	
0.8	1.5	160.0	0.3	0.5	0.00	2.52	3.11	2.00	0.77	-0.00	
0.8	1.5	160.0	0.4	0.4	0.00	5.75	7.94	5.49	2.28	-0.00	
0.8	1.5	160.0	0.4	0.5	0.00	3.42	3.93	2.49	0.97	-0.00	
0.8	1.5	160.0	0.5	0.5	0.00	4.35	4.77	2.37	0.73	-0.00	
0.8	1.5	190.0	0.3	0.3	0.00	5.34	7.14	5.44	2.66	-0.00	
0.8	1.5	190.0	0.3	0.4	0.00	3.80	4.88	3.42	1.44	-0.00	
0.8	1.5	190.0	0.3	0.5	0.00	2.53	3.11	1.97	0.74	-0.00	
0.8	1.5	190.0	0.4	0.4	0.00	5.55	7.92	5.41	2.21	-0.00	
0.8	1.5	190.0	0.4	0.5	0.00	3.39	3.86	2.38	0.88	-0.00	
0.8	1.5	190.0	0.5	0.5	0.00	4.48	4.70	2.23	0.60	-0.00	
0.8	1.5	220.0	0.3	0.3	0.00	5.39	7.17	5.44	2.67	-0.00	
0.8	1.5	220.0	0.3	0.4	0.00	3.79	4.85	3.37	1.39	-0.00	
0.8	1.5	220.0	0.3	0.5	0.00	2.52	3.11	1.97	0.71	-0.00	
0.8	1.5	220.0	0.4	0.4	0.00	5.36	7.84	5.24	2.14	-0.00	
0.8	1.5	220.0	0.4	0.5	0.00	3.36	3.77	2.29	0.81	0.00	
0.8	1.5	220.0	0.5	0.5	0.00	4.52	4.71	2.19	0.52	-0.00	
0.8	1.5	250.0	0.3	0.3	0.00	5.41	7.19	5.42	2.66	-0.00	
0.8	1.5	250.0	0.3	0.4	0.00	3.81	4.81	3.28	1.34	-0.00	
0.8	1.5	250.0	0.3	0.5	0.00	2.51	3.10	1.95	0.69	-0.00	
0.8	1.5	250.0	0.4	0.4	0.00	5.23	7.72	5.02	1.89	-0.00	
0.8	1.5	250.0	0.4	0.5	0.00	3.22	3.65	2.12	0.74	-0.00	
0.8	1.5	250.0	0.5	0.5	0.00	4.58	4.69	2.10	0.44	-0.00	
0.8	1.7	40.0	0.3	0.3	0.00	5.06	7.82	6.54	3.46	-0.00	

ENERGY FACTOR DATA (cont.)

Xnc	Bp(max)	L/G	Ts	Tr	XNI:	-1.8	-1.6	-1.4	-1.2	-1	-0.8
0.8	1.7	40.0	0.3	0.4	0.00	3.96	5.52	4.43	2.35	-0.00	
0.8	1.7	40.0	0.3	0.5	0.00	2.93	3.72	2.87	1.49	-0.00	
0.8	1.7	40.0	0.4	0.4	0.00	6.94	8.90	6.64	3.37	-0.00	
0.8	1.7	40.0	0.4	0.5	0.00	3.65	4.89	4.05	2.21	-0.00	
0.8	1.7	40.0	0.5	0.5	0.00	4.56	6.33	4.87	2.73	-0.00	
0.8	1.7	70.0	0.3	0.3	0.00	5.69	8.30	7.22	3.77	-0.00	
0.8	1.7	70.0	0.3	0.4	0.00	4.51	6.15	4.69	2.30	-0.00	
0.8	1.7	70.0	0.3	0.5	0.00	3.07	4.16	3.04	1.40	-0.00	
0.8	1.7	70.0	0.4	0.4	0.00	7.07	9.33	7.14	3.13	-0.00	
0.8	1.7	70.0	0.4	0.5	0.00	4.09	5.38	3.98	1.90	-0.00	
0.8	1.7	70.0	0.5	0.5	0.00	5.27	6.94	4.54	2.22	-0.00	
0.8	1.7	100.0	0.3	0.3	0.00	6.21	8.58	7.10	3.61	-0.00	
0.8	1.7	100.0	0.3	0.4	0.00	4.63	6.25	4.66	2.19	-0.00	
0.8	1.7	100.0	0.3	0.5	0.00	3.09	4.09	2.88	1.21	-0.00	
0.8	1.7	100.0	0.4	0.4	0.00	7.36	9.80	7.38	3.17	-0.00	
0.8	1.7	100.0	0.4	0.5	0.00	4.39	5.52	3.83	1.67	-0.00	
0.8	1.7	100.0	0.5	0.5	0.00	5.67	7.02	4.23	1.65	-0.00	
0.8	1.7	130.0	0.3	0.3	0.00	6.53	8.73	7.03	3.59	-0.00	
0.8	1.7	130.0	0.3	0.4	0.00	4.68	6.28	4.65	2.11	-0.00	
0.8	1.7	130.0	0.3	0.5	0.00	3.10	4.05	2.77	1.09	-0.00	
0.8	1.7	130.0	0.4	0.4	0.00	7.30	10.15	7.44	3.06	-0.00	
0.8	1.7	130.0	0.4	0.5	0.00	4.53	5.51	3.54	1.45	-0.00	
0.8	1.7	130.0	0.5	0.5	0.00	5.80	7.01	3.80	1.28	-0.00	
0.8	1.7	160.0	0.3	0.3	0.00	6.76	8.92	6.98	3.47	-0.00	
0.8	1.7	160.0	0.3	0.4	0.00	4.77	6.29	4.54	2.00	-0.00	
0.8	1.7	160.0	0.3	0.5	0.00	3.16	4.01	2.63	1.01	-0.00	
0.8	1.7	160.0	0.4	0.4	0.00	7.33	10.31	7.47	2.96	-0.00	
0.8	1.7	160.0	0.4	0.5	0.00	4.58	5.42	3.29	1.27	-0.00	
0.8	1.7	160.0	0.5	0.5	0.00	5.87	7.09	3.51	0.95	0.00	
0.8	1.7	190.0	0.3	0.3	0.00	6.84	9.01	6.99	3.39	-0.00	
0.8	1.7	190.0	0.3	0.4	0.00	4.80	6.27	4.44	1.90	-0.00	
0.8	1.7	190.0	0.3	0.5	0.00	3.17	4.01	2.56	0.96	-0.00	
0.8	1.7	190.0	0.4	0.4	0.00	7.31	10.28	7.37	2.91	-0.00	
0.8	1.7	190.0	0.4	0.5	0.00	4.59	5.34	3.18	1.16	-0.00	
0.8	1.7	190.0	0.5	0.5	0.00	6.02	7.17	3.37	0.80	0.00	
0.8	1.7	220.0	0.3	0.3	0.00	6.90	9.08	6.97	3.35	-0.00	
0.8	1.7	220.0	0.3	0.4	0.00	4.81	6.24	4.34	1.82	-0.00	
0.8	1.7	220.0	0.3	0.5	0.00	3.17	4.01	2.52	0.93	-0.00	
0.8	1.7	220.0	0.4	0.4	0.00	7.08	10.24	7.32	2.80	-0.00	
0.8	1.7	220.0	0.4	0.5	0.00	4.60	5.31	3.05	1.06	-0.00	
0.8	1.7	220.0	0.5	0.5	0.00	6.15	7.28	3.24	0.69	-0.00	
0.8	1.7	250.0	0.3	0.3	0.00	6.92	9.07	6.96	3.34	-0.00	
0.8	1.7	250.0	0.3	0.4	0.00	4.78	6.18	4.26	1.74	-0.00	
0.8	1.7	250.0	0.3	0.5	0.00	3.14	4.00	2.49	0.90	-0.00	
0.8	1.7	250.0	0.4	0.4	0.00	6.79	10.11	7.20	2.70	-0.00	
0.8	1.7	250.0	0.4	0.5	0.00	4.51	5.24	2.95	0.99	-0.00	
0.8	1.7	250.0	0.5	0.5	0.00	6.26	7.31	3.14	0.62	0.00	
0.8	1.9	40.0	0.3	0.3	0.00	5.85	9.82	8.21	4.33	-0.00	

ENERGY FACTOR DATA (cont.)

Xnc	Bp(max)	L/G	Ts	Tr	XNI:	-1.8	-1.6	-1.4	-1.2	-1	-.8
0.8	1.9	40.0	0.3	0.4	0.00	4.95	6.92	5.53	2.94	-0.00	
0.8	1.9	40.0	0.3	0.5	0.00	3.68	4.68	3.59	1.87	-0.00	
0.8	1.9	40.0	0.4	0.4	0.00	7.94	11.03	8.53	4.25	-0.00	
0.8	1.9	40.0	0.4	0.5	0.00	4.55	6.23	5.15	2.80	-0.00	
0.8	1.9	40.0	0.5	0.5	0.00	5.56	8.51	6.26	3.43	-0.00	
0.8	1.9	70.0	0.3	0.3	0.00	6.64	10.22	9.15	4.86	-0.00	
0.8	1.9	70.0	0.3	0.4	0.00	5.55	7.69	5.98	2.92	-0.00	
0.8	1.9	70.0	0.3	0.5	0.00	3.78	5.30	3.92	1.76	-0.00	
0.8	1.9	70.0	0.4	0.4	0.00	8.24	11.89	9.40	3.92	-0.00	
0.8	1.9	70.0	0.4	0.5	0.00	5.20	7.06	5.12	2.40	-0.00	
0.8	1.9	70.0	0.5	0.5	0.00	6.69	9.49	6.41	2.90	-0.00	
0.8	1.9	100.0	0.3	0.3	0.00	7.23	10.49	9.04	4.72	-0.00	
0.8	1.9	100.0	0.3	0.4	0.00	5.68	7.84	5.95	2.81	-0.00	
0.8	1.9	100.0	0.3	0.5	0.00	3.76	5.26	3.74	1.57	-0.00	
0.8	1.9	100.0	0.4	0.4	0.00	8.73	12.35	9.81	4.09	-0.00	
0.8	1.9	100.0	0.4	0.5	0.00	5.58	7.32	5.02	2.15	-0.00	
0.8	1.9	100.0	0.5	0.5	0.00	7.38	9.73	5.86	2.31	-0.00	
0.8	1.9	130.0	0.3	0.3	0.00	7.57	10.70	9.05	4.64	-0.00	
0.8	1.9	130.0	0.3	0.4	0.00	5.74	7.95	5.94	2.70	-0.00	
0.8	1.9	130.0	0.3	0.5	0.00	3.79	5.26	3.59	1.39	-0.00	
0.8	1.9	130.0	0.4	0.4	0.00	8.80	12.66	10.00	4.03	-0.00	
0.8	1.9	130.0	0.4	0.5	0.00	5.78	7.35	4.71	1.91	-0.00	
0.8	1.9	130.0	0.5	0.5	0.00	7.83	9.77	5.27	1.81	0.00	
0.8	1.9	160.0	0.3	0.3	0.00	7.92	10.86	8.98	4.56	-0.00	
0.8	1.9	160.0	0.3	0.4	0.00	5.80	7.95	5.86	2.58	-0.00	
0.8	1.9	160.0	0.3	0.5	0.00	3.82	5.20	3.46	1.28	0.00	
0.8	1.9	160.0	0.4	0.4	0.00	8.79	12.92	10.19	3.84	-0.00	
0.8	1.9	160.0	0.4	0.5	0.00	5.94	7.38	4.39	1.67	-0.00	
0.8	1.9	160.0	0.5	0.5	0.00	7.89	10.09	5.11	1.33	-0.00	
0.8	1.9	190.0	0.3	0.3	0.00	8.05	10.94	8.97	4.48	-0.00	
0.8	1.9	190.0	0.3	0.4	0.00	5.81	7.92	5.76	2.47	-0.00	
0.8	1.9	190.0	0.3	0.5	0.00	3.83	5.18	3.38	1.23	-0.00	
0.8	1.9	190.0	0.4	0.4	0.00	8.70	12.96	10.24	3.75	-0.00	
0.8	1.9	190.0	0.4	0.5	0.00	6.03	7.38	4.20	1.51	-0.00	
0.8	1.9	190.0	0.5	0.5	0.00	8.04	10.43	5.04	1.05	-0.00	
0.8	1.9	220.0	0.3	0.3	0.00	8.17	11.04	8.92	4.37	-0.00	
0.8	1.9	220.0	0.3	0.4	0.00	5.83	7.85	5.61	2.37	-0.00	
0.8	1.9	220.0	0.3	0.5	0.00	3.84	5.16	3.29	1.19	-0.00	
0.8	1.9	220.0	0.4	0.4	0.00	8.42	12.91	10.22	3.62	-0.00	
0.8	1.9	220.0	0.4	0.5	0.00	6.05	7.37	4.05	1.38	-0.00	
0.8	1.9	220.0	0.5	0.5	0.00	8.16	10.60	4.95	0.92	-0.00	
0.8	1.9	250.0	0.3	0.3	0.00	8.20	11.03	8.88	4.32	-0.00	
0.8	1.9	250.0	0.3	0.4	0.00	5.80	7.76	5.47	2.22	-0.00	
0.8	1.9	250.0	0.3	0.5	0.00	3.80	5.12	3.24	1.16	-0.00	
0.8	1.9	250.0	0.4	0.4	0.00	8.28	12.78	10.15	3.55	-0.00	
0.8	1.9	250.0	0.4	0.5	0.00	6.03	7.31	3.92	1.28	-0.00	
0.8	1.9	250.0	0.5	0.5	0.00	8.31	10.71	4.84	0.82	-0.00	
0.8	2.1	40.0	0.3	0.3	0.00	6.48	11.35	10.11	5.32	0.00	

ENERGY FACTOR DATA (cont.)

Xnc	Bp(max)	L/G	Ts	Tr	XNI:	-1.8	-1.6	-1.4	-1.2	-1	-0.8
0.8	2.1	40.0	0.3	0.4	0.00	5.90	8.46	6.79	3.62	-0.00	
0.8	2.1	40.0	0.3	0.5	0.00	4.48	5.76	4.41	2.28	-0.00	
0.8	2.1	40.0	0.4	0.4	0.00	7.93	13.21	11.01	5.25	0.00	
0.8	2.1	40.0	0.4	0.5	0.00	5.45	7.87	6.47	3.46	0.00	
0.8	2.1	40.0	0.5	0.5	0.00	6.37	10.90	8.12	4.20	0.00	
0.8	2.1	70.0	0.3	0.3	0.00	7.32	12.17	11.27	6.13	-0.00	
0.8	2.1	70.0	0.3	0.4	0.00	6.62	9.39	7.49	3.64	-0.00	
0.8	2.1	70.0	0.3	0.5	0.00	4.56	6.56	4.94	2.18	-0.00	
0.8	2.1	70.0	0.4	0.4	0.00	8.59	14.57	12.17	5.09	-0.00	
0.8	2.1	70.0	0.4	0.5	0.00	6.40	9.06	6.61	3.06	-0.00	
0.8	2.1	70.0	0.5	0.5	0.00	8.00	12.38	8.82	3.81	-0.00	
0.8	2.1	100.0	0.3	0.3	0.00	7.83	12.43	11.20	6.02	-0.00	
0.8	2.1	100.0	0.3	0.4	0.00	6.73	9.59	7.48	3.54	-0.00	
0.8	2.1	100.0	0.3	0.5	0.00	4.46	6.57	4.75	1.97	-0.00	
0.8	2.1	100.0	0.4	0.4	0.00	9.50	15.12	12.61	5.20	-0.00	
0.8	2.1	100.0	0.4	0.5	0.00	6.93	9.38	6.44	2.76	-0.00	
0.8	2.1	100.0	0.5	0.5	0.00	8.66	12.76	8.51	3.19	-0.00	
0.8	2.1	130.0	0.3	0.3	0.00	8.14	12.69	11.23	5.95	-0.00	
0.8	2.1	130.0	0.3	0.4	0.00	6.81	9.75	7.48	3.41	-0.00	
0.8	2.1	130.0	0.3	0.5	0.00	4.50	6.60	4.60	1.77	-0.00	
0.8	2.1	130.0	0.4	0.4	0.00	9.81	15.35	12.92	5.30	-0.00	
0.8	2.1	130.0	0.4	0.5	0.00	7.22	9.48	6.18	2.52	-0.00	
0.8	2.1	130.0	0.5	0.5	0.00	9.38	12.89	7.67	2.58	-0.00	
0.8	2.1	160.0	0.3	0.3	0.00	8.43	12.88	11.31	5.92	-0.00	
0.8	2.1	160.0	0.3	0.4	0.00	6.87	9.86	7.46	3.25	-0.00	
0.8	2.1	160.0	0.3	0.5	0.00	4.53	6.60	4.49	1.60	-0.00	
0.8	2.1	160.0	0.4	0.4	0.00	9.91	15.64	13.25	5.12	-0.00	
0.8	2.1	160.0	0.4	0.5	0.00	7.46	9.61	5.86	2.21	-0.00	
0.8	2.1	160.0	0.5	0.5	0.00	9.65	13.31	7.56	2.07	-0.00	
0.8	2.1	190.0	0.3	0.3	0.00	8.51	12.99	11.35	5.90	-0.00	
0.8	2.1	190.0	0.3	0.4	0.00	6.89	9.85	7.38	3.14	-0.00	
0.8	2.1	190.0	0.3	0.5	0.00	4.55	6.61	4.43	1.54	-0.00	
0.8	2.1	190.0	0.4	0.4	0.00	9.90	15.73	13.53	4.95	-0.00	
0.8	2.1	190.0	0.4	0.5	0.00	7.67	9.74	5.64	1.98	-0.00	
0.8	2.1	190.0	0.5	0.5	0.00	9.83	14.01	7.56	1.50	0.00	
0.8	2.1	220.0	0.3	0.3	0.00	8.56	13.01	11.37	5.89	-0.00	
0.8	2.1	220.0	0.3	0.4	0.00	6.82	9.80	7.30	3.02	-0.00	
0.8	2.1	220.0	0.3	0.5	0.00	4.52	6.63	4.39	1.49	-0.00	
0.8	2.1	220.0	0.4	0.4	0.00	9.79	15.75	13.59	4.68	-0.00	
0.8	2.1	220.0	0.4	0.5	0.00	7.81	9.79	5.36	1.80	-0.00	
0.8	2.1	220.0	0.5	0.5	0.00	9.95	14.31	7.53	1.31	-0.00	
0.8	2.1	250.0	0.3	0.3	0.00	8.58	12.99	11.34	5.84	-0.00	
0.8	2.1	250.0	0.3	0.4	0.00	6.77	9.68	7.15	2.85	-0.00	
0.8	2.1	250.0	0.3	0.5	0.00	4.47	6.60	4.33	1.46	-0.00	
0.8	2.1	250.0	0.4	0.4	0.00	9.73	15.55	13.65	4.58	-0.00	
0.8	2.1	250.0	0.4	0.5	0.00	7.82	9.79	5.22	1.67	-0.00	
0.8	2.1	250.0	0.5	0.5	0.00	10.08	14.48	7.48	1.16	0.00	
0.6	1.1	40.0	0.3	0.3	1.06	0.00	1.06	1.53	1.20	-0.56	

ENERGY FACTOR DATA (cont.)

Xnc	Bp(max)	L/G	Ts	Tr	XNI:	-1.8	-1.6	-1.4	-1.2	-1	-.8
0.6	1.1	40.0	0.3	0.4		0.85	0.00	0.85	1.09	0.79	-0.36
0.6	1.1	40.0	0.3	0.5		0.66	0.00	0.66	0.75	0.50	-0.25
0.6	1.1	40.0	0.4	0.4		1.63	0.00	1.63	1.78	1.10	-0.49
0.6	1.1	40.0	0.4	0.5		0.82	0.00	0.82	0.96	0.70	-0.39
0.6	1.1	40.0	0.5	0.5		0.98	0.00	0.98	1.13	0.88	-0.47
0.6	1.1	70.0	0.3	0.3		1.28	0.00	1.28	1.69	1.23	-0.52
0.6	1.1	70.0	0.3	0.4		1.03	0.00	1.03	1.21	0.77	-0.31
0.6	1.1	70.0	0.3	0.5		0.72	0.00	0.72	0.79	0.47	-0.19
0.6	1.1	70.0	0.4	0.4		1.81	0.00	1.81	1.89	1.02	-0.41
0.6	1.1	70.0	0.4	0.5		0.94	0.00	0.94	0.98	0.60	-0.29
0.6	1.1	70.0	0.5	0.5		1.01	0.00	1.01	1.06	0.68	-0.36
0.6	1.1	100.0	0.3	0.3		1.40	0.00	1.40	1.81	1.25	-0.45
0.6	1.1	100.0	0.3	0.4		1.10	0.00	1.10	1.26	0.74	-0.27
0.6	1.1	100.0	0.3	0.5		0.77	0.00	0.77	0.82	0.41	-0.14
0.6	1.1	100.0	0.4	0.4		1.79	0.00	1.79	1.99	1.08	-0.37
0.6	1.1	100.0	0.4	0.5		0.98	0.00	0.98	1.00	0.54	-0.22
0.6	1.1	100.0	0.5	0.5		1.10	0.00	1.10	1.02	0.51	-0.22
0.6	1.1	130.0	0.3	0.3		1.45	0.00	1.45	1.87	1.31	-0.43
0.6	1.1	130.0	0.3	0.4		1.15	0.00	1.15	1.31	0.72	-0.24
0.6	1.1	130.0	0.3	0.5		0.80	0.00	0.80	0.86	0.38	-0.10
0.6	1.1	130.0	0.4	0.4		1.78	0.00	1.78	2.01	1.08	-0.34
0.6	1.1	130.0	0.4	0.5		0.99	0.00	0.99	0.98	0.49	-0.18
0.6	1.1	130.0	0.5	0.5		1.15	0.00	1.15	0.94	0.41	-0.14
0.6	1.1	160.0	0.3	0.3		1.48	0.00	1.48	1.91	1.35	-0.41
0.6	1.1	160.0	0.3	0.4		1.18	0.00	1.18	1.33	0.71	-0.21
0.6	1.1	160.0	0.3	0.5		0.82	0.00	0.82	0.88	0.37	-0.08
0.6	1.1	160.0	0.4	0.4		1.76	0.00	1.76	2.01	1.04	-0.31
0.6	1.1	160.0	0.4	0.5		0.98	0.00	0.98	0.94	0.44	-0.15
0.6	1.1	160.0	0.5	0.5		1.19	0.00	1.19	0.88	0.35	-0.10
0.6	1.1	190.0	0.3	0.3		1.51	0.00	1.51	1.93	1.37	-0.40
0.6	1.1	190.0	0.3	0.4		1.20	0.00	1.20	1.34	0.69	-0.19
0.6	1.1	190.0	0.3	0.5		0.83	0.00	0.83	0.89	0.36	-0.06
0.6	1.1	190.0	0.4	0.4		1.73	0.00	1.73	1.99	0.98	-0.28
0.6	1.1	190.0	0.4	0.5		0.97	0.00	0.97	0.90	0.41	-0.13
0.6	1.1	190.0	0.5	0.5		1.20	0.00	1.20	0.87	0.30	-0.08
0.6	1.1	220.0	0.3	0.3		1.53	0.00	1.53	1.94	1.39	-0.39
0.6	1.1	220.0	0.3	0.4		1.22	0.00	1.22	1.34	0.67	-0.18
0.6	1.1	220.0	0.3	0.5		0.84	0.00	0.84	0.90	0.35	-0.05
0.6	1.1	220.0	0.4	0.4		1.71	0.00	1.71	1.95	0.96	-0.26
0.6	1.1	220.0	0.4	0.5		0.95	0.00	0.95	0.88	0.38	-0.11
0.6	1.1	220.0	0.5	0.5		1.20	0.00	1.20	0.87	0.26	-0.06
0.6	1.1	250.0	0.3	0.3		1.56	0.00	1.56	1.95	1.40	-0.38
0.6	1.1	250.0	0.3	0.4		1.23	0.00	1.23	1.34	0.66	-0.16
0.6	1.1	250.0	0.3	0.5		0.84	0.00	0.84	0.91	0.34	-0.04
0.6	1.1	250.0	0.4	0.4		1.68	0.00	1.68	1.93	0.93	-0.25
0.6	1.1	250.0	0.4	0.5		0.93	0.00	0.93	0.85	0.36	-0.10
0.6	1.1	250.0	0.5	0.5		1.20	0.00	1.20	0.88	0.24	-0.05
0.6	1.3	40.0	0.3	0.3		1.49	0.00	1.49	2.14	1.68	-0.78

ENERGY FACTOR DATA (cont.)

Xnc	Bp(max)	L/G	Ts	Tr	XNI: -1.8	-1.6	-1.4	-1.2	-1	-0.8
0.6	1.3	40.0	0.3	0.4	1.19	0.00	1.19	1.53	1.10	-0.51
0.6	1.3	40.0	0.3	0.5	0.92	0.00	0.92	1.04	0.69	-0.34
0.6	1.3	40.0	0.4	0.4	2.31	0.00	2.31	2.48	1.54	-0.69
0.6	1.3	40.0	0.4	0.5	1.15	0.00	1.15	1.33	0.98	-0.55
0.6	1.3	40.0	0.5	0.5	1.37	0.00	1.37	1.57	1.21	-0.66
0.6	1.3	70.0	0.3	0.3	1.78	0.00	1.78	2.37	1.73	-0.74
0.6	1.3	70.0	0.3	0.4	1.44	0.00	1.44	1.71	1.08	-0.44
0.6	1.3	70.0	0.3	0.5	1.00	0.00	1.00	1.10	0.66	-0.27
0.6	1.3	70.0	0.4	0.4	2.52	0.00	2.52	2.66	1.42	-0.58
0.6	1.3	70.0	0.4	0.5	1.32	0.00	1.32	1.37	0.84	-0.41
0.6	1.3	70.0	0.5	0.5	1.44	0.00	1.44	1.49	0.95	-0.51
0.6	1.3	100.0	0.3	0.3	1.96	0.00	1.96	2.52	1.75	-0.64
0.6	1.3	100.0	0.3	0.4	1.54	0.00	1.54	1.77	1.05	-0.38
0.6	1.3	100.0	0.3	0.5	1.07	0.00	1.07	1.15	0.58	-0.19
0.6	1.3	100.0	0.4	0.4	2.46	0.00	2.46	2.81	1.53	-0.52
0.6	1.3	100.0	0.4	0.5	1.38	0.00	1.38	1.42	0.76	-0.31
0.6	1.3	100.0	0.5	0.5	1.55	0.00	1.55	1.48	0.71	-0.31
0.6	1.3	130.0	0.3	0.3	2.03	0.00	2.03	2.60	1.82	-0.60
0.6	1.3	130.0	0.3	0.4	1.60	0.00	1.60	1.82	1.02	-0.34
0.6	1.3	130.0	0.3	0.5	1.11	0.00	1.11	1.20	0.54	-0.15
0.6	1.3	130.0	0.4	0.4	2.45	0.00	2.45	2.83	1.55	-0.47
0.6	1.3	130.0	0.4	0.5	1.38	0.00	1.38	1.39	0.69	-0.25
0.6	1.3	130.0	0.5	0.5	1.62	0.00	1.62	1.38	0.57	-0.20
0.6	1.3	160.0	0.3	0.3	2.07	0.00	2.07	2.65	1.88	-0.58
0.6	1.3	160.0	0.3	0.4	1.64	0.00	1.64	1.85	0.99	-0.30
0.6	1.3	160.0	0.3	0.5	1.13	0.00	1.13	1.24	0.52	-0.12
0.6	1.3	160.0	0.4	0.4	2.45	0.00	2.45	2.83	1.50	-0.43
0.6	1.3	160.0	0.4	0.5	1.37	0.00	1.37	1.34	0.62	-0.20
0.6	1.3	160.0	0.5	0.5	1.67	0.00	1.67	1.28	0.48	-0.14
0.6	1.3	190.0	0.3	0.3	2.11	0.00	2.11	2.67	1.92	-0.56
0.6	1.3	190.0	0.3	0.4	1.66	0.00	1.66	1.86	0.96	-0.27
0.6	1.3	190.0	0.3	0.5	1.14	0.00	1.14	1.26	0.50	-0.09
0.6	1.3	190.0	0.4	0.4	2.42	0.00	2.42	2.79	1.43	-0.40
0.6	1.3	190.0	0.4	0.5	1.35	0.00	1.35	1.29	0.58	-0.17
0.6	1.3	190.0	0.5	0.5	1.69	0.00	1.69	1.27	0.42	-0.11
0.6	1.3	220.0	0.3	0.3	2.13	0.00	2.13	2.68	1.96	-0.55
0.6	1.3	220.0	0.3	0.4	1.68	0.00	1.68	1.87	0.94	-0.25
0.6	1.3	220.0	0.3	0.5	1.15	0.00	1.15	1.27	0.49	-0.07
0.6	1.3	220.0	0.4	0.4	2.37	0.00	2.37	2.74	1.38	-0.37
0.6	1.3	220.0	0.4	0.5	1.33	0.00	1.33	1.26	0.54	-0.15
0.6	1.3	220.0	0.5	0.5	1.71	0.00	1.71	1.28	0.37	-0.08
0.6	1.3	250.0	0.3	0.3	2.15	0.00	2.15	2.68	1.99	-0.54
0.6	1.3	250.0	0.3	0.4	1.69	0.00	1.69	1.87	0.92	-0.23
0.6	1.3	250.0	0.3	0.5	1.15	0.00	1.15	1.28	0.48	-0.06
0.6	1.3	250.0	0.4	0.4	2.33	0.00	2.33	2.68	1.31	-0.34
0.6	1.3	250.0	0.4	0.5	1.30	0.00	1.30	1.20	0.50	-0.14
0.6	1.3	250.0	0.5	0.5	1.70	0.00	1.70	1.29	0.33	-0.07
0.6	1.5	40.0	0.3	0.3	2.00	0.00	2.00	2.89	2.24	-1.04

ENERGY FACTOR DATA (cont.)

Xnc	Bp(max)	L/G	Ts	Tr	XNI:	-1.8	-1.6	-1.4	-1.2	-1	-.8
0.6	1.5	40.0	0.3	0.4		1.60	0.00	1.60	2.05	1.47	-0.68
0.6	1.5	40.0	0.3	0.5		1.23	0.00	1.23	1.39	0.91	-0.45
0.6	1.5	40.0	0.4	0.4		3.09	0.00	3.09	3.30	2.05	-0.92
0.6	1.5	40.0	0.4	0.5		1.53	0.00	1.53	1.77	1.29	-0.73
0.6	1.5	40.0	0.5	0.5		1.85	0.00	1.85	2.09	1.60	-0.88
0.6	1.5	70.0	0.3	0.3		2.36	0.00	2.36	3.16	2.31	-1.00
0.6	1.5	70.0	0.3	0.4		1.93	0.00	1.93	2.29	1.45	-0.59
0.6	1.5	70.0	0.3	0.5		1.33	0.00	1.33	1.48	0.89	-0.36
0.6	1.5	70.0	0.4	0.4		3.36	0.00	3.36	3.54	1.89	-0.78
0.6	1.5	70.0	0.4	0.5		1.76	0.00	1.76	1.83	1.12	-0.55
0.6	1.5	70.0	0.5	0.5		1.94	0.00	1.94	2.00	1.27	-0.68
0.6	1.5	100.0	0.3	0.3		2.62	0.00	2.62	3.35	2.32	-0.87
0.6	1.5	100.0	0.3	0.4		2.04	0.00	2.04	2.36	1.41	-0.52
0.6	1.5	100.0	0.3	0.5		1.42	0.00	1.42	1.53	0.79	-0.26
0.6	1.5	100.0	0.4	0.4		3.27	0.00	3.27	3.78	2.02	-0.69
0.6	1.5	100.0	0.4	0.5		1.85	0.00	1.85	1.90	1.01	-0.42
0.6	1.5	100.0	0.5	0.5		2.08	0.00	2.08	2.04	0.94	-0.43
0.6	1.5	130.0	0.3	0.3		2.74	0.00	2.74	3.46	2.38	-0.81
0.6	1.5	130.0	0.3	0.4		2.12	0.00	2.12	2.41	1.37	-0.46
0.6	1.5	130.0	0.3	0.5		1.47	0.00	1.47	1.58	0.72	-0.20
0.6	1.5	130.0	0.4	0.4		3.26	0.00	3.26	3.86	2.08	-0.63
0.6	1.5	130.0	0.4	0.5		1.87	0.00	1.87	1.89	0.92	-0.33
0.6	1.5	130.0	0.5	0.5		2.20	0.00	2.20	1.93	0.75	-0.28
0.6	1.5	160.0	0.3	0.3		2.82	0.00	2.82	3.51	2.44	-0.78
0.6	1.5	160.0	0.3	0.4		2.17	0.00	2.17	2.44	1.33	-0.41
0.6	1.5	160.0	0.3	0.5		1.50	0.00	1.50	1.62	0.68	-0.16
0.6	1.5	160.0	0.4	0.4		3.22	0.00	3.22	3.86	2.08	-0.57
0.6	1.5	160.0	0.4	0.5		1.85	0.00	1.85	1.84	0.84	-0.27
0.6	1.5	160.0	0.5	0.5		2.25	0.00	2.25	1.79	0.64	-0.19
0.6	1.5	190.0	0.3	0.3		2.88	0.00	2.88	3.54	2.48	-0.75
0.6	1.5	190.0	0.3	0.4		2.20	0.00	2.20	2.45	1.28	-0.37
0.6	1.5	190.0	0.3	0.5		1.50	0.00	1.50	1.64	0.66	-0.13
0.6	1.5	190.0	0.4	0.4		3.16	0.00	3.16	3.80	2.05	-0.53
0.6	1.5	190.0	0.4	0.5		1.82	0.00	1.82	1.80	0.78	-0.23
0.6	1.5	190.0	0.5	0.5		2.27	0.00	2.27	1.78	0.56	-0.14
0.6	1.5	220.0	0.3	0.3		2.92	0.00	2.92	3.54	2.52	-0.73
0.6	1.5	220.0	0.3	0.4		2.22	0.00	2.22	2.45	1.24	-0.33
0.6	1.5	220.0	0.3	0.5		1.50	0.00	1.50	1.66	0.65	-0.10
0.6	1.5	220.0	0.4	0.4		3.09	0.00	3.09	3.70	1.99	-0.49
0.6	1.5	220.0	0.4	0.5		1.79	0.00	1.79	1.76	0.73	-0.20
0.6	1.5	220.0	0.5	0.5		2.30	0.00	2.30	1.78	0.50	-0.11
0.6	1.5	250.0	0.3	0.3		2.96	0.00	2.96	3.54	2.55	-0.72
0.6	1.5	250.0	0.3	0.4		2.23	0.00	2.23	2.45	1.21	-0.31
0.6	1.5	250.0	0.3	0.5		1.50	0.00	1.50	1.67	0.64	-0.09
0.6	1.5	250.0	0.4	0.4		3.18	0.00	3.18	3.56	1.75	-0.46
0.6	1.5	250.0	0.4	0.5		1.75	0.00	1.75	1.62	0.68	-0.18
0.6	1.5	250.0	0.5	0.5		2.30	0.00	2.30	1.77	0.45	-0.09
0.6	1.7	40.0	0.3	0.3		2.58	0.00	2.58	3.75	2.88	-1.34

ENERGY FACTOR DATA (cont.)

Xnc	Bp(max)	L/G	Ts	Tr	XNI:	-1.8	-1.6	-1.4	-1.2	-1	-0.8
0.6	1.7	40.0	0.3	0.4		2.07	0.00	2.07	2.65	1.89	-0.88
0.6	1.7	40.0	0.3	0.5		1.60	0.00	1.60	1.78	1.16	-0.58
0.6	1.7	40.0	0.4	0.4		3.93	0.00	3.93	4.26	2.63	-1.19
0.6	1.7	40.0	0.4	0.5		1.97	0.00	1.97	2.27	1.66	-0.94
0.6	1.7	40.0	0.5	0.5		2.39	0.00	2.39	2.69	2.04	-1.12
0.6	1.7	70.0	0.3	0.3		3.02	0.00	3.02	4.08	3.01	-1.31
0.6	1.7	70.0	0.3	0.4		2.48	0.00	2.48	2.96	1.88	-0.76
0.6	1.7	70.0	0.3	0.5		1.72	0.00	1.72	1.94	1.16	-0.47
0.6	1.7	70.0	0.4	0.4		4.31	0.00	4.31	4.51	2.43	-1.04
0.6	1.7	70.0	0.4	0.5		2.26	0.00	2.26	2.36	1.46	-0.72
0.6	1.7	70.0	0.5	0.5		2.63	0.00	2.63	2.67	1.66	-0.88
0.6	1.7	100.0	0.3	0.3		3.35	0.00	3.35	4.30	2.98	-1.13
0.6	1.7	100.0	0.3	0.4		2.61	0.00	2.61	3.03	1.83	-0.67
0.6	1.7	100.0	0.3	0.5		1.82	0.00	1.82	1.96	1.03	-0.34
0.6	1.7	100.0	0.4	0.4		4.25	0.00	4.25	4.88	2.60	-0.89
0.6	1.7	100.0	0.4	0.5		2.41	0.00	2.41	2.46	1.31	-0.54
0.6	1.7	100.0	0.5	0.5		2.87	0.00	2.87	2.73	1.24	-0.56
0.6	1.7	130.0	0.3	0.3		3.52	0.00	3.52	4.41	3.01	-1.07
0.6	1.7	130.0	0.3	0.4		2.70	0.00	2.70	3.08	1.79	-0.60
0.6	1.7	130.0	0.3	0.5		1.88	0.00	1.88	2.00	0.94	-0.26
0.6	1.7	130.0	0.4	0.4		4.19	0.00	4.19	5.00	2.68	-0.81
0.6	1.7	130.0	0.4	0.5		2.44	0.00	2.44	2.45	1.19	-0.43
0.6	1.7	130.0	0.5	0.5		2.99	0.00	2.99	2.61	0.97	-0.38
0.6	1.7	160.0	0.3	0.3		3.62	0.00	3.62	4.49	3.04	-1.03
0.6	1.7	160.0	0.3	0.4		2.77	0.00	2.77	3.10	1.73	-0.54
0.6	1.7	160.0	0.3	0.5		1.92	0.00	1.92	2.03	0.89	-0.21
0.6	1.7	160.0	0.4	0.4		4.13	0.00	4.13	5.03	2.70	-0.74
0.6	1.7	160.0	0.4	0.5		2.42	0.00	2.42	2.39	1.09	-0.35
0.6	1.7	160.0	0.5	0.5		3.02	0.00	3.02	2.48	0.81	-0.26
0.6	1.7	190.0	0.3	0.3		3.70	0.00	3.70	4.52	3.07	-0.99
0.6	1.7	190.0	0.3	0.4		2.81	0.00	2.81	3.10	1.66	-0.48
0.6	1.7	190.0	0.3	0.5		1.93	0.00	1.93	2.05	0.87	-0.17
0.6	1.7	190.0	0.4	0.4		4.06	0.00	4.06	5.00	2.67	-0.68
0.6	1.7	190.0	0.4	0.5		2.40	0.00	2.40	2.35	1.01	-0.30
0.6	1.7	190.0	0.5	0.5		3.03	0.00	3.03	2.45	0.71	-0.18
0.6	1.7	220.0	0.3	0.3		3.76	0.00	3.76	4.53	3.09	-0.97
0.6	1.7	220.0	0.3	0.4		2.83	0.00	2.83	3.09	1.61	-0.44
0.6	1.7	220.0	0.3	0.5		1.92	0.00	1.92	2.06	0.85	-0.14
0.6	1.7	220.0	0.4	0.4		4.00	0.00	4.00	4.92	2.61	-0.63
0.6	1.7	220.0	0.4	0.5		2.38	0.00	2.38	2.32	0.95	-0.26
0.6	1.7	220.0	0.5	0.5		3.06	0.00	3.06	2.41	0.65	-0.14
0.6	1.7	250.0	0.3	0.3		3.81	0.00	3.81	4.52	3.11	-0.94
0.6	1.7	250.0	0.3	0.4		2.84	0.00	2.84	3.08	1.56	-0.40
0.6	1.7	250.0	0.3	0.5		1.92	0.00	1.92	2.06	0.83	-0.12
0.6	1.7	250.0	0.4	0.4		3.97	0.00	3.97	4.82	2.50	-0.59
0.6	1.7	250.0	0.4	0.5		2.35	0.00	2.35	2.25	0.89	-0.23
0.6	1.7	250.0	0.5	0.5		3.04	0.00	3.04	2.39	0.60	-0.11
0.6	1.9	40.0	0.3	0.3		3.21	0.00	3.21	4.69	3.61	-1.67

ENERGY FACTOR DATA (cont.)

Xnc	Bp(max)	L/G	Ts	Tr	XNI:	-1.8	-1.6	-1.4	-1.2	-1	-.8
0.6	1.9	40.0	0.3	0.4		2.58	0.00	2.58	3.31	2.36	-1.11
0.6	1.9	40.0	0.3	0.5		1.99	0.00	1.99	2.22	1.45	-0.72
0.6	1.9	40.0	0.4	0.4		4.82	0.00	4.82	5.33	3.27	-1.50
0.6	1.9	40.0	0.4	0.5		2.45	0.00	2.45	2.84	2.07	-1.17
0.6	1.9	40.0	0.5	0.5		3.00	0.00	3.00	3.37	2.54	-1.39
0.6	1.9	70.0	0.3	0.3		3.74	0.00	3.74	5.11	3.80	-1.66
0.6	1.9	70.0	0.3	0.4		3.10	0.00	3.10	3.71	2.36	-0.96
0.6	1.9	70.0	0.3	0.5		2.16	0.00	2.16	2.45	1.46	-0.59
0.6	1.9	70.0	0.4	0.4		5.38	0.00	5.38	5.61	3.08	-1.35
0.6	1.9	70.0	0.4	0.5		2.83	0.00	2.83	2.98	1.85	-0.91
0.6	1.9	70.0	0.5	0.5		3.42	0.00	3.42	3.54	2.10	-1.10
0.6	1.9	100.0	0.3	0.3		4.15	0.00	4.15	5.34	3.72	-1.45
0.6	1.9	100.0	0.3	0.4		3.25	0.00	3.25	3.79	2.31	-0.85
0.6	1.9	100.0	0.3	0.5		2.27	0.00	2.27	2.45	1.31	-0.43
0.6	1.9	100.0	0.4	0.4		5.34	0.00	5.34	6.10	3.26	-1.13
0.6	1.9	100.0	0.4	0.5		3.05	0.00	3.05	3.11	1.65	-0.69
0.6	1.9	100.0	0.5	0.5		3.74	0.00	3.74	3.59	1.62	-0.70
0.6	1.9	130.0	0.3	0.3		4.36	0.00	4.36	5.47	3.73	-1.37
0.6	1.9	130.0	0.3	0.4		3.36	0.00	3.36	3.84	2.27	-0.76
0.6	1.9	130.0	0.3	0.5		2.33	0.00	2.33	2.48	1.21	-0.33
0.6	1.9	130.0	0.4	0.4		5.23	0.00	5.23	6.28	3.36	-1.01
0.6	1.9	130.0	0.4	0.5		3.09	0.00	3.09	3.10	1.49	-0.54
0.6	1.9	130.0	0.5	0.5		3.92	0.00	3.92	3.51	1.22	-0.48
0.6	1.9	160.0	0.3	0.3		4.49	0.00	4.49	5.57	3.74	-1.31
0.6	1.9	160.0	0.3	0.4		3.44	0.00	3.44	3.87	2.20	-0.68
0.6	1.9	160.0	0.3	0.5		2.38	0.00	2.38	2.51	1.13	-0.27
0.6	1.9	160.0	0.4	0.4		5.14	0.00	5.14	6.33	3.38	-0.92
0.6	1.9	160.0	0.4	0.5		3.07	0.00	3.07	3.03	1.37	-0.44
0.6	1.9	160.0	0.5	0.5		3.96	0.00	3.96	3.37	1.00	-0.34
0.6	1.9	190.0	0.3	0.3		4.58	0.00	4.58	5.61	3.76	-1.27
0.6	1.9	190.0	0.3	0.4		3.48	0.00	3.48	3.87	2.13	-0.62
0.6	1.9	190.0	0.3	0.5		2.40	0.00	2.40	2.52	1.10	-0.22
0.6	1.9	190.0	0.4	0.4		5.05	0.00	5.05	6.32	3.37	-0.85
0.6	1.9	190.0	0.4	0.5		3.05	0.00	3.05	3.00	1.28	-0.37
0.6	1.9	190.0	0.5	0.5		4.01	0.00	4.01	3.36	0.91	-0.24
0.6	1.9	220.0	0.3	0.3		4.65	0.00	4.65	5.62	3.76	-1.23
0.6	1.9	220.0	0.3	0.4		3.48	0.00	3.48	3.84	2.07	-0.56
0.6	1.9	220.0	0.3	0.5		2.39	0.00	2.39	2.53	1.08	-0.18
0.6	1.9	220.0	0.4	0.4		4.96	0.00	4.96	6.28	3.31	-0.79
0.6	1.9	220.0	0.4	0.5		3.04	0.00	3.04	2.95	1.20	-0.33
0.6	1.9	220.0	0.5	0.5		4.08	0.00	4.08	3.33	0.83	-0.18
0.6	1.9	250.0	0.3	0.3		4.71	0.00	4.71	5.61	3.77	-1.19
0.6	1.9	250.0	0.3	0.4		3.52	0.00	3.52	3.80	1.94	-0.51
0.6	1.9	250.0	0.3	0.5		2.38	0.00	2.38	2.53	1.06	-0.15
0.6	1.9	250.0	0.4	0.4		4.87	0.00	4.87	6.21	3.23	-0.73
0.6	1.9	250.0	0.4	0.5		3.00	0.00	3.00	2.90	1.13	-0.29
0.6	1.9	250.0	0.5	0.5		4.05	0.00	4.05	3.30	0.77	-0.14
0.6	2.1	40.0	0.3	0.3		3.90	0.00	3.90	5.72	4.40	-2.04

ENERGY FACTOR DATA (cont.)

Xnc	Bp(max)	L/G	Ts	Tr	XNI:	-1.8	-1.6	-1.4	-1.2	-1	-0.8
0.6	2.1	40.0	0.3	0.4		3.15	0.00	3.15	4.04	2.88	-1.35
0.6	2.1	40.0	0.3	0.5		2.42	0.00	2.42	2.71	1.77	-0.89
0.6	2.1	40.0	0.4	0.4		5.87	0.00	5.87	6.53	3.99	-1.85
0.6	2.1	40.0	0.4	0.5		2.99	0.00	2.99	3.48	2.53	-1.43
0.6	2.1	40.0	0.5	0.5		3.67	0.00	3.67	4.20	3.10	-1.70
0.6	2.1	70.0	0.3	0.3		4.53	0.00	4.53	6.22	4.70	-2.08
0.6	2.1	70.0	0.3	0.4		3.77	0.00	3.77	4.54	2.90	-1.19
0.6	2.1	70.0	0.3	0.5		2.63	0.00	2.63	3.02	1.81	-0.73
0.6	2.1	70.0	0.4	0.4		6.52	0.00	6.52	6.83	3.87	-1.70
0.6	2.1	70.0	0.4	0.5		3.46	0.00	3.46	3.71	2.32	-1.13
0.6	2.1	70.0	0.5	0.5		4.32	0.00	4.32	4.59	2.61	-1.36
0.6	2.1	100.0	0.3	0.3		5.05	0.00	5.05	6.48	4.55	-1.83
0.6	2.1	100.0	0.3	0.4		3.95	0.00	3.95	4.63	2.85	-1.05
0.6	2.1	100.0	0.3	0.5		2.75	0.00	2.75	3.00	1.65	-0.53
0.6	2.1	100.0	0.4	0.4		6.53	0.00	6.53	7.43	4.01	-1.43
0.6	2.1	100.0	0.4	0.5		3.76	0.00	3.76	3.85	2.07	-0.86
0.6	2.1	100.0	0.5	0.5		4.73	0.00	4.73	4.75	2.06	-0.84
0.6	2.1	130.0	0.3	0.3		5.29	0.00	5.29	6.62	4.54	-1.73
0.6	2.1	130.0	0.3	0.4		4.08	0.00	4.08	4.70	2.81	-0.94
0.6	2.1	130.0	0.3	0.5		2.83	0.00	2.83	3.03	1.53	-0.41
0.6	2.1	130.0	0.4	0.4		6.36	0.00	6.36	7.70	4.13	-1.26
0.6	2.1	130.0	0.4	0.5		3.84	0.00	3.84	3.87	1.85	-0.68
0.6	2.1	130.0	0.5	0.5		4.95	0.00	4.95	4.68	1.57	-0.60
0.6	2.1	160.0	0.3	0.3		5.46	0.00	5.46	6.76	4.52	-1.63
0.6	2.1	160.0	0.3	0.4		4.19	0.00	4.19	4.72	2.73	-0.85
0.6	2.1	160.0	0.3	0.5		2.90	0.00	2.90	3.04	1.42	-0.33
0.6	2.1	160.0	0.4	0.4		6.24	0.00	6.24	7.78	4.17	-1.14
0.6	2.1	160.0	0.4	0.5		3.82	0.00	3.82	3.79	1.69	-0.55
0.6	2.1	160.0	0.5	0.5		5.04	0.00	5.04	4.59	1.26	-0.43
0.6	2.1	190.0	0.3	0.3		5.55	0.00	5.55	6.81	4.54	-1.58
0.6	2.1	190.0	0.3	0.4		4.23	0.00	4.23	4.72	2.65	-0.77
0.6	2.1	190.0	0.3	0.5		2.92	0.00	2.92	3.06	1.38	-0.27
0.6	2.1	190.0	0.4	0.4		6.08	0.00	6.08	7.78	4.17	-1.04
0.6	2.1	190.0	0.4	0.5		3.79	0.00	3.79	3.75	1.58	-0.46
0.6	2.1	190.0	0.5	0.5		5.17	0.00	5.17	4.59	1.15	-0.31
0.6	2.1	220.0	0.3	0.3		5.63	0.00	5.63	6.82	4.53	-1.54
0.6	2.1	220.0	0.3	0.4		4.23	0.00	4.23	4.69	2.58	-0.70
0.6	2.1	220.0	0.3	0.5		2.91	0.00	2.91	3.07	1.36	-0.23
0.6	2.1	220.0	0.4	0.4		5.94	0.00	5.94	7.75	4.09	-0.96
0.6	2.1	220.0	0.4	0.5		3.76	0.00	3.76	3.69	1.49	-0.40
0.6	2.1	220.0	0.5	0.5		5.27	0.00	5.27	4.59	1.07	-0.23
0.6	2.1	250.0	0.3	0.3		5.69	0.00	5.69	6.81	4.53	-1.50
0.6	2.1	250.0	0.3	0.4		4.28	0.00	4.28	4.65	2.42	-0.63
0.6	2.1	250.0	0.3	0.5		2.90	0.00	2.90	3.06	1.33	-0.19
0.6	2.1	250.0	0.4	0.4		5.85	0.00	5.85	7.68	3.98	-0.91
0.6	2.1	250.0	0.4	0.5		3.72	0.00	3.72	3.61	1.41	-0.36
0.6	2.1	250.0	0.5	0.5		5.29	0.00	5.29	4.56	1.00	-0.17

$$t_r/\lambda : 0,3, 0,4, 0,5$$

$$X_{ni} : -1,8, -1,6, -1,4, -1,2, -1, -0,8$$

In order to limit the current in the winding 70 kA is chosen as mmf limit during this computation.

3.4 OBSERVATIONS ON THE OBTAINED ENERGY FACTOR DATA

Typical energy factor vs normalized switch-on position (X_{ni}) curves for different conduction periods are shown in fig. 3.8, as seen from this figure energy factor increases while normalized conduction period (X_{ni}) is increased. Therefore unity conduction period maximizes energy factor. Additionally it is observed that (X_{ni}) value which corresponds to peak of this curve shifts toward -1.6 from -1.2 while conduction period is increased. However, optimum (X_{ni}) value is also affected by $B_{p(max)}$ and t_s/λ , t_r/λ as discussed below. Therefore shifting from -1.6 to -1.2 in (X_{ni}) value denoted in fig. 3.8 is valid for this special case only.

In fig. 3.9, energy factor vs. normalized switch-on position curves for different B values are shown. As seen from this figure energy factor is increased by increasing $B_{p(max)}$ and it is maximized when $B_{p(max)} = 2,1 T$. It is observed that increasing $B_{p(max)}$ shifts X_{ni} value which corresponds to peak of the curve,

Fig. 3.9 Energy Factor vs X_{ni} Curves

$t_s/\lambda = 0.3$
 $t_r/\lambda = 0.4$
 $\lambda/g = 100$
 $X_{nc} = 1$

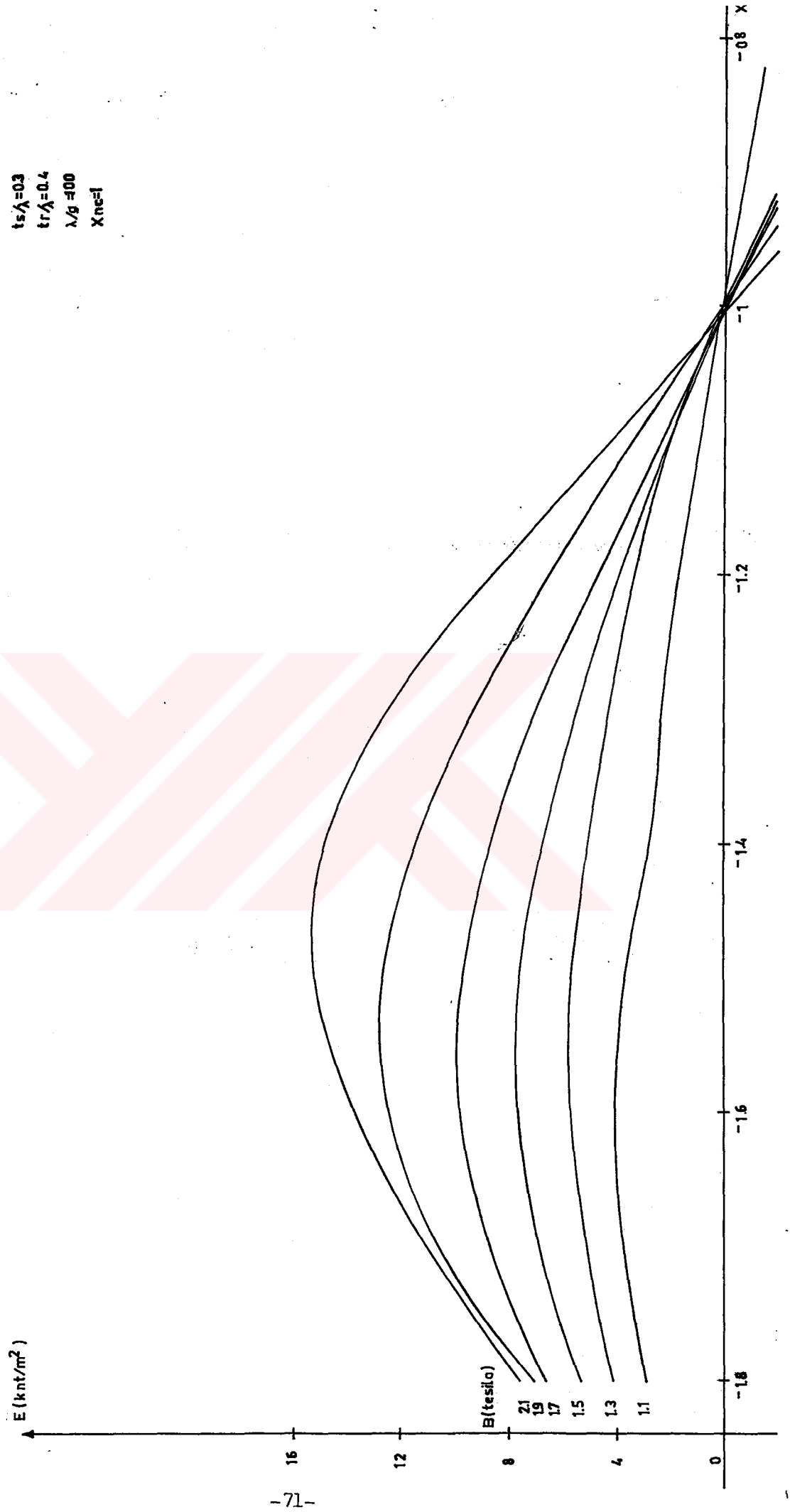
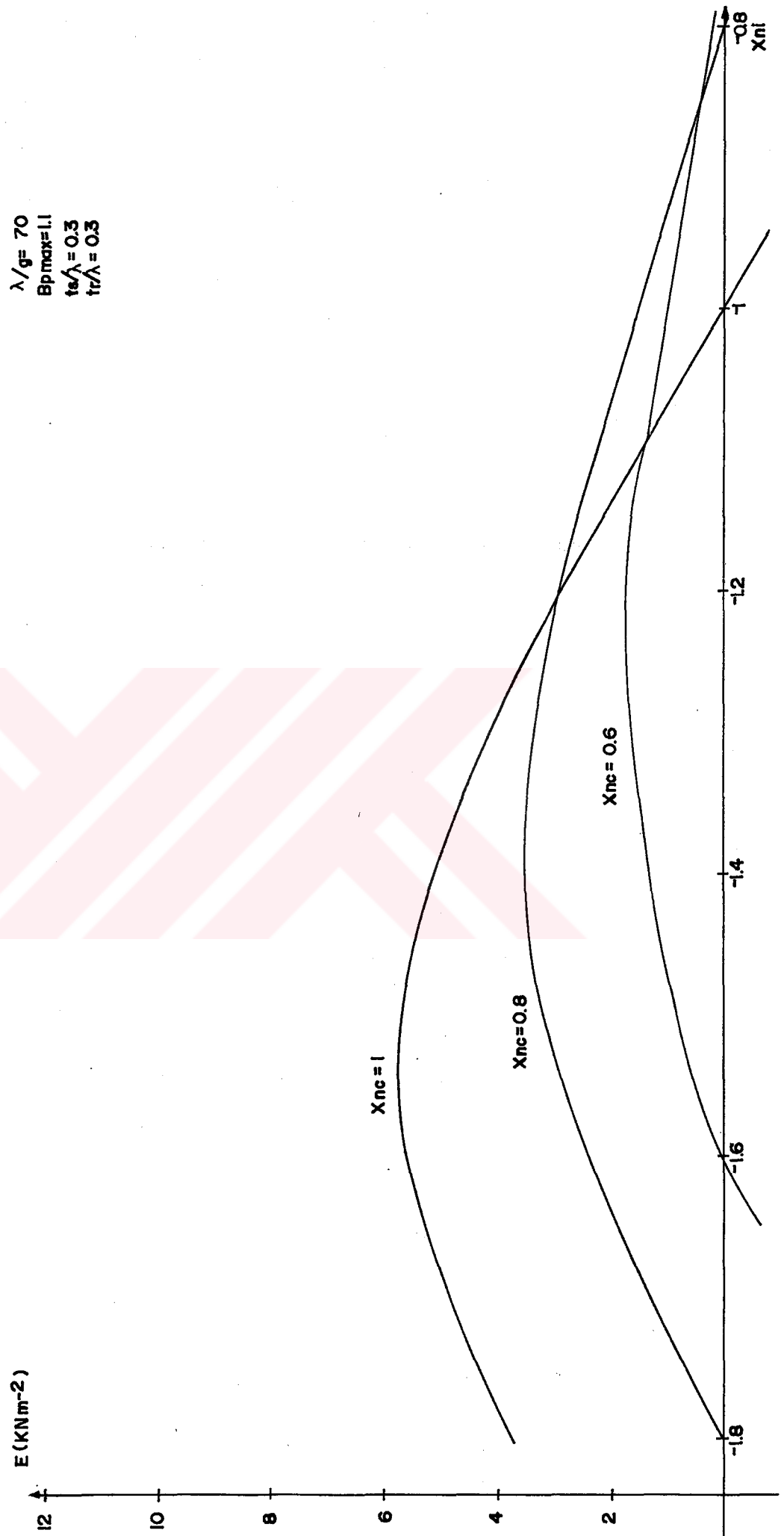


Fig. 3.8 Energy Uactor vs X_{ni} Curves

$\lambda/g = 70$
 $Bp_{max} = 1.1$
 $t_e/\lambda = 0.3$
 $t_r/\lambda = 0.3$



from -1.6, to -1.4,

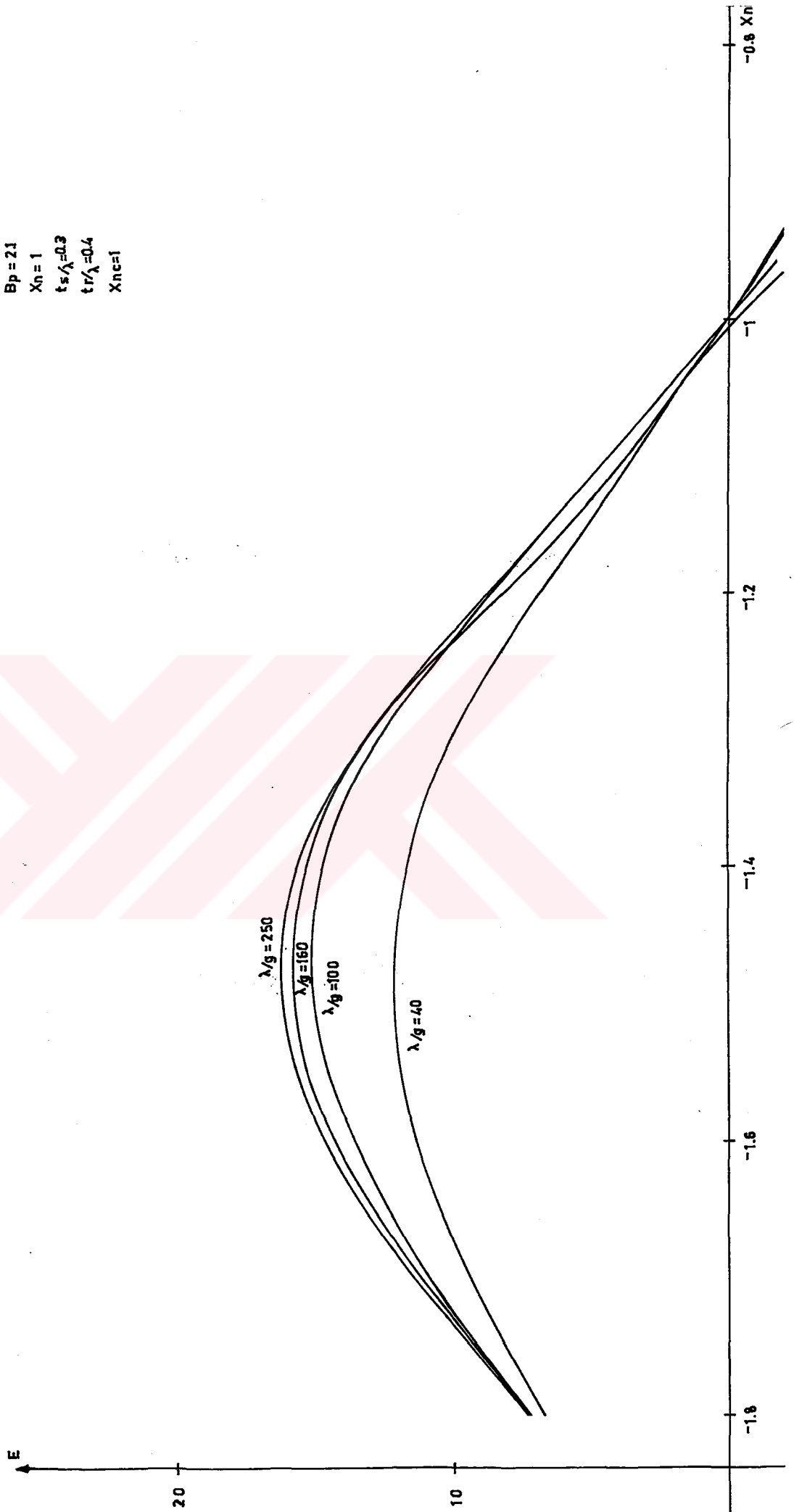
In fig. 3.10 energy factor vs X_{ni} curves with respect to different λ/g values are shown. This figure shows that increasing λ/g does not change optimum X_{ni} value. As seen from same figure, increasing λ/g also maximizes energy factor at $B_{p(max)} = 2.1 T$. In fig 3.11, effect of $B_{p(max)}$ on energy factor vs λ/g curves are shown. For $B_{p(max)}$ values higher than 1.3 T, optimum λ/g occurs at 250. However, for lower $B_{p(max)}$ values (i.e lower than 1.3) optimum occurs at lower λ/g values also depending on tooth widths. For larger tooth widths this optimum value is shifted lower λ/g values as well, for example at $B_{p(max)} = 1.3 T$ optimum λ/g occurs at 250, 190, 160 for normalized tooth widths 0.3, 0.4, 0.5 respectively.

For $\lambda/g = 100$ and for $B_{p(max)} = 1.7$ only 4% increase in energy factor is observed by making λ/g larger than 160 at 2.1 T. Therefore it is not meaningful to air-gap larger than λ/g 's than 160.

In fig. 3.12 the effects of available tooth widths on energy factor are shown. It is observed that $t_s/\lambda = t_r/\lambda = 0.4$ maximizes energy factor. But in order to observe the effect of tooth width on energy factor accurately, E vs $(t_s/\lambda$ or $t_r/\lambda)$ curves should be used. For each Energy factor vs $(t_r/\lambda, t_s/\lambda)$ curves there are 3 points computed. Therefore in order to draw

Fig. 3.10 Energy Factor vs X_{ni} Curves

$Bp = 2.1$
 $Xn = 1$
 $ts/\lambda = 0.3$
 $tr/\lambda = 0.4$
 $Xnc = 1$



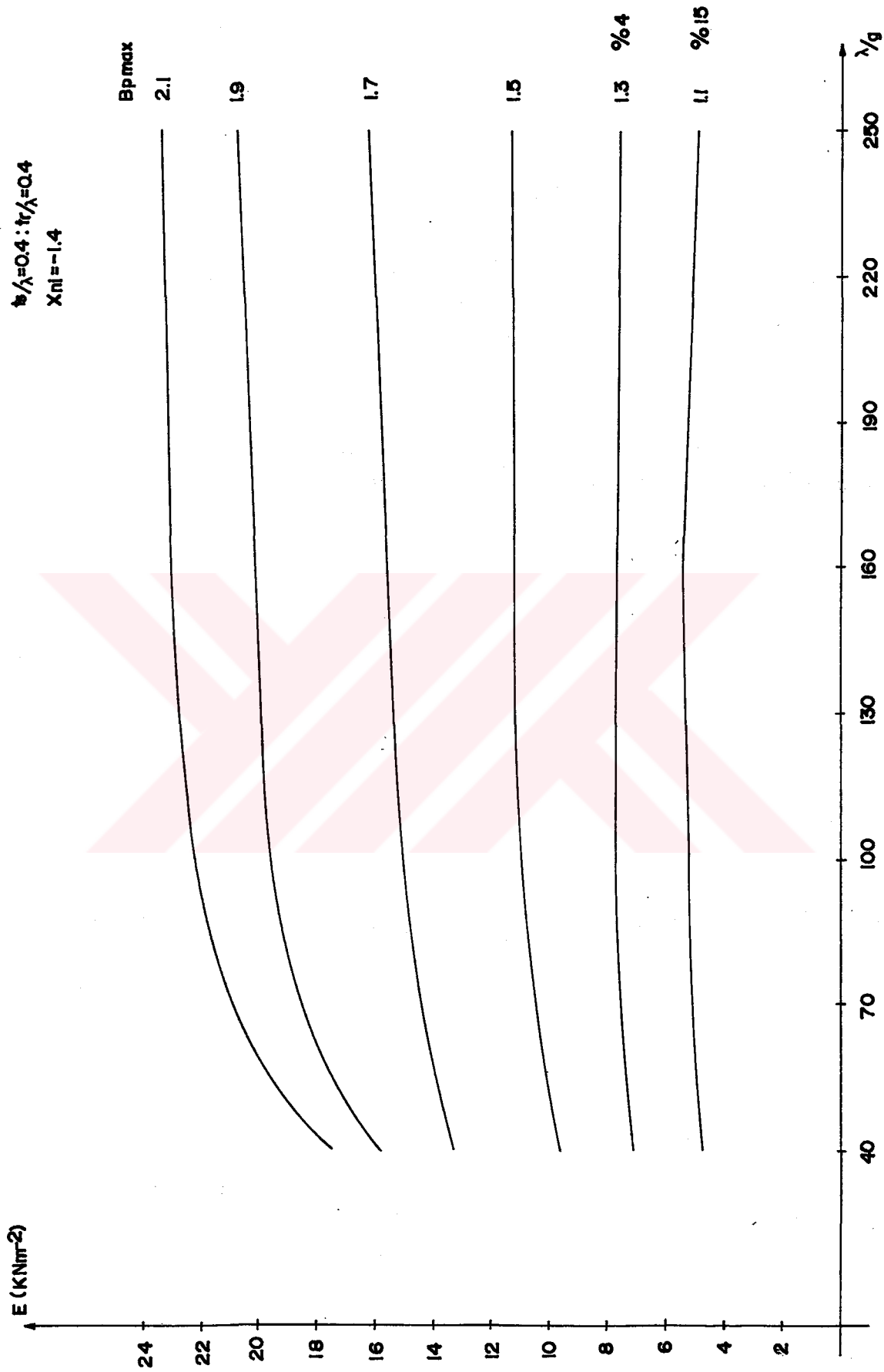
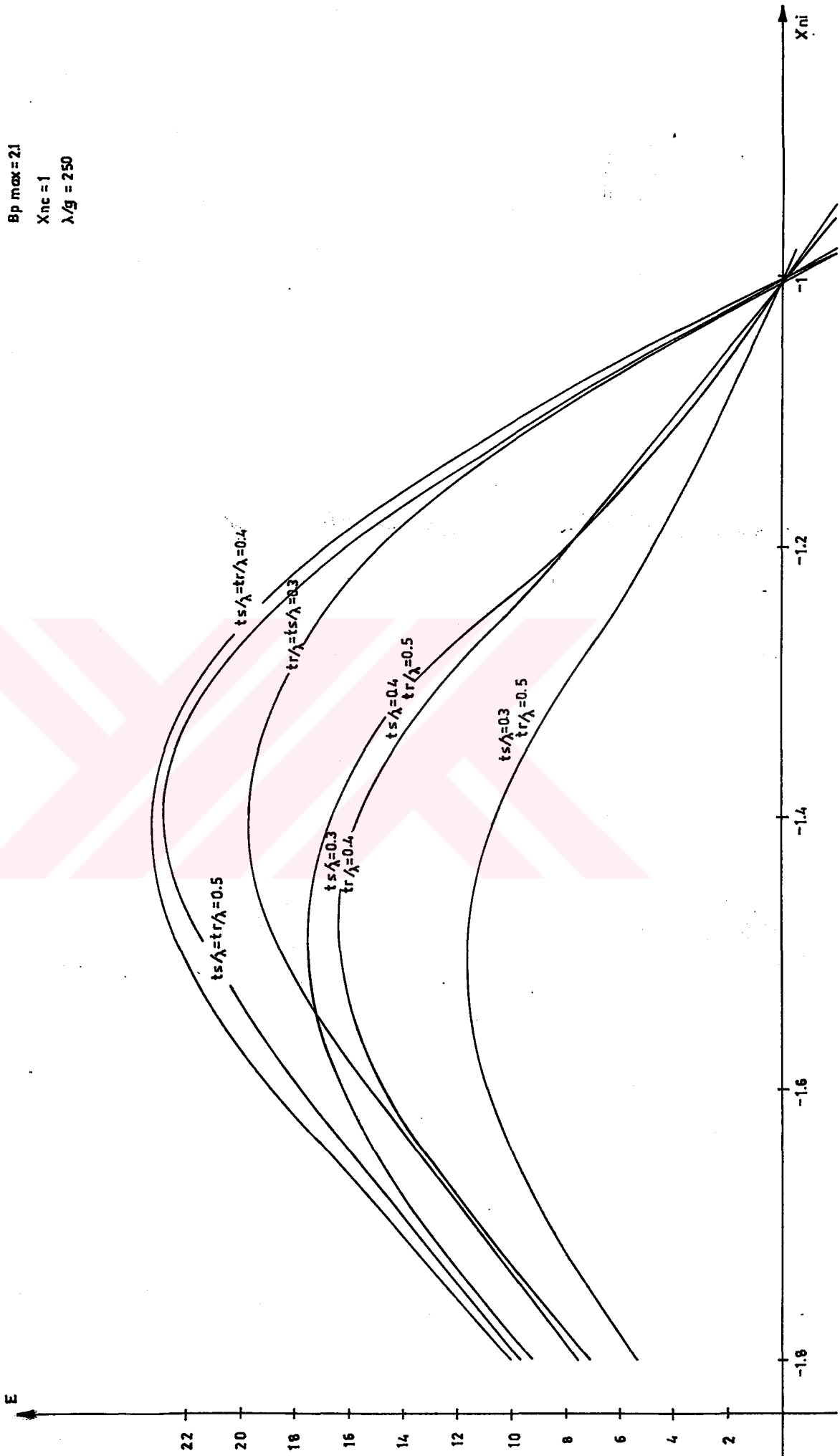


Fig. 3.11 Energy Factor vs λ/g Curves

Fig. 3.12 Energy Factor vs X_{ni} Curves



exact shape of these curves, energy factors of intermediate tooth width values are also computed for this part of the work. However, for obtaining accurate optimum value of accurate calculation should be done for rest of the parameters. This will be given in optimization work in chapter 4. Therefore this approach done here is, only for obtaining exact shape of energy factor vs $(t_s/\lambda, t_r/\lambda)$ curves.

In fig. 3.13, energy factor vs t_r/λ curve for different t_s/λ values are shown. It is observed that energy factor decreases while the difference between rotor and stator tooth width increases. In other words, while the tooth widths of rotor and stator converge to each other, energy factor increases and it is maximized when tooth widths of stator and rotor are equal to each other.

Since, rotor tooth width can not be less than stator tooth width because of the constraint $t_s/\lambda \geq t_r/\lambda$, then each curve starts at different t_r/λ value which is $t_r/\lambda = t_s/\lambda$. Therefore the peak value of energy factor is beginning point of this curve as seen in fig. 3.13. As discussed above, increasing in value of $B_{p(max)}$ increases energy factor. It is possible to see same effect of $B_{p(max)}$ in fig 3.13. Additionally it is observed that the difference between energy factor vs t_r/λ curves for different t_s/λ values get closer to each other.

$\chi_{nc} = -1.4$
 $\lambda/g = 250$

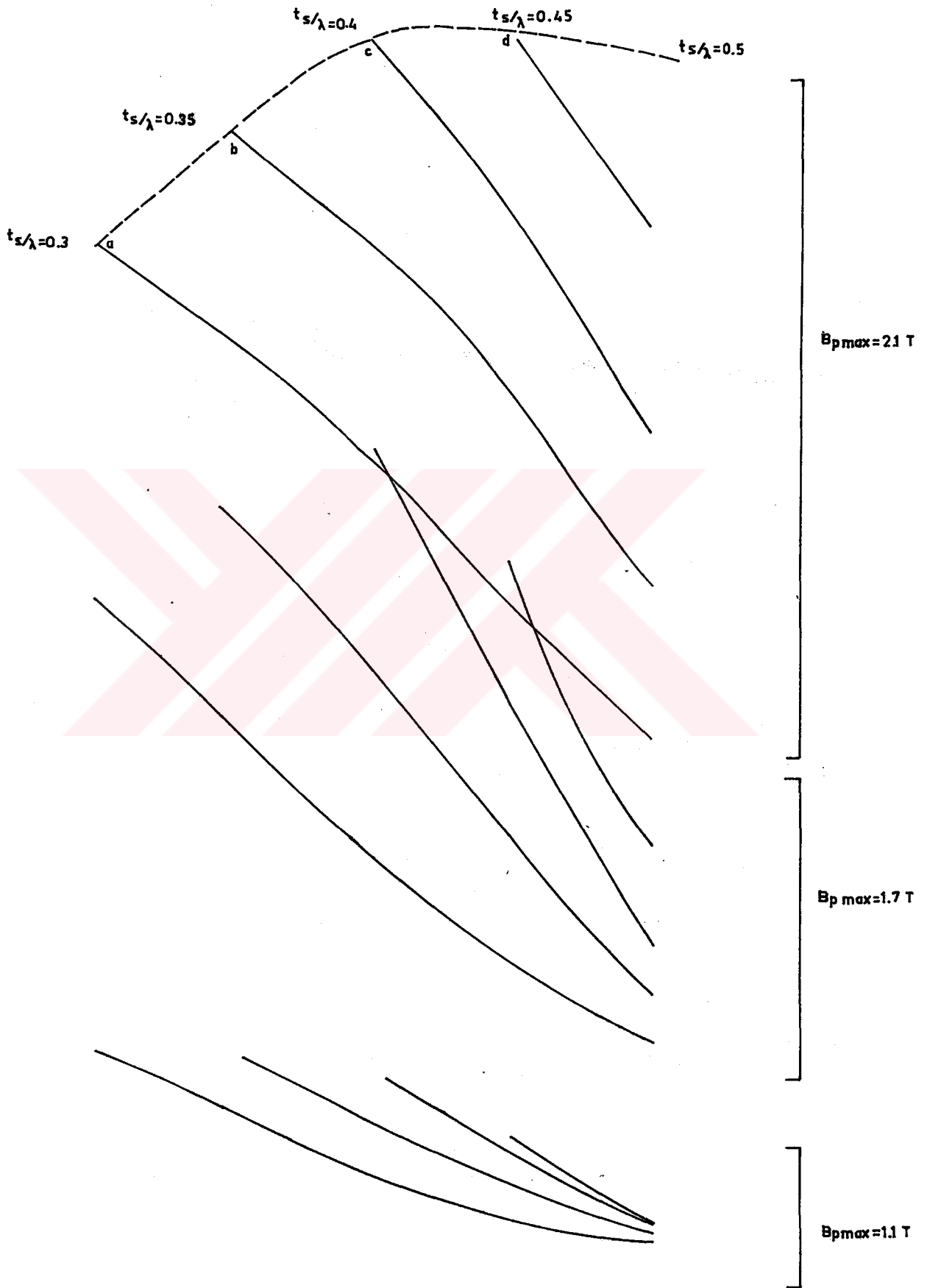
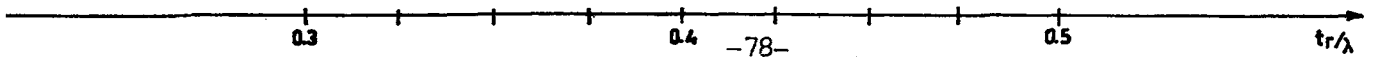


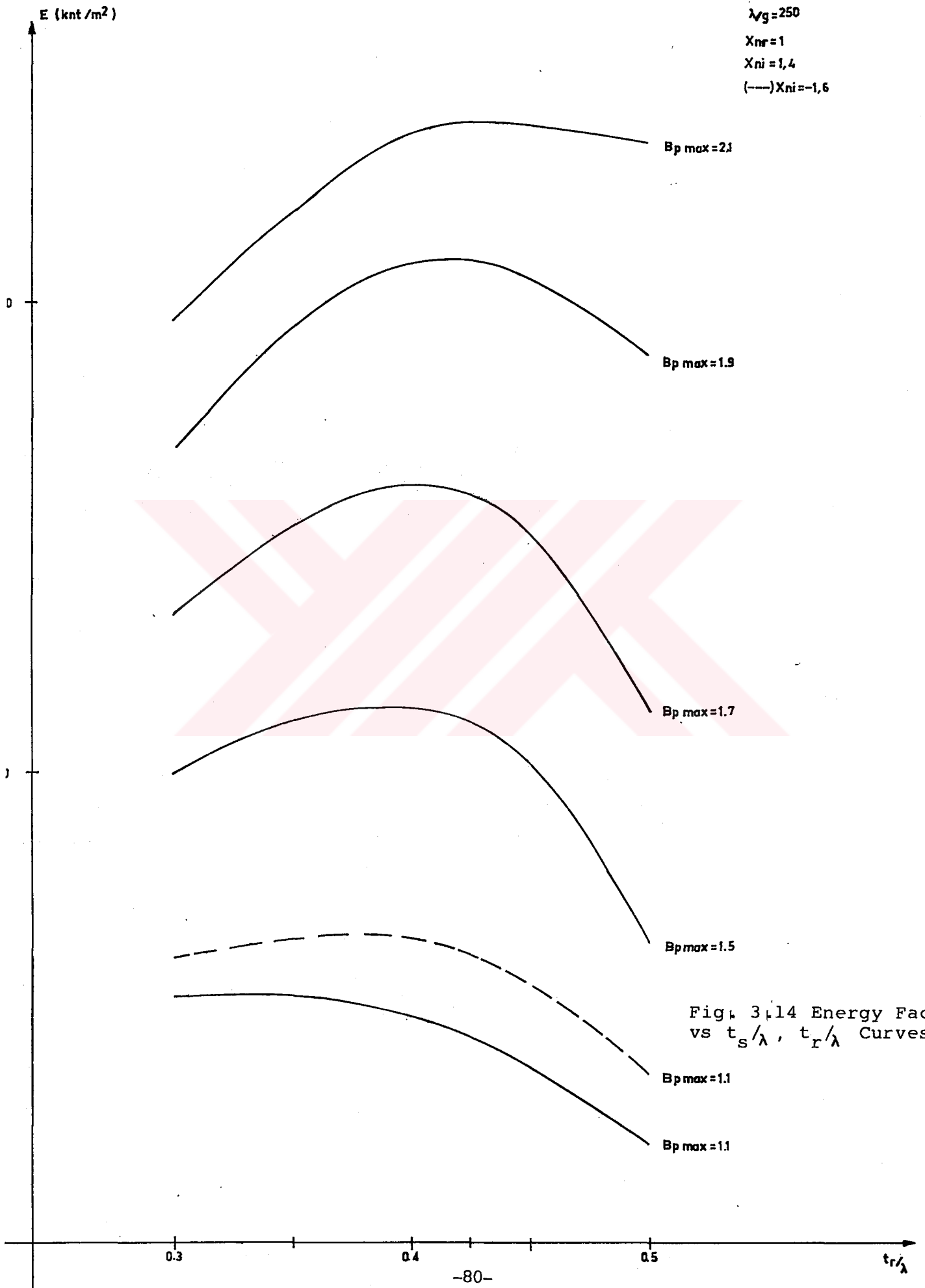
Fig. 3.13 Energy Factor vs t_r/λ Curves



As mentioned above for a fixed stator tooth width, energy factor is maximized when stator-rotor pairs are identical and this situation correspond to the points marked with letters a, b, c, d in fig, 3,13 of these curves, Therefore it is possible to observe the variation of energy factor while stator and rotor tooth widths change equally without destroying symmetry between them as denoted by dotted line in fig, 3,13,

Since it is understood that energy factor maximizes if rotor and stator tooth widths are equal to each other, then the effect of variation of identical tooth pair on energy factor should be investigated,

In fig, 3,14, energy factor vs identical tooth width curves for different $B_{p(max)}$ values are shown, In order to draw exact shape of the curve, energy factor values are also computed for intermediate values of tooth widths which are not available in table (3,7), As seen from fig 3,24, it is observed that the value of tooth width which maximizes energy factor depends on $B_{p(max)}$, As seen from this figure for $B = 1,1T \ t_s/\lambda = t_r/\lambda = 0,35$ maximizes energy factor, but while B increases the optimum value of tooth width shifts toward 0,4, But, these curves have X_{ni} value which is -1,4, However, it is known from earlier discussions that while B_t reduces, the X_{ni} value which maximizes energy factor shifts from -1,4 to -1,6, Therefore the optimum value of tooth width



E (KN/m²)

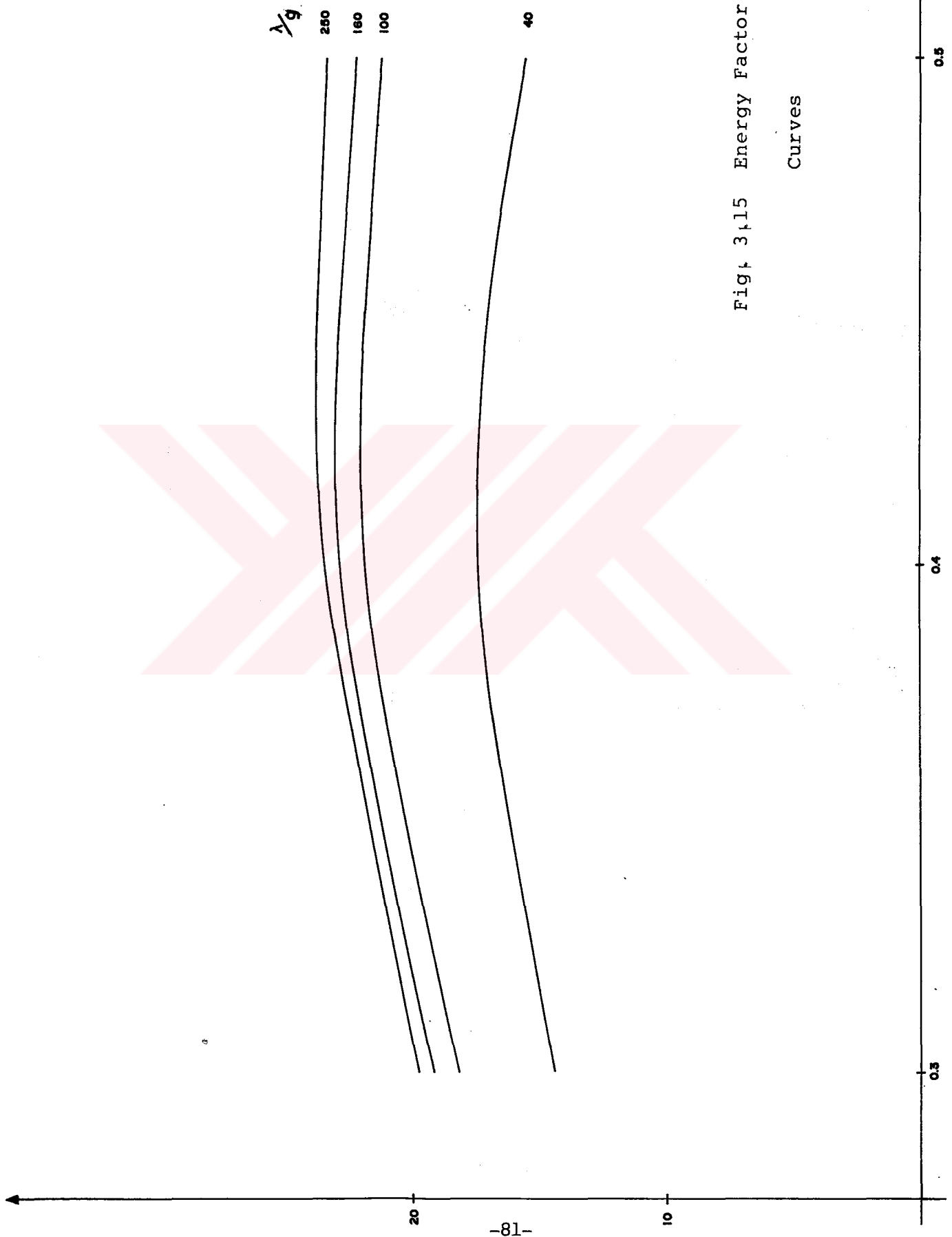


Fig. 3.15 Energy Factor vs t_s/λ , t_r/λ
Curves

should be investigated at $X_{ni} = -1.6$ for low values of B_p . As denoted by dotted line, for $B_p = 1.1 T$, optimum tooth width is about 0.40 for $B = 2.1$ it is observed that the optimum tooth width is 0.42 while $\lambda/g = 250$, $X_{nc} = 1$ and $X_{ni} = -1.4$. This result for optimum tooth width verifies the result of non-linear theory developed by Harris Lawrenson and Huges.

Although it is known that $\lambda/g = 250$ maximizes energy factor at $B_{p(max)} = 1.3 T$, the effect of λ/g on energy factor vs tooth width should also be investigated. As shown in fig. 3.15 varying λ/g does not change the optimum value of tooth width. It is known from earlier discussions in this section that while λ/g is increased, energy factor increases but smaller in amount for $B_{p(max)}$ higher than 1.3 T. Same property may be seen in this figure.

Until here, some observations for the effect of parameters on energy factor are determined. According to these observations, it is understood that following parameter values maximize energy factor.

$$X_{ni} = -1.4 \quad : \quad X_{nc} = 1 \quad : \quad B_{p(max)} = 2.1 \quad : \quad \lambda/g = 250 \quad :$$

$$t_s/\lambda = t_r/\lambda = 0.42$$

But, since these observations have been obtained

by using the computed energy factor data tabulated in table (3,7), can not give accurate values of parameters which maximize energy factor. Above results can only give rough values of parameters.

Mmf Limit: As mentioned in section 3,3,4 upper limit of mmf is chosen as 70 kA. Whole energy factor data tabulated in table(3,7) are computed under this restriction. Besides that, in order to see the effect of this constrain, energy factor is computed for different mmf limits. In fig, 3,16 energy factor vs mmf limit curves of optimum design found above with respect to different $B_{p(max)}$ values are shown. As may be seen from this figure, energy factor increases while mmf limit increases and after certain value of this limit, it becomes asymptotical. However this value of mmf limit reduces by decreasing $B_{p(max)}$ so that energy factor vs mmf limit curve becomes nearly asymptotical at $B_{p(max)} = 1,1$ Tesla.

As mentioned earlier, these curves are belong to optimum design which is found in this section at 70 kA mmf limit. But, as demonstrated in optimization work given in chapter 4, for mmf limits lower than 40 kA, the optimum values of parameters change. Therefore, this situation should be taken into account in choosing mmf limits design stage.

CONCLUSION:

In this chapter, energy factor data of U_{dss}

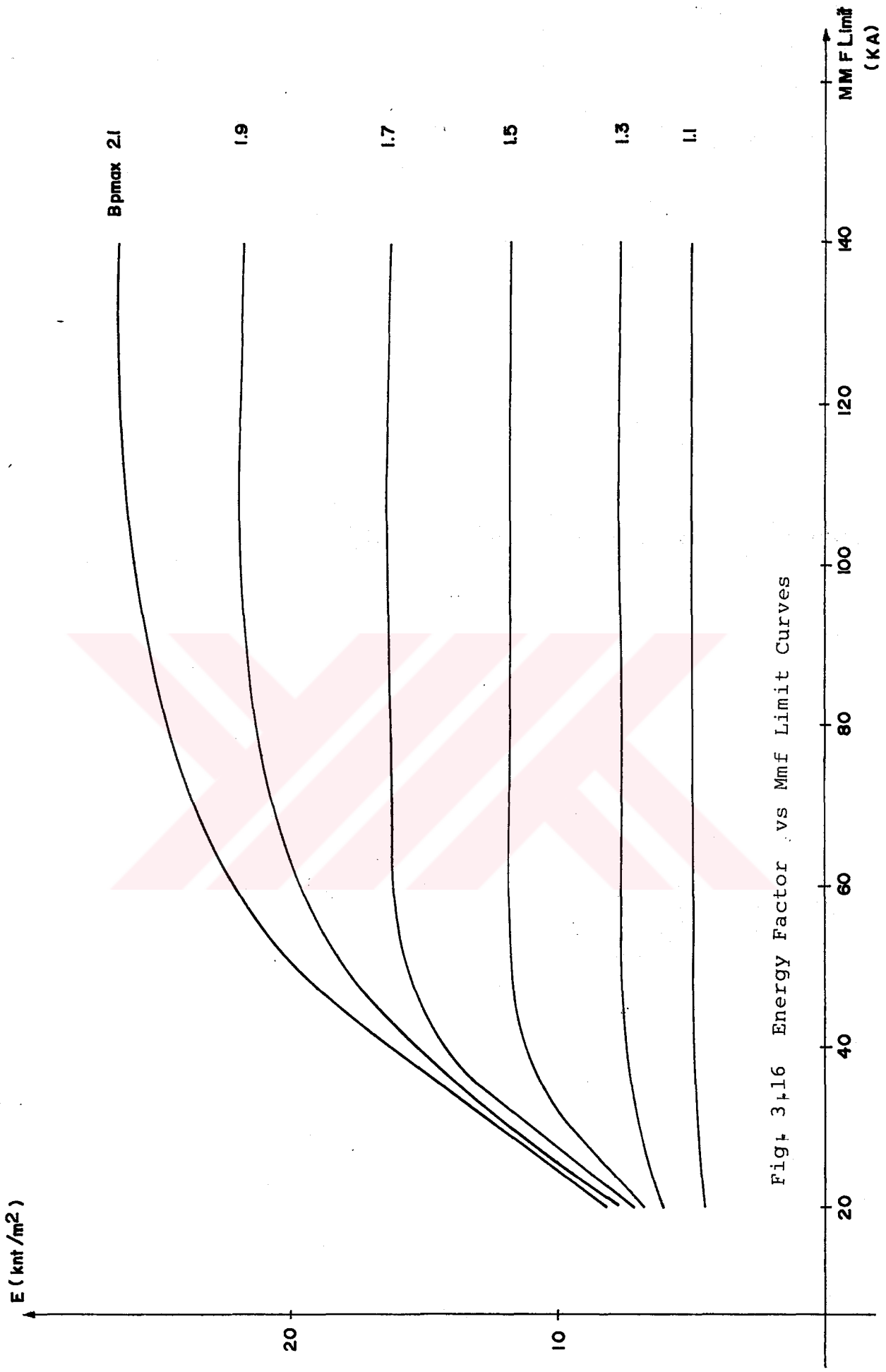


Fig. 3.16 Energy Factor vs Mmf Limit Curves

under different magnetic loading switching conditions are computed by applying the method described in previous chapter with the aid of a computer program.

The effect of air-gap parameters on energy factor are observed by using computed energy factor data. Observation taken from this data that energy factor is maximized when conduction period X_{nc} , maximum flux density $B_{p(max)}$ take highest values in their ranges. Whenever normalized switch-on instant is concerned, it is observed that optimum value of X_{ni} depends on the value of $B_{p(max)}$ and X_{nc} . However, while $B_{p(max)}$ and X_{nc} take their optimum values (i.e. 2.1 T and 1 respectively), $X_{ni} = -1.4$ maximizes energy factor.

Whenever λ/g is considered, it is understood that for $B_{p(max)} = 1.5$ T energy factor is increased by increasing λ/g so that $\lambda/g = 250$ maximizes energy factor. As seen from fig. 3.11 after certain value of λ/g rise in energy factor is not so considerable. This value of λ/g depends on $B_{p(max)}$ mainly. For example at $B_{p(max)} = 2.1$ T the increasing of energy factor is 24% by changing λ/g from 160 to 250 provides only 2% increase in energy factor. Therefore it is not meaningful to increase λ/g larger than 160. Nevertheless, last percentage given above decreases by decreasing $B_{p(max)}$ so that at $B_{p(max)} = 1.5$ T it tends to zero. Under the value of 1.5 T, optimum λ/g is shifted to lower λ/g values by increasing tooth

widths,

The most important result found here is to understand that energy factor increases while tooth widths of rotor and stator converge to each other so that energy factor is maximized when rotor -stator tooth widths become identical. While other parameters take their optimum values, for maximizing energy factor, it is observed that normalized tooth widths of rotor and stator should be 0.42. But as $B_{p(max)}$ reduces to 1.1T it is observed that optimum t_s/λ and t_r/λ is 0.35 which is the result found in the works in literature. But this value of tooth widths maximize energy factor at $X_{ni} = -1.4$. If it is remembered from above discussions, optimum X_{ni} value shifts toward -1.6 while $B_{p(max)}$ decreases. Therefore for $B_{p(max)} = 1.1 T$ optimum t_s/λ and t_r/λ values should be searched at $X_{ni} = -1.6$. At this situation it is understood that optimum normalized tooth widths of rotor and stator is around 0.4 as denoted by dotted line in fig. 3.14.

An upper limit of mmf has been chosen 70 kA for limiting the current in the winding. Whole computed energy factor in this chapter and therefore observations are valid under this restriction. However in order to see the effect of this constraint on energy factor, energy factor vs mmf limit curves are obtained and it is seen that while mmf limit increases, energy factor increases

as expected. After certain value of this limit, it becomes asymptotical as shown in fig. 3.16. This value of mmf limit reduces by decreasing $B_{p(max)}$. In obtaining of these curves in fig. 3.16 optimum design found in this chapter is used. However as will be shown in next chapter optimum design changes by varying mmf limit. Therefore energy factor should be computed.

In this chapter, the rough values of optimum air-gap parameters found. However, since the main purpose of this work is to find optimum air-gap design, the values of parameters should be computed more accurately. For this purpose an optimization method should be used.

In the next chapter the approach used for finding accurate optimum values of air-gap parameters by the help of an optimization method will be presented.

CHAPTER 4

OPTIMIZATION

4.1 INTRODUCTION

Until here, energy factor results for U_{dss} have been obtained by using the method described in chapter 2. These results are important for observing the variations of energy factor with respect to different motor parameters. However, the main purpose of this thesis is to find the optimum air-gap parameter values of U_{dss} which produces maximum steady-state average torque. The results above can only give a rough idea for optimum parameters of U_{dss} . For obtaining more accurate result, the values in the parameter sets should be increased. But, it means that ten thousands of energy factor values must be calculated. This is not a practical solution for obtaining optimum values of motor parameters. Therefore an optimization method which can find the optimum parameter values in desired accuracy and in a short time period should be used.

In this work, such an optimization method which may be called "A Form of Directional Search" has been used. This chapter presents the theory and application of this method.

4.2 GENERAL OPTIMIZATION APPROACH

An optimization problem may be generally formulated as follows

Optimize $F(\bar{X})$

Subject to $g_i(\bar{X})$ for $i=1, \dots, m$

where $f(\bar{X})$ is the function to be maximized and $g_i(\bar{X})$ is the constraint functions and \bar{X} is a vector which contains independent optimization parameters. The optimization and constraint functions are computed by using independent optimization parameters. A general optimization procedure of the SRM design, the following stages should be considered,

- 1) Independent motor parameters should be chosen from which the performance may be calculated.
- 2) The constraints should be identified.
- 3) A method for computing of performance function in terms of independent parameters should be available, In chapter 2 such a method has been presented for obtaining energy factor of U_{dss} .

4.2.1 INDEPENDENT MOTOR PARAMETERS

Following parameters are chosen as the independent optimization parameters in this work.

- 1) λ/g : rotor tooth pitch over air-gap length,
- 2) t_s/λ : stator tooth width over rotor tooth pitch,
- 3) t_r/λ : rotor tooth width over rotor tooth pitch,
- 4) X_{ni} : normalized switch-on position,
- 5) X_{nc} : normalized conduction period,
- 6) B_p : peak value of stator pole average flux density,

4.2.2 CONSTRAINTS

Some practical restrictions in manufacturing and in utilizing of SRM for optimum design should be taken into account. These constraints and their reasons may be summarized as follows.

a) Constraints on t_s/λ and t_r/λ : There are two separate constraints on teeth widths of rotor and stator.

1- In order to increase winding space

$$t_r/\lambda \geq t_s/\lambda$$

2- In order to minimize OUT position inductance

$$t_r/\lambda + t_s/\lambda \leq 1$$

b) Constraint on mmf value: If a practical motor is assumed, current limit action should be taken into account as mentioned in chapter 3. Therefore, for this work, an upper limit of 70 kA is assumed for limiting the current in the winding. This is a value which will saturate a Udss having identically slotted teeth pairs with a normalized tooth width 0.4 and with an λ/g value which is 70 to an average flux density of 2.1 T for IN position. But in order to see effect of this limit an optimum values of parameters different mmf limits are used in next sections of this chapter.

4.3 THEORY OF OPTIMIZATION METHOD USED IN THIS WORK

Since the independent parameters vector is,

$$X = (X_{nc}, B_p, \lambda/g, t_s/\lambda, t_r/\lambda, X_{ni})$$

This method here, chooses gradient vector which has the highest positive magnitude. Then the maximum value of the performance function is sought, and the value of related parameter which corresponds to peak value of that curve is found. Then, while this parameter is held constant at that value, new gradient vector which belongs to other parameters are calculated as mentioned above. This procedure is

repeated until the magnitude of all gradient vectors have zero or negative value. These last values of parameters correspond to maximum value of optimization function.

4.4 APPLICATION OF THE METHOD

In this work, the described optimization method has been applied by the aid of a computer program. The program flow-chart and its detailed description is given in Appendix B.

The procedure for finding of optimum values of parameters may be mainly split into two different searching steps. One of them may be called as coarse search and it is valid from initial point to local maxima. The other searching step is fine search and it is valid from local maxima found at the end of course search, up to maxima is found.

The parameter intervals in two searching steps are not same. In coarse search, the searching step length of any parameter is higher than the step length of fine search for that parameter. The aim of the coarse search is to make the procedure faster and find the rough values of optimum parameters. The purpose of fine search is to find accurate optimum values of parameters. Briefly, by using fine search step lengths of parameters along the whole optimization application, then time consumption is

very high,

In this work, the step lengths for coarse and fine search are chosen as follows,

	<u>Coarse Search(Step 1)</u>	<u>Fine Search(Step 2)</u>
X_{nc}	0.2	0.05
B_p	0.2	0.05
λ/g	30	10
$t_s/\lambda, t_r/\lambda$	0.1	0.01
X_{ni}	0.2	0.01

Moreover, number of points defines mmf vs B countour is increased from 20 to 40 for fine search,

Therefore, those independent parameters may take the following values during the coarse search,

- X_{nc} : 0.6, 0.8, 1
- B_p : 1.1, 1.3, 1.5,, 2.1
- λ/g : 40, 70, 100,, 250
- $t_r/\lambda, t_s/\lambda$: 0.3, 0.4, 0.5
- X_{ni} : -1.8, -1.6, -1.4,, -0.8

Coarse and fine searches contain two separate mode, one of them is searching mode and the other is progress mode. As explained in Appendix B, search mode finds the parameter which can maximize energy factor and in the other mode this parameter is incremented in maximum energy factor direction.

The procedure followed by the computer program written may be summarized as follows.

This program strats to search the local maximum point from any initialpoint which can be arbitrarily chosen by the user. At this instant program is in teh search mode. It searches the parameter which maximizes energy factor. To do this, only one parameter is changed while others are held constant as described. For this purpose, energy factor is computed and rate of change of function is found as follows.

$$\text{Average rate of change of } E(\bar{X}) = \frac{E(X_1) - E(X_2)}{X_1 - X_2} \quad 4.3$$

For other directions of rate of change of the function $E(\bar{X})$ is also found in a similar manner. For the problem here, since there are 6 variables, 12 rate of change vaues (for increment and decrement) are calculated and parameter which has highest rate of change in magnitude and its direction (increment or decrement) are found.

This above process continues until all rate of change of parameters have values zero or less than zero. Then, program jumps to the second mode which is maximum. The indicated parameter in search mode is changed in the direction found in search mode (increment or decrement). When energy factor starts to decrease, then that parameter is held constant at last value and program jumps again to search mode in order to seek new parameter and new direction which maximizes energy factor.

The above process continues until none of the parameters increases energy factor any more in search mode. Then the last set of values of parameters found correspond to coarse local maximum value of energy factor. Then program jumps to step 2 where fine search is done in order to find the local maximum point with better accuracy, smaller values of step lengths are used which are given above. The same procedure used in coarse search (step 1) is followed for this step, but the initial point in this case is the coarse local maxima found at the end of coarse search.

During the computations of energy factor values for optimization, intermediate values are found by using cubic spline and linear interpolation techniques since t_{sn} , t_{rn} parameter sets contain less number of values cubic spline method is used for these two parameters. For other parameters linear interpolation method is used.

4.5 RESULT OF OPTIMIZATION

In all optimization methods the maxima found depends on initial point if $f(\bar{X})$ has local maximums more than one,

During this optimization work, different initial points are tried, But it is observed that for parameter ranges and step lengths of coarse search given in previous section, 3 different local maximums are found as denoted in table (4.1). As may be seen from this table, it is observed that parameters B_p , X_{nc} , X_{ni} , λ/g reach same values for all local maximum whatever they take initial values, Therefore local maximums found are independent of initial values of these parameters, But same thing can not be said for t_s/λ and t_r/λ . It is observed that t_s/λ and t_r/λ don't reach same values at local maximums, Therefore it is understood that the local maximum found depends on the initial values of t_r/λ and t_s/λ .

Common and important properties of these three local maximums are, all of them have rotor and stator tooth widths which are equal to each other (i.e. $t_s/\lambda = t_r/\lambda$). In other words, whatever initial Udss has tooth widths, they become identical at local maximums. It is understood that energy factor function has peak values at each $t_s/\lambda = t_r/\lambda$ points while other parameters are held constant. Since the sets of t_s/λ and t_r/λ for the coarse search are,

$$t_s/\lambda : (0.3, 0.4, 0.5)$$

$$t_r/\lambda : (0.3, 0.4, 0.5)$$

Then the combination of these two set offers 3 separate symmetrical pairs as below,

$$t_s/\lambda = 0.3 \quad t_r/\lambda = 0.3$$

$$t_s/\lambda = 0.4 \quad t_r/\lambda = 0.4$$

$$t_s/\lambda = 0.5 \quad t_r/\lambda = 0.5$$

Therefore, for the coarse search conditions given in previous section, three type of symmetrically slotted Udss are taken into account in the search, three different local maximas are found.

If the previous step length condition is changed from 0.1 to 0.05 for t_s/λ and t_r/λ , it is observed that local maximas found have similar properties as the case of step length 0.1 as shown in table (4.2). But in this new case (step length= 0.05) the number of found maximas is 5. This is an expected result because for the new coarse search condition the values of t_s/λ and t_r/λ are,

$$t_s/\lambda : (0.3, 0.35, 0.4, 0.45, 0.5)$$

$$t_r/\lambda : (0.3, 0.35, 0.4, 0.45, 0.5)$$

INITIAL POINT (Desing)							LOCAL MAXIMA						
Xnc	Bp	l/g	ts/l	tr/l	Xni	Receiving time	Xnc	Bp	l/g	ts/l	tr/l	Xni	Max.En.Factor
0.60	1.10	40.00	0.30	0.30	-1.80	00:03:52	1.00	2.10	250.00	0.30	0.30	-1.40	20.012
0.60	1.30	190.00	0.40	0.30	-1.80	00:04:01	1.00	2.10	250.00	0.40	0.40	-1.40	23.838
0.80	1.50	160.00	0.50	0.30	-1.20	00:03:28	1.00	2.10	250.00	0.30	0.30	-1.40	20.012
0.80	1.90	130.00	0.50	0.50	-0.80	00:03:24	1.00	2.10	250.00	0.50	0.50	-1.40	22.950
1.00	1.10	100.00	0.50	0.40	-1.00	00:04:15	1.00	2.10	250.00	0.40	0.40	-1.40	23.838
1.00	1.10	220.00	0.40	0.40	-1.60	00:02:47	1.00	2.10	250.00	0.40	0.40	-1.40	23.838
0.60	2.10	40.00	0.40	0.40	-1.00	00:05:13	1.00	2.10	250.00	0.40	0.40	-1.40	23.838

Table 4.1 Optimization results concerning 3 different local maximas

INITIAL POINT (Desing)							LOCAL MAXIMA						
(nc	Bp	l/g	tr/l	ts/l	Xni	Receiving time	Xnc	Bp	l/g	tr/l	ts/l	Xni	Max.En.Factor
0.60	1.10	40.00	0.30	0.30	-1.80	00:09:00	1.00	2.10	250.00	0.30	0.30	-1.40	20.012
0.60	1.50	100.00	0.45	0.35	-1.60	00:22:22	1.00	2.10	250.00	0.45	0.45	-1.40	23.752
0.80	1.70	190.00	0.50	0.40	-1.20	00:20:19	1.00	2.10	250.00	0.45	0.45	-1.40	23.752
1.00	1.10	70.00	0.50	0.40	-1.80	00:15:58	1.00	2.10	250.00	0.45	0.45	-1.40	23.752
1.00	1.90	220.00	0.35	0.30	-1.40	00:09:47	1.00	2.10	250.00	0.35	0.35	-1.40	22.104
0.80	1.70	40.00	0.50	0.30	-1.40	00:08:09	1.00	2.10	250.00	0.50	0.50	-1.40	22.950
1.00	1.30	250.00	0.50	0.35	-1.00	00:16:42	1.00	2.10	250.00	0.45	0.45	-1.40	23.752
1.00	1.50	220.00	0.40	0.30	-1.20	00:11:23	1.00	2.10	250.00	0.40	0.40	-1.40	23.838
0.80	2.10	40.00	0.50	0.50	-0.80	00:05:07	1.00	2.10	250.00	0.50	0.50	-1.40	22.950
0.60	1.30	250.00	0.40	0.30	-1.00	00:08:52	1.00	2.10	250.00	0.40	0.40	-1.40	23.838
0.80	2.10	130.00	0.50	0.45	-1.60	00:12:52	1.00	2.10	250.00	0.45	0.45	-1.40	23.752

Table 4.2 Optimization results concerning 5 different local maximas

The combination of these two sets offers 5 symmetrically slotted Udss which are,

$$t_s/\lambda = 0.3 \quad t_r/\lambda = 0.3$$

$$t_s/\lambda = 0.35 \quad t_r/\lambda = 0.35$$

$$t_s/\lambda = 0.4 \quad t_r/\lambda = 0.4$$

$$t_s/\lambda = 0.45 \quad t_r/\lambda = 0.45$$

$$t_s/\lambda = 0.5 \quad t_r/\lambda = 0.5$$

Then, it can be said that energy factor function has a peak value at each $t_s/\lambda = t_r/\lambda$ while other parameters are hold constant. Therefore, in order to maximize energy factor, tooth widths of stator should be identical. Then for obtaining optimum values of air-gap parameters, search should be made by considering only symmetrically slotted Udss. For this purpose t_r/λ and t_s/λ are simultaneously incremented in the optimization and a new optimum is sought.

As seen from table (4.1) and (4.2) the optimum values of t_r/λ and t_s/λ should be around $t_r/\lambda = t_s/\lambda = 0.4$.

At the end of the fine search the following values of air-gap parameters are found for 70 kAT mmf limit.

$$X_{nc} = 1 : B_{p(max)} = 2,1 : \lambda/g = 250 : t_s/\lambda = 0,4 : t_r/\lambda = 0,4$$

$$X_{ni} = -1,3$$

$$\text{Energy Factor} = 24,406 \text{ kN/m}^2$$

The fact that the optimum occurs at limiting value of X_{nc} and $B_{p(max)}$ is excepted in view of the results found in section (3,4). Since optimum $B_{p(max)}$ value obtained here is 2,1 T, optimum value of λ/g which is 250 is also excepted result as observed in above mentioned section.

An interesting result here is the fact that the energy factor is optimized for $t_r/\lambda = t_s/\lambda = 0,4$. As it is well known from the point of view of average torque optimization, optimum values are reported to be 0,42 or this parameter in literature. The inspection here in the case that the optimum of this parameter is also dependent upon the switching instant. If switching instant was $X_{ni} = -1,4$ instead of the value found here ($X_{ni} = -1,3$) indeed the optimum tooth widths ratio would have been around 0,42. The difference between the optimum found here and the optimum at $X_{ni} = -1,4$ is about 6,4% and energy factor values are $24,406 \text{ KNm}^{-2}$ respectively.

4.6 EFFECT OF Mmf LIMITS ON OPTIMUM VALUES OF PARAMETERS

As mentioned in section (4.2.1), an upper limit of mmf has been chosen 70 kA for limiting the current in the winding. The optimum values of air-gap parameters presented in previous section are obtained under this restriction. However in order to observe the effect of this restriction on optimum air-gap parameters, different mmf limits have been also tried. In table (4.3) related computer output is given Upper limit of $B_p(\max)$ is chosen vs 2.1 T for this search. As seen from this table, after 100 kA mmf limit there is no rise in energy factor. Additionally to increase mmf limit 80 to 100 kA the rising percentage of energy factor is 4%. Therefore it may not be meaningful to shift mmf limit to values higher than 80 kA for $B_p(\max)$ 2.1 T.

Whenever optimum values of parameters are considered, it is seen that for mmf limits higher than 40 kA optimum normalized tooth widths t_s/λ , t_r/λ is 0.4. But under this value of mmf limit t_s/λ , t_r/λ is shifted to 0.48 by decreasing mmf limit. Additionally X_{ni} change its optimum value from -1.3 to -1.24 at 20 kA. Other parameters prevent their values whatever mmf limit is.

4.7 EFFECT OF $B_p(\max)$ ON OPTIMUM VALUES OF PARAMETERS

All optimization work up to here, considers that upper limit of $B_p(\max)$ is 2.1 T. In this section

INITIAL DESIGN							OPTIMUM DESIGN						
Xnc	Bp	l/g	tr/l	ts/l	Xni	MMF Limit	Xnc	Bp	l/g	tr/l	ts/l	Xni	Max.En.Factor
0.60	1.10	40.00	0.30	0.30	-1.80	20	1.00	2.10	250.00	0.48	0.48	-1.24	9.241
0.60	1.10	40.00	0.30	0.30	-1.80	30	1.00	2.10	250.00	0.45	0.45	-1.30	13.870
0.60	1.10	40.00	0.30	0.30	-1.80	40	1.00	2.10	250.00	0.43	0.43	-1.30	17.861
0.60	1.10	40.00	0.30	0.30	-1.80	50	1.00	2.10	250.00	0.40	0.40	-1.30	20.836
0.60	1.10	40.00	0.30	0.30	-1.80	60	1.00	2.10	250.00	0.40	0.40	-1.30	23.174
0.60	1.10	40.00	0.30	0.30	-1.80	70	1.00	2.10	250.00	0.40	0.40	-1.30	24.406
0.60	1.10	40.00	0.30	0.30	-1.80	80	1.00	2.10	250.00	0.40	0.40	-1.30	25.350
0.60	1.10	40.00	0.30	0.30	-1.80	90	1.00	2.10	250.00	0.40	0.40	-1.30	26.127
0.60	1.10	40.00	0.30	0.30	-1.80	100	1.00	2.10	250.00	0.40	0.40	-1.30	26.496
0.60	1.10	40.00	0.30	0.30	-1.80	110	1.00	2.10	250.00	0.40	0.40	-1.30	26.498
0.60	1.10	40.00	0.30	0.30	-1.80	120	1.00	2.10	250.00	0.40	0.40	-1.30	26.498

Table 4.3 Optimum air-gap parameters with respect to different Mmf limit

INITIAL DESIGN							OPTIMUM DESIGN						
Xnc	Bpmax	l/g	tr/l	ts/l	Xni	Upper lim.of Bpmax	Xnc	Bpmax	l/g	tr/l	ts/l	Xni	Max.En.Factor
0.60	1.10	40.00	0.30	0.30	-1.80	2.1	1.00	2.10	250.00	0.40	0.40	-1.30	24.406
0.60	1.10	40.00	0.30	0.30	-1.80	2.0	1.00	2.00	250.00	0.41	0.41	-1.40	22.474
0.60	1.10	40.00	0.30	0.30	-1.80	1.9	1.00	1.90	245.00	0.40	0.40	-1.40	20.906
0.60	1.10	40.00	0.30	0.30	-1.80	1.8	1.00	1.80	220.00	0.40	0.40	-1.48	18.830
0.60	1.10	40.00	0.30	0.30	-1.80	1.7	1.00	1.70	220.00	0.40	0.40	-1.50	17.361
0.60	1.10	40.00	0.30	0.30	-1.80	1.6	1.00	1.60	190.00	0.40	0.40	-1.50	15.307
0.60	1.10	40.00	0.30	0.30	-1.80	1.5	1.00	1.50	190.00	0.40	0.40	-1.50	13.159
0.60	1.10	40.00	0.30	0.30	-1.80	1.4	1.00	1.40	190.00	0.40	0.40	-1.50	11.188
0.60	1.10	40.00	0.30	0.30	-1.80	1.3	1.00	1.30	190.00	0.40	0.40	-1.50	9.364
0.60	1.10	40.00	0.30	0.30	-1.80	1.2	1.00	1.20	160.00	0.40	0.40	-1.60	7.902
0.60	1.10	40.00	0.30	0.30	-1.80	1.1	1.00	1.10	160.00	0.40	0.40	-1.60	6.600

Table 4.4 Optimum air-gap parameters with respect to different B_{p(max)} limit

of the work, the effect of $B_{p(max)}$ on optimum motor parameters are observed. In table (4,4) the variation of energy factor with $B_{p(max)}$ is shown for 70 kA mmf limit. As seen from this table normalized conduction period X_{nc} and normalized tooth widths t_s/λ , t_r/λ do not show any change in their previous optimum values with changing $B_{p(max)}$ values. It is also observable that for maximizing energy factor, it is observed that $B_{p(max)}$ and X_{nc} take their permitted highest values as excepted from the observations done in chapter 3.

Whatever λ/g is concerned, it is observed that optimum values of λ/g is decreased by decreasing $B_{p(max)}$. As remembered in section (3,4), this situation is clearly seen in table (4,4). For this part of the work only step length of λ/g is chosen as 5 for denoting variation of optimum λ/g values with respect to different upper limits of $B_{p(max)}$.

If the effect of normalized switch-on position, X_{ni} is considered, it is observed that optimum X_{ni} value is shifted from -1,3 to -1,6 by decreasing $B_{p(max)}$ as discussed in section (3,4).

In order to illustrate variation of optimum design parameters under both $B_{p(max)}$ and mmf limits, the table shown in table (4,5) is prepared. By using this

O P T I M U M D E S I G N

Upper limit of Epmax	MMF= 50										MMF= 80										MMF= 110											
	Xnc	Epmax	l/g	tr/l	ts/l	Xni	En.fac.	Per.	Xnc	Epmax	l/g	tr/l	ts/l	Xni	En.fac.	Per.	Xnc	Epmax	l/g	tr/l	ts/l	Xni	En.fac.	Per.	Xnc	Epmax	l/g	tr/l	ts/l	Xni	En.fac.	Per.
1.1	1.00	1.10	250	0.40	0.40	-1.48	5.01	% 5	1.00	1.10	160	0.40	0.40	-1.60	6.60	% 32	1.00	1.10	160	0.40	0.40	-1.60	6.60	% 32	1.00	1.10	160	0.40	0.40	-1.60	6.60	% 32
1.3	1.00	1.30	250	0.41	0.41	-1.41	6.40	% 0	1.00	1.30	190	0.40	0.40	-1.50	9.36	% 22	1.00	1.30	190	0.40	0.40	-1.50	9.36	% 22	1.00	1.30	190	0.40	0.40	-1.50	9.36	% 22
1.5	1.00	1.50	250	0.40	0.40	-1.30	7.19	% 1	1.00	1.50	220	0.40	0.40	-1.50	13.20	% 16	1.00	1.50	190	0.40	0.40	-1.50	13.16	% 15	1.00	1.50	190	0.40	0.40	-1.50	13.16	% 15
1.7	1.00	1.70	250	0.46	0.46	-1.30	8.62	% 15	1.00	1.70	250	0.40	0.40	-1.41	16.19	% 0	1.00	1.70	220	0.40	0.40	-1.60	16.32	% 1	1.00	1.70	220	0.40	0.40	-1.60	16.32	% 1
1.9	1.00	1.90	250	0.46	0.46	-1.26	8.98	% 13	1.00	1.90	250	0.40	0.40	-1.32	18.69	% 2	1.00	1.90	250	0.40	0.40	-1.40	21.51	% 2	1.00	1.90	250	0.40	0.40	-1.40	21.79	% 2
2.1	1.00	2.10	250	0.47	0.47	-1.22	9.23	% 11	1.00	2.10	250	0.40	0.40	-1.30	20.84	% 6	1.00	2.10	250	0.40	0.40	-1.30	25.35	% 2	1.00	2.10	250	0.40	0.40	-1.30	26.50	% 1

Table 4.5 Optimum designs with respect to Mmf Limits and B_{p(max)} Limits

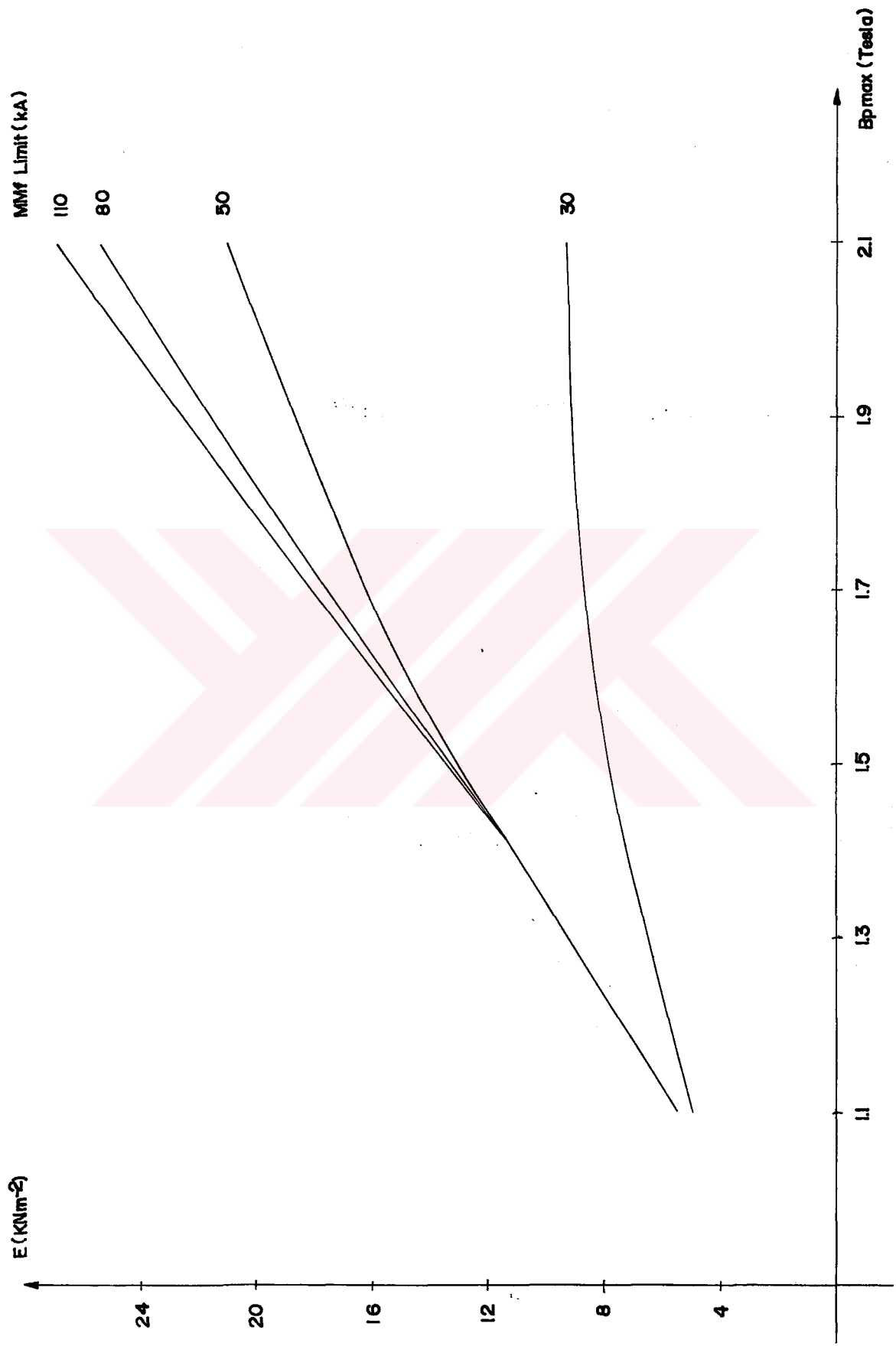


Fig. 4.6 Energy Factor vs $B_{p(\max)}$ Curves

table, energy factor vs $B_{p(max)}$ curves for different mmf limits are shown in fig 4.6. This figure indicates that approximately 20% increase is achieved by increasing $B_{p(max)}$ from 1.9 T to 2.1 T at 80 kA. Similarly at 110 kA same increase is observed in energy factor with increasing $B_{p(max)}$ (i.e from 1.9 T to 2.1T).

Percentages shown in this table indicate the difference between energy factors of design found in chapter 3 section 4 which is $X_{ni} = -1.4 \lambda/g = 250$, $t_s/\lambda = t_r/\lambda = 0.42$, and optimum designs are found by optimization method at same mmf and $B_{p(max)}$ limits.

4.8 CONCLUSION

In this chapter, accurate values of optimum air-gap parameters of SRM has been found by the help of the optimization method given in section (4.3). By using this method, optimum values of parameters are found in a couple of minutes. Otherwise, if the whole data is calculated in desired accuracy for selecting highest energy factor among computed data, it would take several hours or may be days.

Optimization method used here, is briefly searches local maximum point by progressing in the direction of maximum. This method involves two steps which are coarse and fine search. The purpose of coarse search is to reduce processing time. Coarse search is used until

reaching the vicinity of local maxima, Fine search is used for founding accurate values of optimum parameters around local maxima and naturally searching step length is lowered for accuracy.

During the optimization work, it is understood that energy factor function has peaks (i.e. local maxima) at each $t_s/\lambda = t_r/\lambda$ points while other parameters are held constant. This verifies the observations done in chapter 3 about tooth widths. Optimization procedure stops the search when it finds any local maxima although there may be other maxima having higher energy factor value. In order to overcome this problem and to find local maxima having highest energy factor value, search is done among symmetrically slotted structures.

In this optimization work, optimum values of parameters are found under different mmf limits and different $B_{p(max)}$ limits. During this search it is seen that optimum normalized conduction period is always unity whatever upper limit of $B_{p(max)}$ and mmf limit are.

It is also observed that optimum $B_{p(max)}$ value is always equal to its upper limiting value. However normalized switch-on position X_{ni} depends on upper limit of $B_{p(max)}$ and mmf limits as well. t_s/λ t_r/λ are equal to each other and for mmf 20kA they are equal to 0.4. But at mmf mmf, 20kA, optimum t_s/λ , t_r/λ are shifted from 0.4 to 0.48 by increasing $B_{p(max)}$.

If the optimum design found in chapter 3 by the help of observations is used in place of optimum designs found here at the same mmf and $B_{p(max)}$ limits the difference of energy factors of them is between 0 and 32% as shown in table (4,5). This implies the importance of optimization work done here.

By obtaining optimum values of air-gap parameters under different constraint values general frame of optimum design criteria is identified. In the next chapter, results and observations taken during this work will be summarized.

CHAPTER 5

CONCLUSION

In the last 20-25 years, product quality and production speed has been improved by developing improved forms of controlled electrical drives, drive based on switching reluctance motors (SRM) is regarded as a new alternative in the competition between AC and DC drives. Srm offers high power output, per unit volume, high system efficiency and low manufacturing cost. The drive circuitry of SRM is simple and dependable compared to inverter fed induction motors.

However, because of the effects of saturation for the performance functions are not available. Therefore, instead of using analytical expressions, experimentally measured or numerically computed data are used for the purpose of design. Current SRM design techniques are generally based on experimentally obtained information. However, in order to obtain optimum design parameters, performance function should be accurately found. For obtaining these performance functions in desired accuracy, field solutions should be used. However, especially for the design purpose, it is a very time consuming process and is not desirable.

The purpose of this thesis is to find optimum values of parameters of asymmetrically slotted structures with acceptable accuracy but with limited effort. To do

this, a method recently developed and used for symmetrically slotted SRM's is adopted to asymmetrically slotted structures by the help of the digital computer programs. By using this approach, it is possible to compute steady state average torque a doubly salient structure under specified magnetic loading and switching condition by the aid of energy factor concept. Energy factor is simply coenergy of the scaled model of original geometry of SRM.

An important advantage of this work is its applicability on a personal computer rather than a main frame system. Problems that originate from P.C's slow execution time is overcome by developing some techniques as presented in chapter 3.

Available data for this work is permeance vs stator flux density B_t curves of symmetrically slotted structures. In order to cover the parameter range encountered in SRM's, the available data is extended and also put into a suitable form for this work by using some interpolation and extrapolation techniques.

By the help of the method mentioned above, energy factor data of asymmetrically slotted SRM's are computed and tabulated in the table 3.7. The purpose of this approach is to observe the variation of energy factor with respect to air-gap parameters and to find rough values of parameters which maximize energy factor.

During these observations, it is seen that, maximum peak flux density $B_{p(max)}$ and normalized conduction period X_{nc} , take their highest permitted values whatever the values of other parameters are. However, optimum value of normalized switch-on position X_{ni} depends on the values of $B_{p(max)}$ and X_{nc} . Therefore for maximizing energy factor, X_{ni} should be selected according to the values of $B_{p(max)}$ and X_{nc} . Whenever, rotor tooth pitch over air-gap length; λ/g is concerned, it is observed that optimum λ/g value depends on the value of $B_{p(max)}$ and low $B_{p(max)}$ values (i.e. lower than 1.5 T) it also depends on the value of tooth widths. While $B_{p(max)}$ increases optimum λ/g increases so that for $B_{p(max)}=2.1$ T optimum λ/g value is its limiting value which is 250. For $B_{p(max)}=1.3$ T optimum $\lambda/g=250, 190, 160$ while normalized stator and rotor tooth widths t_s/λ , t_r/λ is equal to 0.3, 0.4, 0.5 respectively. The most important observation of this work, is about tooth widths. It is seen that tooth widths of rotor and stator should be identical for maximizing energy factor. In other words, it is understood that while tooth widths of stator and rotor converge to each other, energy factor maximizes.

In order to hold the current in reasonable level in the winding, 70 kA mmf limit is found to be suitable. Therefore all computations is done under

this constraint,

By the help of the computed energy factor data mentioned above, one can easily predict optimum design parameter values. These, however, will be rough values of parameters. By the above approach, in order to find accurate values, more than ten thousands of energy factor should be computed. This is not a practical solution for optimization. Hence, an optimization method is used in this work, for finding accurate values of air-gap parameters of SRM. The essence of the method given in chapter 4 is to seek local maxima by progressing in direction which maximizes the objective function so that there is no need to compute energy factors of all structures. By the help of this procedure optimum values of parameters are found in a couple of minutes on an IBM PC XT computer. During this part of the work, it is observed that, optimum designs found there have identical teeth pairs whatever the initial design is. Therefore it is understood that energy factor function has peaks (or local maximas) at each identically slotted structures while other parameter are held fixed. Optimization method stops the search after finding any local maxima although there may be an other maxima having higher energy factor value. In order to find local maxima having highest energy factor, search is also done among symmetrically

slotted SRM's. In optimization work done in this thesis, accurate optimum values of parameters are also found under different mmf limits and different $B_{p(max)}$ limits. During this search it is found that it is not meaningful to increase mmf limit beyond kA as further increase, increases energy factor marginally at practical $B_{p(max)}$ values (i.e. 1.9 - 2.1 T). For smaller $B_{p(max)}$ limits mmf limit may be safely taken as 50 kA. Whenever effect of $B_{p(max)}$ is concerned, it may be stated $B_{p(max)}$ is directly proportional to energy factor and therefore the design should aim highest $B_{p(max)}$ values. Mmf limit and upper limit of $B_{p(max)}$ also affects optimum values of air-gap parameters summarized as in table 4.5 so that optimum t/λ ratio at practical mmf limits (mmf limit greater than 50 kA) is found to be 0.4. This value however also depended on the switching angle. In the optimization work here, the switching angle X_{ni} is assumed to be adjustable as desired. It is observed that if X_{ni} is held at -1.4 to optimum t/λ occurs at 0.42 for $B_{p(max)}=2.1$ T. $B_{p(max)}$ For smaller mmf limits when X_{ni} is left free to vary, optimum t/λ approaches 0.47 by increasing $B_{p(max)}$. If on the other hand X_{ni} is limited, optimum value is found to be around 0.35. Whenever λ/g is considered, at $B_{p(max)}=2.1$ T only 5% increase is observed in energy factor by increasing λ/g from

160 to 190 and this percentage decreases with decreasing $B_{p(max)}$. Therefore there is no meaningful λ/g larger than 160 for $B_{p(max)} = 1.5 T$. For lower values of $B_{p(max)}$ optimum λ/g values shown in table (4.5) should be taken in to account.

In summary, general guideline are set for the designer and the effect of all possible parameters on the performance is clearly illustrated. Since, only a complete understanding of SRM behaviour can clarify whether SRM has any chance as variable speed industrial drive system. This thesis may help to provide answer to this question.

LIST OF REFERENCES

- 1) Harris M.R., Huges A., Lawrenson P.J., "Static Torque Production in Saturated Doubly-Salient Machines", PROC. IEE, Vol. 122, No 10, OCTOBER 1975
- 2) Harris M.R., Andşargholi V., Lawrenson P.J., Huges A., Ertan B., "Unifying Approach to the Static Torque of Stepping-Motor Structures", IEE, Vol. 124, No. 12, DECEMBER 1977
- 3) Ertan H.B., "Asimetrik Çıkık Kutuplu Manyetik Yapılarda Kuvvetin Hesabı", Doçentlik Tezi, 1982
- 4) Ertan H.B., "Analytical Prediction of Torque and Inductance Characterisitcs of Identically Slotted Doubly-Salient Reluctance Motors", IEE, Vol. 133, No. 4 JULY 1986
- 5) Tohumcu M., "Optimum Design of Switching Reluctance Motors", Phd Thesis in METU, JUNE 1985
- 6) Aktaş Z., Öncül H., Ural S., Aksu H., "Numerical Analysis", METU, Department of Computer Science, 1973
- 7) Kuo S.S., "Cömputer Applications of Numerical Methods", Addison Wesley, 1972
- 8) Accarnley P.P., "Stepping Motors", Peter Peregrinus Ltd, 2nd edittion, 1984

- 9) Fitzgerald A, E, Kingsley C, Kuskoski A, "Electric Machinery", Mc Graw Hill, 1971
- 10) Pierre A, D, "Optimization Theory with Applications", John Willey & Sons, 1969



APPENDIX A

Cubic Spline Interpolation

Given a number of points which represent a function $f(x)$, it is possible to obtain $f(x)$ for intermediate values of x , by using cubic spline interpolation. Advantage of this method is that it assures the continuity of the function and its derivative. Given n pivotal points, a cubic polynomial is used to interpolate the function in each interval, that passes through the end points of the interval. Let $g(x)$ denotes the entire interpolating function $f(x)$. Since it is cubic polynomial in each interval, its second derivative is piecewise linear function as shown in the figure.

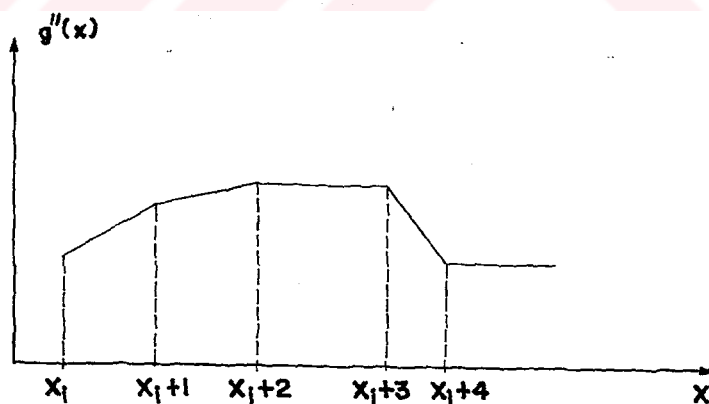


Fig. A.1.1. Second derivative of function $f(x)$
The second derivative of $f(x)$ at any interval of x can be written as piecewise linear function.

$$g''(x) = g''(x_i) + \frac{x - x_i}{x_{i+1} - x_i} (g''(x_{i+1}) - g''(x_i)) \quad (A-1)$$

where $x_i < x < x_{i+1}$

Integrating this equation twice and applying the conditions that $g(x_i) = f(x_i)$ and $g(x_{i+1}) = f(x_{i+1})$, one can find;

$$F_i(x) = g(x) = \frac{g''(x_i)}{6} \left[\frac{(x_{i+1} - x)^3}{\Delta x_i} - \Delta x_i (x_{i+1} - x) \right] + \frac{g''(x_{i+1})}{6} \left[\frac{(x - x_i)^3}{\Delta x_i} - \Delta x_i (x - x_i) \right] + f(x_i) \left[\frac{x_{i+1} - x}{\Delta x_i} \right] + f(x_{i+1}) \left[\frac{x - x_i}{\Delta x_i} \right] \quad (A-2)$$

where $\Delta x_i = x_{i+1} - x_i$. But in this equation second derivatives $g''(x_i)$ ($i = 1, \dots, n$) are still unknown. In any function, left and right derivatives must be equal to each other. Then, in order to satisfy it

$$F_i'(x_i) = F_{i-1}'(x_i) \quad (A-3)$$

$$F_i''(x_i) = F_{i-1}''(x_i) \quad (A-4)$$

Applying this condition and collecting terms yields a set of linear simultaneous equations of the form,

should obtain two additional equation, which are simply,

$$g''(x_0) \text{ and } g''(x_n) = 0 \quad (\text{A-7})$$

With there last two equation and the matrix (A-6), it can be possible to obtain $g''(x)$ value.

Then equation (A-2) is used to find $F_i(x)$ where x in

$$x_i < x < x_i + 1$$

As shown eq. (A-6) the A matrix is tridiagonal, and it contains at most three unknown. But if this method is used for equal intervals of x then the A matrix becomes,

$$A = \begin{bmatrix} 4 & 1 & 0 & 0 & \dots & 0 \\ 1 & 4 & 1 & 0 & & \\ 0 & 1 & 4 & 1 & & \\ & & \dots & \dots & \dots & \\ & & & & & 0 \\ & & & & & 1 \\ 0 & \dots & 0 & 1 & & 4 \end{bmatrix}$$

Which is constant for equal interval cases. Then for any function where x intervals are equal to each other, intermediate values can be found by using eq. (A-6) once. The obtained $g''(x_i)$ for $i=0, \dots, n$, are valid for calculating for all intermediate values in eq. (A-6). This situation brings considerable simplicity of evaluating of this method,

APPENDIX B

DESCRIPTIONS OF PROGRAM USED IN THIS WORK

As mentioned before, from first step to last step of this work several computer programs have been used. However these programmes have been applied on a personal computer instead of a main frame computer.

Since the memory area and speed of PC's are limited with respect to those systems, in developing these programmes pre-cautions have been taken. In this section, flow-charts and brief description of some important programs used during this work are presented as well as the techniques adopted to able to solve the problems on a PC.

(B.1.2) PROGRAM FOR COMPUTATION OF PvsB CURVES OF ASYMMETRICALLY SLOTTED STRUCTURES

The flow-chart of program used for computing PvsB curves of asymmetrically slotted structures and its sub-routine are shown in fig (B-1) and fig (B-2) Input data for this program is normalized PvsB curves for symmetrically slotted structures. This data has been located in the computer file as denoted in fig (B-3).

In this program, identification of parameter values for corresponding symmetrical pair is done according to the equations and constrains given in chapter 2. In order to find the permeance data of corresponding structure from the input data, program uses a search and interpolation sub-routine.

If desired structure has unavailable parameter values, this routine is capable of calculating its permeance value by using an interpolation routine. The interpolation method is linear, because of the reasons described in chapter 3. However, any other interpolation method can be applied to this program by making minor changes in it.

The search method adopted for finding permeance value of desired structure is quite interesting in this program. Instead of comparing the parameters of a structure with structures available in the data, computing the array number of that structure by using a method described below has been used. In this manner considerable advantage is gained from the point of view of computer execution time.

As shown in fig (B-3), the input data is loaded into the computer memory in sequential manner instead of random manner. In other words every parameter has a specific number N so that each parameter changes at every Nth permeance data. For this work, parameters have N values as follows.

<u>Parameter</u>	<u>N_i</u>
B	1
λ/g	21
t/λ	168
X_n	504

Then, related parameter takes specified value firstly after array number which can be found as,

$$\text{Array Number, } S_i = (K_i - 1) \times N_i \quad \text{eq. (B.1)}$$

where $i = 1, 5$

where k is the order number of related parameter values in that parameter range. If the above equation is applied to each parameter separately then summation of those results plus 1 denotes the exact array number of desired structure in the whole data. For presenting this method clearly, an example may be useful. Let's suppose that a structure has following parameter values.

$$X_n = 0.8, \quad t_n = 0.4, \quad \lambda/g = 190, \quad B = 1.5 \text{ T}$$

For X_n : For this step of the work X_n has following values.

$$\begin{matrix} (0.0, & 0.2, & 0.4, & 0.6, & 0.8, & 1) \\ 1 & 2 & 3 & 4 & 5 & 6 \end{matrix}$$

As seen above 0.8 is 5th value in X_n set. Therefore $k=5$ for $X_n=0.8$. Then array number of X_n denoted by S_{xn} is,

$$S_{xn} = (5-1) \times 504 = 2016$$

It means that all structure which have $X_n=0.8$ value start after 2016th array whatever other parameters have.

For t/λ : t/λ may take following values for this step of the work.

(0.3 , 0.4 , 0.5)
 1 2 3

As seen above 0.4 is 2nd value in t/λ set. Therefore $k=2$ for $t/\lambda = 0.4$.

Then array number of $t/\lambda = 0.4$ is

$$S_{t/\lambda} = (2-1) \times 168 = 168$$

For λ/g : λ/g set contain following values for this work.

(40 , 70 , 100 , 130 , 160 , 190 , 220 , 250)
 1 2 3 4 5 6 7 8

As seen above 190 is 6th value in λ/g set, then $k=6$.

Therefore,

$$S_{\lambda/g} = (6-1) \times 21 + 105$$

For B : 1.5 T is the 15th value in B set shown below.

(0.1, 0.2, 0.3, 0.4, 0.5, , 1.4, 1.5, 1.6, 1.7, 1.8, 1.9, 2.0, 2.1)
 1 2 3 4 6 14 15 16 17 18 19 20 21 .

Then $k=15$, the array number of B1.5 T is found as,

$$S_B = (15-1) \times 1 + 14$$

After computing the array numbers of parameters separately, the location S of permeance value in the data can be found as,

$$S = S_{xn} = S_{t/\lambda} + S_{\lambda/g} + S_{B+1}$$

Then

$$S = 2304$$

It means that the 2304th permeance value in the whole data belongs to the structure given above.

As seen from above example by using this method the search of permeance value of desired structure in the data can be made considerably than the procedure of comparing the desired structure parameter with the available data one by one until it is found. Since this program needs to find permeance of the structures many times, this method provides a great saving of computer run-time.

Additionally, since there is no need to load parameter values to the computer memory. In otherwords to load only permeance values is sufficient. It is enough to know the location form of the parameters in the data file as mentioned above. This situation provides a saving of memory area by the percentage of 80%.

Since this method offers a solution to the speed

and memory area problems in a PC applications, same technique is used in further programs in this work.

(B.1.2) PROGRAM FOR COMPUTATION OF ENERGY FACTOR DATA.

In energy factor calculation similar search and interpolation techniques are used. The area of B vs F contour has been computed by using trapezoidal rule. Since practical motor parameters have been assumed throughout this work, the mmf side of the contour has been limited at 70 k AT. However this program is capable to limit the mmf at any other desired mmf value. Nevertheless, the variation of energy factor with respect to mmf limits mentioned in chapter 4 has been found by using this facility of the program. The flow-chart of this program is shown in fig (B-4)

(B.1.3) OPTIMIZATION PROGRAM

An other important program developed in this work is the optimization program. The procedure of optimization technique has been given in chapter 4 and the flow-chart of related program is given in fig (B.5). The major property of this program is to contain several sections and sub-sections. In order to distinguish, these sections in the text, they are named in the following manner.

Step 1, Step 2: These are the main sections

in the program. Step 1 refers the section which does the coarse search. It starts from initial point and continues until reaching a local maxima, Step 2 is the fine search section and it starts from local maxima found in Step 1 and end at accurate maximum point. Basically program follows the same routine for these two sections, however the step lengths in the searches are not the same.

Search Mode, Progress Mode: These sections behave as sub-sections of both Step 1 and Step 2 (coarse and fine search).

Search mode tries to find parameter and its direction which maximizes energy factor. The search progresses with the direction found in progress mode while other parameters are kept constant. Progress mode changes the identified parameter in the defined direction until energy factor decreases.

Direction phase: Direction phase is a sub-section in search mode. It provides to examine the parameter in two direction by increasing and decreasing the value of related parameter.

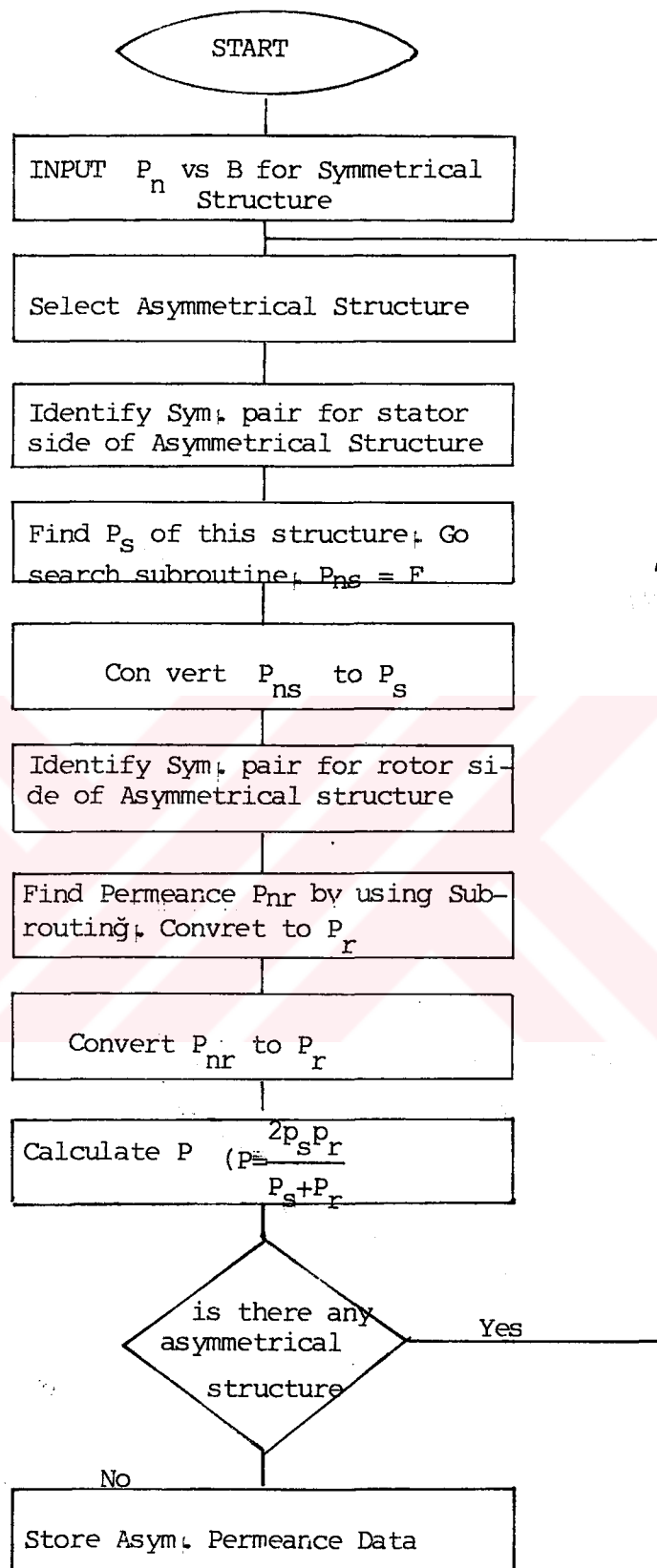
As seen from the program flow-chart, this program has a compact form. In other words, all sections and sub-sections utilize useful part of each other. Therefore at necessary instants, program should know its current situation. This can be provided by the help of the program flags. All necessary sections are defined

by these flags which can be set or reset (0.1). Some of the other important symbols and functions of these flags are as follows.

<u>Flag</u>	<u>Reset (0)</u>	<u>Set(1)</u>
SWI (Step Flag)	Defines Coarse Search	Defines Fine Search
MD (Mode Flag)	Defines Search Mode	Defines Progress Mode
SW (Direction Flag)	Defines that parameter is examined in one direction	Defines that parameter is examined into two direction.

Energy factor program which has been previously described are used as a sub-routine in this program. However for interpolation, $t_{s/\lambda}$, $t_{r/\lambda}$ and x_{ni} cubic spline interpolation technique and for other parameters linear interpolation technique have been used.

Fig. B.1 FLOW-CHART FOR COMPUTATION OF ASYM? P vs B CURVES



END

TABLE B.2 SUB-ROUTINE FOR SEARCHING AN INTERPOLATING

P(J) : Parameter

where P(1)=B, P(2)= λ/g ,
P(3)= ϕ/λ , P(4)= X_n

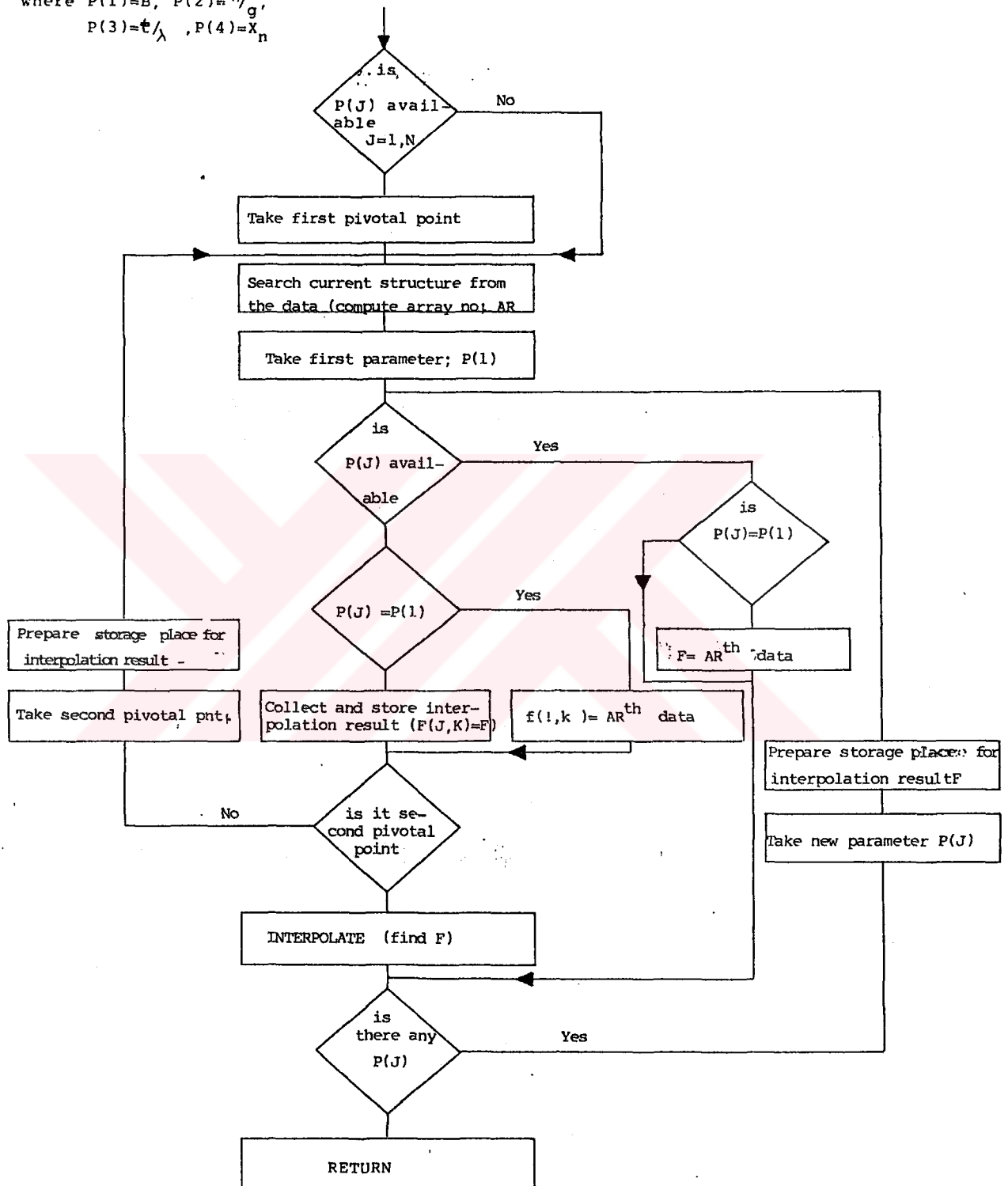


Fig. B.3
 FLOW-CHART OF ENERGY
 FACTOR PROGRAM

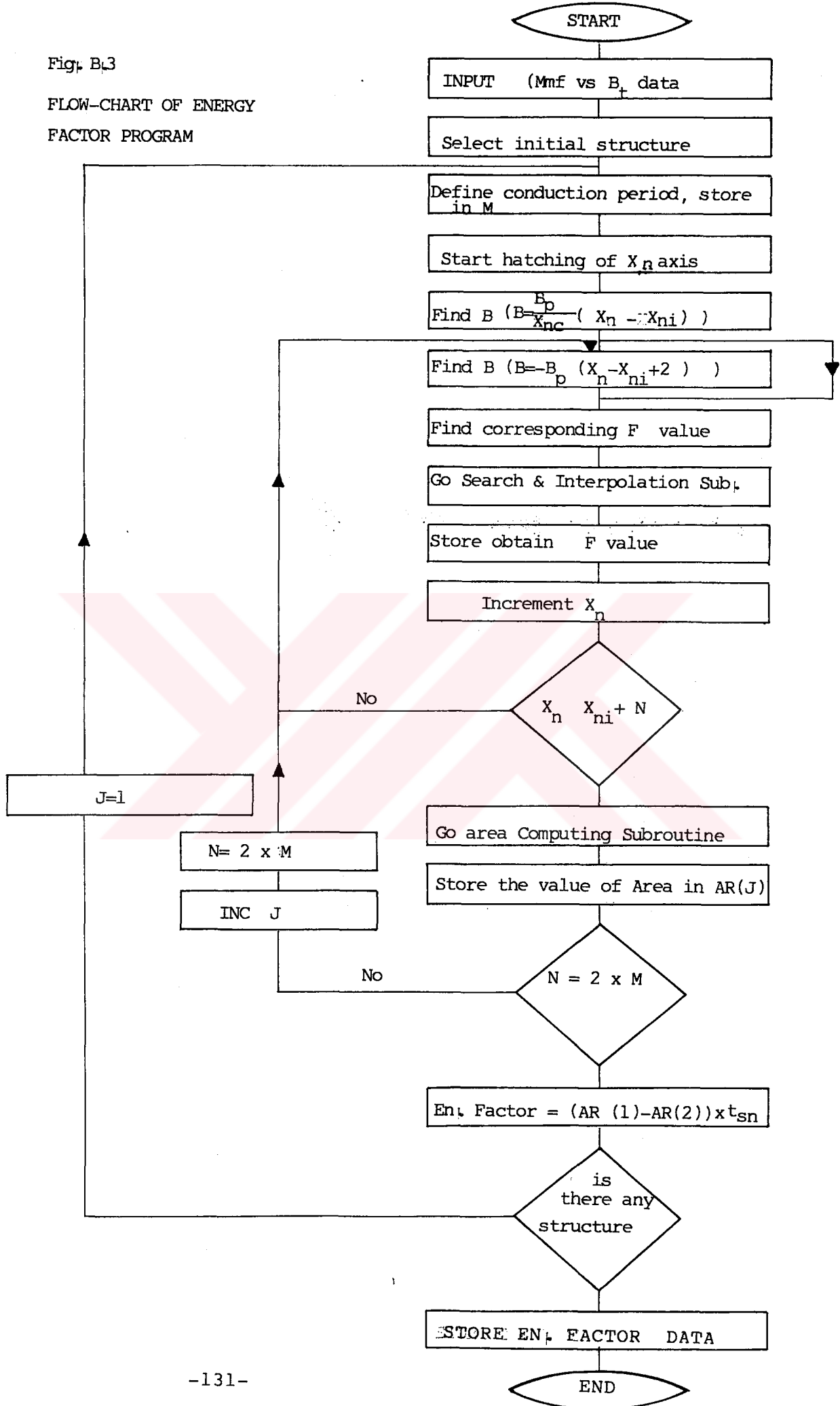


Table B.4 OPTIMIZATION PROGRAM FLOW-CHART

